Applications of Numerical Methods in Heterotic Calabi-Yau Compactification

Wei Cui

Dissertation submitted to the Faculty of the
Virginia Polytechnic Institute and State University
in partial fulfillment of the requirements for the degree of

Doctor of Philosophy
in
Physics

James Gray, Chair
Lara Anderson
Eric Sharpe
Shengfeng Cheng

August 7th, 2020
Blacksburg, Virginia

Keywords: Numerical methods, Heterotic String Compactification

Applications of Numerical Methods in Heterotic Calabi-Yau Compactification

Wei Cui

(ABSTRACT)

In this thesis, we apply the methods of numerical differential geometry to several different problems in heterotic Calabi-Yau compactification. We review algorithms for computing both the Ricci-flat metric on Calabi-Yau manifolds and Hermitian Yang-Mills connections on poly-stable holomorphic vector bundles over those spaces. We apply the numerical techniques for obtaining Ricci-flat metrics to study hierarchies of curvature scales over Calabi-Yau manifolds as a function of their complex structure moduli. The work we present successfully finds known large curvature regions on these manifolds, and provides useful information about curvature variation at general points in moduli space. This research is important in determining the validity of the low energy effective theories used in the description of Calabi-Yau compactifications. The numerical techniques for obtaining Hermitian Yang-Mills connections are applied in two different fashions in this thesis. First, we demonstrate that they can be successfully used to numerically determine the stability of vector bundles with qualitatively different features to those that have appeared in the literature to date. Second, we use these methods to further develop some calculations of holomorphic Chern-Simons invariant contributions to the heterotic superpotential that have recently appeared in the literature. A complete understanding of these quantities requires explicit knowledge of the Hermitian Yang-Mills connections involved. This feature makes such investigations prohibitively hard to pursue analytically, and a natural target for numerical techniques.

Applications of Numerical Methods in Heterotic Calabi-Yau Compactification

Wei Cui

(GENERAL AUDIENCE ABSTRACT)

String theory is one of the most promising attempts to unify gravity with the other three fundamental interactions (electromagnetic, weak and strong) of nature. It is believed to give a self-consistent theory of quantum gravity, which, at low energy, could contain all of the physics that we known, from the Standard Model of particle physics to cosmology. String theories are often defined in nine spatial dimensions. To obtain a theory with three spatial dimensions one needs to hide, or "compactify," six of the dimensions on a compact space which is small enough to have remained unobserved by our experiments. Unfortunately, the geometries of these spaces, called Calabi-Yau manifolds, and additional structures associated to them, called holomorphic vector bundles, turns out to be extremely complex. The equations determining the exact solutions of string theory for these quantities are highly non-linear partial differential equations (PDE's) which are simply impossible to solve analytically with currently known techniques. Nevertheless, knowledge of these solutions is critical in understanding much of the detailed physics that these theories imply. For example, to compute how the particles seen in three dimensions would interact with each other in a string theoretic model, the explicit form of these solutions would be required. Fortunately, numerical methods do exist for finding approximate solutions to the PDE's of interest. In this thesis we implement these algorithmic techniques and use them to study a variety of physical questions associated to the attempt to link string theory to the physics observed in our experiments.

Dedication

I dedicate this thesis to my parents for their understanding and support!

Acknowledgments

I would like to express my gratitude to Professor James Gray for his invaluable guidance and support. It is impossible to finish this thesis without his help. I would also like to thank Professor Lara Anderson and Professor Eric Sharpe for useful conversations on math and string theory.

I am grateful to my fellow graduate students and friends Jirui Guo, Ruoxu Wu, Chen Sun, Zhuo Chen, Hadi Parsian, He Feng, Wei Gu, Juntao Wang, Mohsen Karkheiran and Hao Zou in office 212A for interesting discussion and encouragement during my PhD period. Many thanks also goes to Xin Gao, Seung-Joo Lee, Paul-Konstantin Oehlmann and Nikhil Raghuram for organizing the weekly string theory seminar and for interesting discussion.

Contents

Chapter 1

Introduction

1.1 String Phenomenology

The basic idea of string theory is that the fundamental constituents of nature are one-dimensional strings rather than point-like particles [1, 2]. The strings, objects described by a world-sheet theory with one temporal and one spatial dimension, vibrate as they travel through spacetime (also referred to as the target space). Different vibrational modes look, to a low energy observer who can't resolve the length of the string, like different particles. Among these particles are a massless graviton and gauge bosons, which makes string theory a promising attempt to unify gravity with the other three fundamental interactions. The typical length scale associated to a string $l_s = \sqrt{\alpha'}$ is a constant which appears in the description of the worldsheet. This is the only free parameter of the theory. All other details which appear, including the coupling constant g_s which determines how strongly the strings interact and even the geometry of space-time, are determined dynamically.

Despite the appealing features of string theories, not every theory of this type is consistent and those that are often naively seem to be very far from what we observe in nature. Firstly, in order to avoid tachyons, world-sheet supersymmetry is often introduced giving rise to superstring theory [2, 3]. Secondly, in many string theories, in order to make sure the theory is anomaly free, it is necessary that spacetime be ten-dimensional. There are five consistent

superstring theories in ten dimensions, namely type IIA, type IIB, type I and the heterotic theories with gauge groups $SO(32)$ or $E_8 \times E_8$. These different looking theories are related by a network of dualities, and are conjectured to all be part of a more inclusive structure known as M-theory, which can be described in eleven-dimensional terms in certain regimes.

String phenomenology attempts to construct vacua of string theories, such as those discussed above, whose effective field theory can reproduce experimentally observed physics (for an overview see [4]). As a starting point, it is interesting to find a model that leads to an apparently four dimensional theory that includes the standard model of particle physics. Such "model building" attempts often are chosen to preserve some of the supersymmetry of the theory. This is because $N = 1$ supersymmetry in four dimensions is one of the best solutions to the Hierarchy problem and also allows for the unification of gauge couplings at a realistic scale. Thus, the goal of such research is to search for models which reproduce the Minimal Supersymmetric Standard Model (MSSM) [5].

In this thesis, we shall focus largely on the Heterotic string. In the low energy limit, the heterotic superstring reduces to a ten-dimensional supergravity coupled to gauge theories [6]. In order to build "realistic" four-dimensional models, one usually assumes that the ten-dimensional space-time M_{10} is a direct product of a non-compact four-dimensional space M_4 and a compact six-dimensional (internal) space X. The extra six dimensions are considered to have a characteristic length l_c that is small enough that it is consistent that their existence has evaded direct observation to date. If one tries to solve the equations of motion and consistency constraints of the string theory in such a manner as to preserve $N = 1$ supersymmetry, one arrives at a surprisingly varied set of possibilities [7, 8, 9]. However, if one further requires that M_4 is Minkowski space and that the Neveu-Schwarz three-form field strength has vanishing expectation value, then a relatively simple set of solutions is arrived at. The internal space X must be a Calabi-Yau three-fold and the vector bundle

$V \to X$, upon which the gauge fields in the theory are a connection, must be holomorphic, slope-zero and poly-stable [6, 10].

In a Calabi-Yau compactification, the four-dimensional physics can be derived from the topology and geometry of the string vacuum. In terms of model building, the goal is to find a vacuum, i.e. a choice of X and V, such that the four-dimensional theory reproduces the MSSM. As a first step, one requires that the effective field theory has the gauge group $SU(3)\times SU(2)\times U(1)$ and the MSSM spectrum. To achieve this, first, an X and V are identified which give rise to a supersymmetric Grand Unified Theory (GUT) in four dimensions. Then, the compactification is modified by the addition of a Wilson line such that the supersymmetric GUT theory is broken to the MSSM. Following this approach, several heterotic models have been found with the correct gauge group and charged spectrum (additional uncharged moduli fields are also present) [11, 12, 13, 14, 15, 16, 17, 18]. More recently over two thousand such models have been built in this manner. These compactifications are known as Heterotic Line Bundle Models [19, 20, 21].

Given heterotic models with the correct gauge group and spectrum, an obvious next step is to compute Yukawa couplings. In supersymmetric theories, the physical Yukawa couplings contain two parts. The first part is determined in terms of a holomorphic function of the fields in the theory called the superpotential, while the second is a normalization factor depending upon a real function called the Kähler potential. The former is quasi-topological and can be computed algebraically [22, 23, 24, 27, 28, 29, 30, 33, 34, 35, 36] while computation of later is in general difficult [1]. This is because computation of the Kähler potential depends

[1] In special cases, this quantity has been worked out, for example in the standard embedding [37] and in the presence of "large" flux [38]. The other possible approach is using the mirror symmetry [39], in which the effective theory of a Calabi-Yau compactification can be determined by the mirrored orbifold compactification. The matter Kähler potential of orbifold compactification can be computed in [40, 41, 42, 43, 44]. This duality is well-understood for the standard embedding models [45, 46, 47]. However, although progress has been made in [48, 49, 50, 51], it has not been extended to the realistic models yet.

on the explicit expression for a specific metric on the Calabi-Yau manifold X and a specific connection on V. The partial differential equations (PDEs) that govern these quantities are exceptionally difficult to solve. The eventual computation of the normalizing factor for the Yukawa couplings is one of the key long-term motivations for the numerical methods in Calabi-Yau compactification that we will discuss.

Although model building has proven to be very successful in heterotic compactifications, the issue of "moduli stabilization" has proven more problematic. The issue can be described as follows. Mathematically, the moduli space of a compactification corresponds to the allowed deformations of the geometry that preserve the equations of motion in general, and supersymmetry in particular. These deformations give rise to fields in the low energy theory, called moduli, that correspond to flat directions in the four-dimensional potential. These fields are not observed in nature and they must therefore be given a mass in order to lift them from the low energy spectrum. Progress in this direction has been made in recent years, for example in the works in [52, 53, 54, 55, 56, 58, 59] which will be discussed to some extent in this thesis, but a supersymmetric compactification with all of the moduli stabilized appears difficult to achieve [54]. Recent progress in understanding one of the ingredients of the theory that is crucial for moduli stabilization [60] requires explicit knowledge of the gauge connection on V to be completely understood. Thus numerical methods in Calabi-Yau compactification are important in both model building and moduli stabilization, again motivating their study in this thesis.

1.2 Details of Heterotic Calabi-Yau Compactification

In the low-energy limit, $E_8 \times E_8$ heterotic string can be described by 10-dimensional $N = 1$ supergravity coupled to a 10-dimensional $E_8 \times E_8$ super Yang-Mills theory [6]. This theory

contains two multiplets, namely the gravity multiplet which consists of the metric g, the NS two-form B, the dilaton ϕ as well as their fermionic partners, the gravitino ψ and the dilatino λ, and an $E_8 \times E_8$ Yang-Mills multiplet with gauge field A and associated field strength $F = dA + A \wedge A$ as well as its superpartners, the gauginos χ. To first order in α', the bosonic part of the associated 10-dimensional action is given by [6]

$$S = \frac{1}{2\kappa_{10}} \int d^{10}x \sqrt{-g} e^{-2\phi} \left[(R + 4(\partial\phi)^2 - \frac{1}{2}H^2) - \frac{\alpha'}{4}(\mathrm{tr}F^2 - \mathrm{tr}R^2) \right] + O(\alpha'^2) \tag{1.1}$$

where κ_{10} is the ten-dimensional gravitational coupling constant and the three form H is

$$H = dB - \frac{\alpha'}{4} \left(\omega_{\mathrm{YM}} - \omega_{\mathrm{L}} \right) \ . \tag{1.2}$$

Here ω_{YM} and ω_{L} are the gauge and gravitational Chern-Simons forms, respectively,

$$\omega_{\mathrm{YM}} = \mathrm{tr}(A \wedge dA + \frac{2}{3} A \wedge A \wedge A) \ , \tag{1.3}$$

$$\omega_{\mathrm{L}} = \mathrm{tr}(\Theta \wedge d\Theta + \frac{2}{3} \Theta \wedge \Theta \wedge \Theta) \tag{1.4}$$

where Θ is the spin connection of X. Together with F and R, the three form H should satisfy the Bianchi identity given below

$$dH = \alpha' \left(\mathrm{tr}(R \wedge R) - \mathrm{tr}(F \wedge F) \right) \ . \tag{1.5}$$

To construct a supersymmetric vacuum, the variation of the fermionic fields

$$\delta\psi_A = \frac{1}{\kappa} D_A \eta + \frac{\kappa}{32 g^2 \phi} (\Gamma_A^{BCD} - 9\delta_A^B \Gamma^{CD}) \eta H_{BCD} + (\text{Fermi})^2 = 0 \ , \tag{1.6}$$

$$\delta\lambda = -\frac{1}{\sqrt{2}\phi} (\Gamma . \partial\phi)\eta + \frac{\kappa}{8\sqrt{2} g^2 \phi} \Gamma^{MNP} \eta H_{MNP} + (\text{Fermi})^2 = 0 \ , \tag{1.7}$$

$$\delta\chi = -\frac{1}{4g\sqrt{\phi}} \Gamma^{AB} F_{AB} \eta + (\text{Fermi})^2 = 0 \ , \tag{1.8}$$

should vanish in the background [6]. Here η is the Majorana-Weil spinor parameter for the supersymmetric variation and Γ^{AB} are the anti-symmetrizations of products of ten-dimensional Gamma matrices. More specifically, these equations should be solved, for the field values in vacuum, for four appropriate η's such as to preserve $N = 1$ supersymmetry in four dimensions.

If we consider compactifications that are a direct product of four-dimensional Minkowski space and a compact manifold X,

$$M_{10} = \mathbb{R}^{3,1} \times X \tag{1.9}$$

then the requirements of solving (1.6), (1.7), (1.8) and (1.9) leads us to a subset of the cases described by the Strominger system [7]. If we restrict ourselves further to solutions with

$$H = 0 \ , \quad \phi = \text{const} \tag{1.10}$$

then the situation becomes rather simple. With the condition (1.10) and (1.9), one can show that (1.6) becomes

$$D_a \nu = 0$$

where D_a is the covariant derivative on X and ν is the spinor supersymmetry parameter

associated to X arising from the decomposition of η under the factoring of the ten dimensional Lorentz group. We thus have that ν is covariantly constant spinor on X. This implies that the manifold has $SU(3)$ holonomy and a manifold with this property is called a Calabi-Yau three-fold [61, 62, 63, 64]. The equation (1.7) vanishes automatically. The equation (1.8) becomes

$$F_{ab} = F_{\bar{a}\bar{b}} = 0, \tag{1.11}$$

$$g^{\bar{b}a} F_{a\bar{b}} = 0. \tag{1.12}$$

These are the Hermitian Yang-Mills (HYM) equations and their solutions are called HYM connections [65, 66]. The solution of (1.11) and (1.12) are in one to one correspondence with vector bundles V which are holomorphic, poly-stable and slope-zero. We will discuss the meaning of these algebraic concepts in detail in the later Chapters[2].

Heterotic models also need to satisfy a consistency condition following from the Bianchi identity (1.5). The vector bundle V is often written as $V = V_v \oplus V_h$ where the visible sector V_v and hidden sector V_h vector bundles are associated to the two separate E_8 factors of the ten dimensional gauge group. In addition, heterotic vacua can have five-branes wrapping holomorphic two-cycles in X, with class $[W] \in H_2(X, \mathbb{Z})$, and still preserve supersymmetry. Given that $c_1(TX) = c_1(V_v) = c_1(V_h) = 0$, the integrability condition associated to (1.5) can then be written as,

$$c_2(TX) - c_2(V_v) - c_2(V_h) = [W] \ . \tag{1.13}$$

The quantities appearing above are Chern classes, topological properties of the bundles that

[2]For the reader who is unfamiliar with mathematical concepts which appear in this introduction, such as stability, Chern-classes and cohomology groups, review material for much of the required technology will be provided in Chapters 2 and 4. If the reader wishes to ignore such technicalities it is hoped that they can still glean an overview of the discussion in this introduction in the absence of such details.

are associated to the construction. For now it is enough to note that (1.13) represents a topological constraint on the ingredients of the compactification, X and V.

1.2.1 Model Building

In this subsection, we will describe in more detail how the four-dimensional physics, the matter sector in particular, is derived from the heterotic Calabi-Yau compactification. We will take one of the E_8 factors as visible sector and study the model building there. The other E_8 factor will work as the hidden sector which is useful for anomaly cancellation, moduli stabilization and supersymmetry breaking. Model building in Calabi-Yau compactification takes place in two stages. First, one uses a gauge bundle V to reduce E_8 to a GUT group. Second, Wilson lines are introduced to break the GUT symmetry to the Standard Model symmetry (plus possibly $U(1)$ factors) [6]. A complete heterotic string model must therefore be constructed using a Calabi-Yau manifold with non-vanishing fundamental group, so that non-trivial Wilson lines exist on X.

Let G be the structure group of V. Then the four-dimensional gauge group H in the visible sector is given by the commutant of G within E_8. All of the charged degrees of freedom that appear in ten-dimensions are charged under the adjoint, the 248 dimensional representation, of E_8. Therefore, in order to find the matter field representations that could possibly appear in four dimensions, we have to decompose the adjoint **248** of E_8 under $G \times H$, which is, in general, given by

$$\mathbf{248} \to (1, \mathrm{Ad}(H)) \oplus (\mathrm{Ad}(G), 1) \oplus \bigoplus_i (R_i, r_i) \tag{1.14}$$

where $\mathrm{Ad}(H)$ denotes the adjoint representation of H, $\mathrm{Ad}(G)$ that of G, and $\{(R_i, r_i)\}$ are a set of representation of G and H.

The above group-theoretic considerations tell us which matter field representations could possibly appear. To determine which representations will actually appear in the massless spectrum, and in what multiplicities, we must appeal to more detailed physics of the compactification. Let $A^{(6)}$ be the solution to the Hermitian Yang-Mills equations being considered on V. The scalar components of the four-dimensional matter fields C^I arise from fluctuations of the gauge field of the form

$$A = A^{(6)} + \nu_I C^I \ , \tag{1.15}$$

where ν_I are bundle-valued one-forms. It can be shown that the 4-dimensional field C^I is massless if and only if the associated ν_I is harmonic. Therefore, the number of supermultiplets in each representation r_i is given by $n_{r_i} = h^1(X, V_{R_i})$, where r_i, R_i are defined by the decomposition (1.14) and V_{R_i} is the corresponding associated bundle. The singlets under H appearing in (1.14) correspond to bundle moduli in the four dimensional theory. The above arguments show that there is no matter appearing in the $\mathrm{Ad}(H)$ representation because $h^1(X, \mathcal{O}) = 0$. However, this representation does appear in the low energy theory in the form of gauge bosons. The relevant cohomology groups, and hence the multiplicities of different low-energy representations for charged matter, can then be computed as summarized in Table 1.1. So far, we have discussed a theory with a GUT-type gauge group. This is typically constructed "upstairs" on a simply connected manifold X. In order to break the GUT group to the standard-model group, we require a freely-acting symmetry Γ on the Calabi-Yau manifold X. The vector bundle V should descend to the quotient Calabi-Yau X/Γ, that is, it should have a Γ-equivariant structure. "Downstairs," on the manifold X/Γ, we then add a Wilson line, defined by a representation W of Γ into the GUT group.

The downstairs spectrum can be computed in a group-theoretical fashion from the upstairs spectrum. Consider a certain type of upstairs multiplet with associated bundle K. Because of the Γ-equivariant structure of V, the cohomology $H^1(X, K)$, associated to the upstairs

$G \times H$	Breaking Pattern for Adjoint Representation	Particle Spectrum
$\mathrm{SU}(3) \times \mathrm{E}_6$	$(\mathbf{1},\mathbf{78}) \oplus (\mathbf{3},\mathbf{27}) \oplus (\overline{\mathbf{3}},\overline{\mathbf{27}}) \oplus (\mathbf{8},\mathbf{1})$	$n_{27} = h^1(V)$ $n_{\overline{27}} = h^1(V^\vee) = h^2(V)$ $n_1 = h^1(V \otimes V^\vee)$
$\mathrm{SU}(4) \times \mathrm{SO}(10)$	$(\mathbf{1},\mathbf{45}) \oplus (\mathbf{4},\mathbf{16}) \oplus (\overline{\mathbf{4}},\overline{\mathbf{16}}) \oplus (\mathbf{6},\mathbf{10}) \oplus (\mathbf{15},\mathbf{1})$	$n_{16} = h^1(V)$ $n_{\overline{16}} = h^1(V^\vee) = h^2(V)$ $n_{10} = h^1(\wedge^2 V)$ $n_1 = h^1(V \otimes V^\vee)$
$\mathrm{SU}(5) \times \mathrm{SU}(5)$	$(\mathbf{1},\mathbf{24}) \oplus (\mathbf{5},\mathbf{10}) \oplus (\overline{\mathbf{5}},\overline{\mathbf{10}}) \oplus (\mathbf{10},\overline{\mathbf{5}}) \oplus (\overline{\mathbf{10}},\mathbf{5}) \oplus (\mathbf{24},\mathbf{1})$	$n_{10} = h^1(V)$ $n_{\overline{10}} = h^1(V^\vee) = h^2(V)$ $n_5 = h^1(\wedge^2 V^\vee)$ $n_{\overline{5}} = h^1(\wedge^2 V)$ $n_1 = h^1(V \otimes V^\vee)$

Table 1.1: *A vector bundle V with structure group G can break the E_8 gauge group into a GUT group H. The representations after this breaking are found from the branching of the* **248** *adjoint of E_8 under $G \times H$ and the spectrum is obtained by computing the indicated bundle cohomology groups (see for example [67, 68]).*

multiplet, becomes a Γ-representation. Each potential downstairs multiplet, ψ, acquires an induced Γ-representation denoted χ_ψ which is determined by the Wilson line and its hypercharge. To calculate the spectrum of a certain type, ψ, of downstairs multiplet contained in $H^1(X,K)$ we should determine the Γ-singlet part of $H^1(X,K) \otimes \chi_\psi$ [17, 20, 33]. It should be noted that only some of the degrees of freedom in the four dimensional theory associated to X will appear in that associated to the quotient. Indeed, the chiral index can be written as an integral and hence will divide by the group order in transitioning between these two cases. Therefore, to obtain three net-generations of quarks and leptons, we must have

$$-\frac{1}{2}\int_X c_3(V) = h^1(X,V) - h^2(X,V) = 3|\Gamma| \ , \tag{1.16}$$

where $|\Gamma|$ is the order of the discrete group Γ, with which we have quotiented X.

Once a model with the MSSM spectrum has been obtained, a natural next structure to

study is the Yukawa couplings. According to Table 1.1, if a matter multiplet transforms as a representation r_i under H, then the associated vector bundle V_{R_i} is that paired with the representation R_i of G. Consider three representations (R_i, r_i) with $i = 1, 2, 3$ such that $R_1 \otimes R_2 \otimes R_3$ contains a singlet. Three matter fields in these representations are associated with harmonic bundle-valued (0,1)-forms $\nu_i \in H^1(X, V_{R_i})$. Then, the associated holomorphic Yukawa couplings can be computed with

$$\lambda(\nu_1, \nu_2, \nu_3) = \int_X \Omega \wedge \mathrm{tr}(\nu_1 \wedge \nu_2 \wedge \nu_3) \ , \tag{1.17}$$

where Ω is the holomorphic $(3, 0)$ form on X. It can be shown that (1.17) is be evaluated using any choice of representatives in $H^1(X, V_{R_i})$. This property simplifies the computation a lot and (1.17) can be computed in many cases.

However, the holomorphic Yukawa couplings (1.17) are not what we measure in experiment. To obtain the physical Yukawa couplings, we have to canonically normalize the associated matter fields. This requires knowledge of the matter field Kähler metric

$$G_{I\bar{J}} = \frac{1}{2V} \int_X \nu_I \wedge \bar{\star}_V(\nu_J) \ , \tag{1.18}$$

where $\bar{\star}_V$ refers to a Hodge dual combined with a complex conjugation and an action of the hermitian bundle metric on V. Unlike the holomorphic Yukawa coupling, this object is not quasi-topological. Thus, to compute it, we have to use the harmonic forms in $H^1(X, V_{R_i})$. This, and evaluation of the expression (1.18), requires explicit knowledge of the metric on the Calabi-Yau three-fold which solves the string theory equations of motion. The metric in question is not known analytically, and thus this forms one of our main motivations to introduce numerical algorithms in the subject of Calabi-Yau compactification.

1.2.2 Moduli Stabilization

The need for moduli stabilization is a problem for almost all theories arising from compactification, and dimensional reduction of heterotic string theory on Calabi-Yau manifolds is no exception. Fields, called moduli, appear in the four dimensional theory which correspond to certain possible deformations of X and V. These moduli are massless and indeed are associated with flat directions of the potential. However, these degrees of freedom are not observed in experiment. What is more, if their expectation values were changing over time then quantities such as gauge couplings which depend on them would vary in unobserved ways. Thus, the moduli should be given a mass, or stabilized, in the 4-dimensional theory. For Calabi-Yau compactifications of heterotic theories, the moduli are $h^{2,1}(X)$ complex structure moduli, $h^{1,1}(X)$ Kähler moduli, $h^1(X, V \otimes V^*)$ bundle moduli and the dilaton ϕ. There are a variety of mechanisms that have been discussed in the literature to stabilize various subsets of these moduli. We will give two examples of such effects here, that will be of relevance elsewhere in this thesis, and another will be discussed in Chapter 5.

As was stated in (1.11) and (1.12), to preserve the supersymmetry, the vector bundle V should be holomorphic, slope zero and poly-stable. Even these basic properties can lead to the stabilization of some moduli [52, 53, 57, 58, 59]. With the help of the Bianchi identity (1.5), pieces of the ten-dimensional action (1.1) can be written as

$$S_{partial} \sim \int_X \sqrt{-g} \left\{ (-\frac{1}{2} \operatorname{tr}(F_{a\bar{b}} g^{a\bar{b}})^2 + \operatorname{tr}(F_{ab} F_{\bar{a}\bar{b}} g^{a\bar{a}} g^{b\bar{b}}) \right\}. \tag{1.19}$$

This term is a positive semi-definite contribution to the 4-dimensional potential. It vanishes when the HYM equations are satisfied. However, if, due to some fluctuations of the moduli, HYM equations fail to be satisfied, then this potential is non-trivial and the fluctuations of the moduli along these directions are stabilized. We will now describe this in more detail.

Let us start by considering an effect that arises from asking that $F_{ab} = 0$ be preserved under moduli variations so that the second potential term in (1.19) is minimized [52, 53]. We begin with a supersymmetric background with complex structure tensor $\zeta^{(0)}$ and gauge connection $A^{(0)}$. Consider the following deformations of the complex structure and connection:

$$\zeta = \zeta^{(0)} + i v_I \delta\mathfrak{z}^I \ , \tag{1.20}$$

$$A_a = A_a^{(0)} + \delta A_a \tag{1.21}$$

where v_I are a harmonic basis of $H^1(X, TX)$ and $\delta\mathfrak{z}^I$ are the deformation of complex structure moduli. Substituting these varied quantities into the equation $F_{ab} = 0$ and working to linear order in the variations one arrives at the following expression that the fluctuations must obey to stay in vacuum [52, 53],

$$\delta\mathfrak{z}^I v^c_{I[\bar{a}} F^{(0)}_{|c|\bar{b}]} + 2 D^{(0)}_{[\bar{a}} \delta A_{\bar{b}]} = 0 \ . \tag{1.22}$$

Here, $D^{(0)}_{\bar{a}}$ is the gauge covariant derivative associated to $A^{(0)}_{\bar{a}}$. This result tells us that complex structure deformations $\delta\mathfrak{z}^I$, for which there exists δA satisfying (1.22), will be modului. However, if for some deformations $\delta\mathfrak{z}^I$ no δA exists which obeys (1.22), then those complex structure deformations are stabilized. Geometrically, this corresponds to the bundle V not being able to adjust to remain holomorphic when the complex structure tensor of the base is varied in such a manner.

The above discussion has an equivalent description in terms of Atiyah classes. Using such a formulation it is straightforward to see that for a given bundle V, at most $h^2(X, V \otimes V^*)$ complex structure moduli can be fixed. From a four-dimensional perspective, this effect can sometimes be phrased in terms of F-term constraints arising from a Gukov-Vafa-Witten superpotential [69].

Next, let us consider an effect, arising from the first term in (1.19), that results in stabilization of Kähler moduli. For vacua with $h^{(1,1)}(X) \geq 2$, the combined Kähler and vector bundle moduli space generically decomposes into supersymmetric regions where equation (1.12) is satisfied and regions where it is not; that is, $\mathcal{N} = 1$ supersymmetric and non-supersymmetric regions respectively. These are separated by "walls of stability," where equation (1.12) and, hence, supersymmetry continue to be satisfied, but where the bundle must decompose into a direct sum of smaller pieces $V = \bigoplus_\alpha U_\alpha$ in order to achieve this. This splitting causes additional Green-Schwarz anomalous $U(1)$ factors to appear in the low energy gauge group. All the matter fields in the theory, which includes new degrees of freedom that arise when the bundle splits, carry a charge under the additional $U(1)$ symmetries. There are D-terms associated to the extra $U(1)$ factors which take the following form [35, 57, 58, 59]

$$D_\alpha^{U(1)} = f_\alpha - \sum_{I\bar{J}} Q_I^L G_{I\bar{J}} C^I \bar{C}^{\bar{J}} \tag{1.23}$$

where Q_α^I are the charges of the matter fields C_I, $G_{I\bar{J}}$ is the positive-definite matter field Kähler metric and the Fayet-Iliopoulos (FI) term f_α is given (to lowest order in α') by

$$f_\alpha = \frac{\mu(U_\alpha)}{\mathcal{V}} \, . \tag{1.24}$$

Here $\mu(U_\alpha)$ is the slope of the bundle factor U_α and $\mathcal{V}$ is the volume of the Calabi-Yau manifold expressed in terms of Kähler moduli. The slope, and so the FI term, vanishes on the stability wall and is positive or negative on either side of it. Thus, if in a given theory all of the matter fields have zero charge under this $U(1)$, then (1.23) shows that the Kähler moduli would be forced to lie on the locus of the stability wall. Some of the Kähler moduli are stabilized. Geometrically this corresponds to a poly-stable bundle that becomes unstable on either side of that locus. At higher orders this effect receives modifications which includes

the dilaton as well as the Kähler moduli.

Using the mechanisms discussed above, it has been argued that all but one linear combination of the dilaton, complex structure and Kähler moduli can be stabilized [54]. The remaining linear combination, together with the vector bundle moduli can potentially be stabilized by other effects. There are several ongoing attempts using non-perturbative contributions to the superpotential such as gaugino condensation and membrane instantons [54, 70, 71, 72, 73, 74, 75, 76, 77, 78, 79, 80]. Additional ingredients for the puzzle of moduli stabilization, involving the vacuum value of holomorphic Chern-Simons invariant contributions to the superpotential have recently been highlighted [60, 81, 82, 83, 84]. We will discuss this further in Chapter 6.

The rest of this thesis is structured as follows. In Chapter 2 we provide some introductory material on the geometry of Calabi-Yau manifolds and describe how numerical techniques can be used to compute Ricci flat metrics on them. In Chapter 3, based upon our paper [85], we describe how these techniques can be used to check the validity of effective theories in string compactifications. In Chapter 4 we give an introduction to the geometry of holomorphic vector bundles and numerical techniques for computing Hermitian-Yang-Mills connections on them. In Chapter 5, which is based upon work to appear in a forthcoming publication, we present an application of these techniques of direct relevance to the subject of moduli stabilization. Finally in Chapter 6 we briefly summarize and conclude. It should be noted that, while Chapters 2 and 4 are largely review material they do contain some new results. In particular, all plots shown were obtained with code written by the author, and Chapter 4 contains an analysis of a bundle with structure qualitatively different to any that has appeared in the literature to date.

Chapter 2

Numerical Metrics

As we have seen in the introduction, one way in which to preserve supersymmetry in the four-dimensional effective field theory associated to a compactification of the heterotic string is to take the internal space to be a compact Kähler manifold with $SU(3)$ holonomy [10]. Such spaces are called Calabi-Yau manifolds, and they, and Ricci-flat metrics on them, have important applications in string theory model building. In this chapter, we will review the definition and proprieties of Calabi-Yau manifolds, the Ricci-flat metrics, and how to compute them with numerical algorithms.

2.1 Calabi-Yau Manifolds

An n dimensional Calabi-Yau manifold (Calabi-Yau n-fold) X is a Kähler manifold satisfying one of the following equivalent conditions: [86]

1. $\mathrm{Hol}(g) = SU(n)$ (or $\mathrm{Hol}(g) \subseteq SU(n)$)
2. The first Chern class vanishes, $c_1(X) = 0$,
3. The Ricci form vanishes,
4. The canonical bundle is trivial,
5. X admits a globally defined and nowhere vanishing holomorphic n-form.

These properties impose strong constraints on the topology and geometry of Calabi-Yau manifolds which will be discussed in the rest of this section.

2.1.1 Hodge Numbers

One feature that can distinguish Calabi-Yau manifolds topologically is their cohomology[1]. On a compact Kähler manifold, the de Rahm cohomology can be decomposed according to its holomorphic and anti-holomorphic index structure as

$$H^k(X,C) = \bigoplus_{k=p+q} H^{p,q}(X), \quad k = 0, \ldots, n \; . \tag{2.1}$$

The dimension of $H^{p,q}(X)$ is called a Hodge number, denoted by $h^{p,q}$, and can be organized in the form of Hodge diamond as we will show shortly. Not all of these Hodge numbers are independent: there are symmetries between them. For a Calabi-Yau manifold, the symmetries are [86]

1. The complex conjugation duality $h^{p,q} = h^{q,p}$.

2. The Hodge star duality $h^{p,q} = h^{3-q,3-p}$.

3. The holomorphic duality $h^{0,q} = h^{0,3-q}$. Given a $(0,q)$ cohomology class a, there is a unique $(0,3-q)$ cohomology class b such that $\int_M a \wedge b \wedge \Omega = 1$ with Ω the nowhere vanishing holomorphic $(n,0)$ form.

Since the canonical bundle of a Calabi-Yau manifold is trivial, we have $h^{n,0} = 1$. If we focus on the compact and simply connected three-folds, then $h^{0,0} = 1$ and $h^{0,1} = h^{1,0} = 0$.

[1]The intersection form, Hodge numbers and second Pontryagin class suffice to distinguish homotopy types of Calabi-Yau three-folds as real six manifolds (Wall's theorem [89]).

The Hodge diamonds of Calabi-Yau one-fold, two-fold and three-fold are displayed in (2.2).

$$\begin{array}{ccccccc} & & & 1 & & & \\ & & 1 & & 1 & & \\ & 1 & & 0 & & 0 & \\ 1 & & 1 & & 1 & & 1 \\ & 1 & & 0 & & 0 & \\ & & 1 & & 1 & & \\ & & & 1 & & & \end{array} \qquad \begin{array}{ccccccc} & & & 1 & & & \\ & & 0 & & 0 & & \\ & 0 & & h^{1,1} & & 0 & \\ 1 & & h^{2,1} & & h^{2,1} & & 1 \\ & 0 & & h^{1,1} & & 0 & \\ & & 0 & & 0 & & \\ & & & 1 & & & \end{array} \tag{2.2}$$

From the Hodge diamonds above, we find that there is an unique one-fold (the torus T^2) and an unique two-fold (the $K3$ surface aside from T^4). While the situation is different for three-folds because they depend on two integers $h^{1,1}$ and $h^{2,1}$. It is known that $h^{1,1}$ and $h^{2,1}$ can not be arbitrary numbers [87], however, whether there are finite of them is still an open question (progress has made in [90, 91, 92, 93, 94, 95, 96, 97]).

As was mentioned before, $h^{1,1}$ and $h^{2,1}$ are the dimensions of $H^{1,1}(X)$ and $H^{2,1}(X)$. These cohomologies describe the possible deformations of the Kähler form and the complex structure tensor of X. By definition,

$$H^{p,q}(X) \simeq H^q(X, \wedge^p T^*X) \ , \tag{2.3}$$

so, we have

$$H^{1,1}(X) = H^1(M, T^*X), \qquad H^{2,1}(X) \simeq H^{1,2}(X) = H^2(X, T^*X) \simeq H^1(X, TX) \ . \tag{2.4}$$

In the above we have used the fact that a Calabi-Yau three-fold has trivial canonical bundle and, as such, $\wedge^3 TX = \mathcal{O}$. Another important topological invariant is the Euler characteristic

of a Calabi-Yau three-fold, defined as follows

$$\chi = \sum_{k=0}^{2n} (-1)^k b^k = 2(h^{1,1} - h^{2,1}) \ . \tag{2.5}$$

Since Calabi-Yau three-folds are the most interesting case for heterotic string compactifications, we will focus on them in the following discussion.

2.1.2 Ricci Flat Metrics

By Yau's theorem [63, 64], given a Calabi-Yau manifold with fixed complex structure and Kähler class, there exists an unique metric such that the Ricci tensor is zero. This metric is called the Ricci-flat metric. We have seen in the introduction that knowledge of this quantity can be important for addressing questions in string theory model building. Therefore, in this section, we will discuss it in detail.

A complex manifold is a topological space covered by complex coordinate charts such that the transition functions between overlapping charts are holomorphic. The complex structure is captured by a $(1,1)$ tensor ζ^a_b, satisfying [88]

- $\zeta^2 = -I$
- Vanishing Nijenhuis tensor $N(\zeta) = 0$ where,

$$N^k_{ab} = \zeta^d_a(\partial_d \zeta^c_b - \partial_b \zeta^c_d) - \zeta^d_b(\partial_d \zeta^c_a - \partial_a \zeta^c_d) \ . \tag{2.6}$$

The existence of a tensor satisfying these two conditions guarantees that we can find a complex chart such that the transition functions are holomorphic. A local holomorphic

coordinate system can be chosen such that the complex structure tensor is given by,

$$\zeta_b^a = i\delta_b^a, \qquad \zeta_{\bar{b}}^{\bar{a}} = -i\delta_{\bar{b}}^{\bar{a}} \ . \tag{2.7}$$

It is easy to check that ζ is invariant under a holomorphic change of coordinates.

The Kähler form J is a no-where vanishing real $(1,1)$ form on X. A complex manifold is Kähler if it admits a J that is closed, which then defines a cohomology class $[J] \in H^{1,1}(X)$. Each representative in the Kähler class defines an Hermitian metric called a Kähler metric [88]

$$J_{ab} = g_{ab} = J_{\bar{a}\bar{b}} = g_{\bar{a}\bar{b}} = 0, \quad J_{a\bar{b}} = -J_{\bar{a}b} = ig_{a\bar{b}}. \tag{2.8}$$

The Kähler metric is, of course, symmetric in its two indices

$$g_{ab} = g_{ba} = 0, \quad g_{\bar{a}\bar{b}} = g_{\bar{b}\bar{a}} = 0, \quad g_{a\bar{b}} = g_{\bar{b}a}. \tag{2.9}$$

The reality property of the Kähler form translates to an analogous property for the Kähler metric

$$\overline{g_{a\bar{b}}} = g_{\bar{a}b}, \quad \overline{g_{\bar{a}b}} = g_{a\bar{b}}. \tag{2.10}$$

Given the above discussion, we only need to study the $g_{a\bar{b}}$ components of the metric, and these form an Hermitian matrix

$$(g_{a\bar{b}})^+ = \overline{g_{b\bar{a}}} = g_{\bar{b}a} = g_{a\bar{b}}. \tag{2.11}$$

We will use this fact in our numerical computations in the next section. In terms of the

metric, the Kähler form is [88]

$$J = ig_{a\bar{b}}dz^a \otimes dz^{\bar{b}} - ig_{\bar{a}b}dz^{\bar{a}} \otimes dz^b = ig_{a\bar{b}}dz^a \wedge dz^{\bar{b}}.$$

On a Kähler manifold, because J is closed, i.e. $dJ = (\partial + \bar{\partial})J = 0$, it is possible to describe the Kähler metric in terms of Kähler potential K, at least locally [88].

$$g_{a\bar{b}} = \partial_a \partial_{\bar{b}} K.$$

The Kähler potential is a real scalar function and two K's give rise to the same metric it they differ by a Kähler transformation,

$$K' = K + F + \bar{F} \ ,$$

where F is a holomorphic function.

To give an example of a Kähler form that will be useful in future sections, consider complex projective space,

$$\mathbb{P}^n = \frac{\{\mathbf{C}^{n+1} \setminus \{0\}\}}{\sim}, \quad \mathbf{Z} \sim \lambda \mathbf{Z}', \quad \lambda \in \mathbf{C}^* \ , \tag{2.12}$$

where $\mathbf{Z} = [Z_0, Z_1, \ldots, Z_n]$ are the homogeneous coordinates of $\mathbb{P}^n$. In the open patch U_A defined by $Z_A \neq 0$, part of the standard open cover of $\mathbb{P}^n$, the affine coordinates are $\{z_\alpha\} = Z_\alpha / Z_A$. There is a natural metric on $\mathbb{P}^n$ called the Fubini-Study metric. Its Kähler potential is [88]

$$K = \ln Z_A \bar{Z}^A \tag{2.13}$$

in terms of homogeneous coordinates. On a patch U_A, it is

$$K = \ln(1 + z_\alpha \bar{z}^{\bar{\alpha}}) = \ln(1 + \delta_{\alpha\bar{\beta}} z^\alpha \bar{z}^{\bar{\beta}})$$

and the corresponding metric is given by

$$g_{\alpha\bar{\beta}} = \frac{(1 + |\mathbf{z}|^2)\delta_{\alpha\bar{\beta}} - \bar{z}_\alpha z_\beta}{(1 + |\mathbf{z}|^2)^2}. \tag{2.14}$$

Here $|\mathbf{z}|^2 = z_\alpha \bar{z}^\alpha$.

Given a Kähler metric $g_{i\bar{j}}$, we can compute the Levi-Civita connection. The only non-vanishing components of the Christoffel symbols are [88]

$$\Gamma^a_{bc} = g^{a\bar{d}} \partial_b g_{\bar{d}c} \qquad \Gamma^{\bar{a}}_{\bar{b}\bar{c}} = \overline{\Gamma^a_{bc}}. \tag{2.15}$$

Given these, the Riemann tensor can be expressed as,

$$R^a_{b\bar{c}d} = \partial_{\bar{c}} \Gamma^a_{bd} = \partial_{\bar{c}} (g^{\bar{e}a} \partial_b g_{d\bar{e}}) \qquad R^{\bar{a}}_{\bar{b}c\bar{d}} = \overline{R^a_{b\bar{c}d}}, \tag{2.16}$$

where $g^{\bar{b}a} = (g_{a\bar{b}})^{-1}$ is the inverse of metric. Sometimes, it is convenient to work with it in following form

$$R_{\bar{a}b\bar{c}d} = g_{e\bar{a}} R^e_{b\bar{c}d}, \tag{2.17}$$

which makes the symmetries of this object explicit.

$$R_{\bar{a}b\bar{c}d} = R_{\bar{c}b\bar{a}d}, \quad R_{\bar{a}b\bar{c}d} = R_{\bar{a}d\bar{c}b}, \quad R_{\bar{a}b\bar{c}d} = R_{\bar{c}d\bar{a}b}. \tag{2.18}$$

Notice that the complex conjugate of the Riemann tensor is

$$(R_{\bar{a}b\bar{c}d})^* = R_{\bar{b}a\bar{d}c} \ . \tag{2.19}$$

The Ricci tensor is ,

$$R_{\bar{b}c} = -\partial_c \Gamma^{\bar{a}}_{\bar{b}\bar{a}}, \quad R_{\bar{b}c} = -R_{c\bar{b}} \ , \tag{2.20}$$

so that the Ricci form is simply [88]

$$R = iR_{a\bar{b}} dz^a \wedge d\bar{z}^{\bar{b}} \ . \tag{2.21}$$

The Ricci form defines a non-trivial element in the second cohomology of the manifold X,

$$c_1(M) = \left[\frac{R}{2\pi}\right] \in H^2(M, R) \ . \tag{2.22}$$

It was conjectured by E. Calabi [61, 62] and later proven by S.T. Yau [63, 64] that for a Kähler manifold with fixed complex structure and Kähler class, if $c_1(M) = 0$, there exists an unique Kähler metric such that,

$$R_{a\bar{b}} = \partial_a \bar{\partial}_{\bar{b}} \ln \det g_{a\bar{b}} = 0 \ . \tag{2.23}$$

Kähler manifolds with vanishing first Chern class are thus called Calabi-Yau manifolds and this unique metric is referred to as the Ricci-flat metric.

Unfortunately, Yau's proof is not constructive. To compute the Ricci-flat metric, we still need to solve (2.23), which is a nonlinear partial differential equation (PDE) and very difficult to solve analytically. It will be helpful to note for later sections of this thesis that, with the help of the nowhere vanishing holomorphic $(n, 0)$ form Ω, the Ricci-flat metric can be shown

to obey a different equation which is simpler to use in some numerical applications than (2.23). Consider the top forms

$$\mu_\Omega = (-i)^n \Omega \wedge \overline{\Omega} \quad , \quad \mu_J = \frac{J^n}{n!} \, . \tag{2.24}$$

Here, μ_Ω is constructed solely from Ω and as such depends only on the complex structure, and μ_ω is constructed from the Kähler form J. Since $h^{3,3} = 1$, these two top forms must be proportional and their ratio $\eta = \mu_\omega / \mu_\Omega$ is simply a function. It can be shown that when η is a constant, then the corresponding metric is the Ricci-flat one [63, 64]. It is often convenient to set this constant, which can be chosen simply by scaling the forms involved by constant factors, to be

$$\eta = \frac{\mu_\omega}{\mu_\Omega} = \langle \eta \rangle \, , \quad \langle \eta \rangle = \frac{\int_X \eta \, \mu_\Omega}{\int_X \mu_\Omega}. \tag{2.25}$$

Here $\langle \eta \rangle$ is the average of the ratio over the Calabi-Yau manifold. We will often use (2.25) rather than the nonlinear PDE (2.23) in the later chapters.

2.1.3 Complete Intersection Calabi-Yau Manifolds

Large numbers of Calabi-Yau three-folds have been constructed explicitly in the literature. The first large dataset, consisting of 7890 cases, was classified in [99, 100, 101, 102, 103, 104, 105]. These examples, where the Calabi-Yau three-fold is constructed as a complete intersection of hypersurfaces in products of complex projective spaces, are called the complete intersection Calabi-Yau manifolds (CICYs). Other classes exist, with the largest dataset of smooth, compact Calabi-Yau three-folds consisting of the hypersurfaces in ambient toric four-folds which was constructed in [106, 107, 108]. This class leads to a data set of more than 473800776 manifolds. We will focus on the CICYs in this thesis. This is because the construction is more straightforward than the toric hypersurface case, where singular

ambient spaces frequently arise. The CICYs will prove to be a rich enough construction to illustrate the physics we wish to study.

CICYs can be described as intersections of the zero loci of K polynomials $\{p_j\}_{j=1,\ldots,K}$ in an ambient space $A = \mathbb{P}^{n_1} \times \ldots \times \mathbb{P}^{n_m}$ given by a product of m ordinary projective spaces with dimensions n_r. This definition can be expressed in terms of a $m \times K$ called configuration matrix [98, 99, 100].

$$X = \left[\begin{array}{c|cccc} \mathbb{P}^{n_1} & q_1^1 & q_2^1 & \ldots & q_K^1 \\ \mathbb{P}^{n_2} & q_1^2 & q_2^2 & \ldots & q_K^2 \\ \vdots & \vdots & \vdots & \ddots & \vdots \\ \mathbb{P}^{n_m} & q_1^m & q_2^m & \ldots & q_K^m \end{array}\right]^{h^{1,1},h^{1,2}}_{\chi} \tag{2.26}$$

Here, each column gives the multi-degree of one of the defining polynomials, with the q_j^r being the degree of the homogeneous polynomial p_j in the coordinates of the factor $\mathbb{P}^{n_r}$ in A. The Calabi-Yau condition in this context is given by the following.

$$\sum_{j=1}^{K} q_j^r = n_r + 1 \ , \qquad \forall r = 1, \ldots, m.$$

If X is a three-fold, then we require

$$\sum_{r=1}^{m} n_r - K = 3 \ .$$

Let $J_r, r = 1, \ldots, m$ be the normalized Kähler form of $\mathbb{P}^{n_r}$, i.e.

$$\int_{P^{n_r}} J_r^{n_r} = 1 \ .$$

A CICY is called "favorable" if a basis for $H^{1,1}(X)$ descends from the Kähler forms of the

ambient space factors. Favorable CICYs have several nice properties, of which we will just mention two. First, at least in the simple cases that we will study, the Kähler cone, that is the set of allowed Kähler forms J on X, can be described by $\{J = t^r J_r \,|\, t^r \geq 0\}$, where the t^r are the Kähler moduli. Second, the set of all possible line bundles on X, the Picard group $\mathrm{Pic}(X)$, is isomorphic to $\mathbb{Z}^m$, so line bundles on X can be characterized by an integer vector $\mathbf{k} = (k^1, \ldots, k^m)$[2]. For line bundles over favorable CICYs these integers simply denote an expansion of the first Chern class in a basis of $(1,1)$ forms given by the pullback of the J_r to X under the embedding map (we denote these pullbacks by the same symbol where no confusion can arise).

$$c_1(\mathcal{O}(k^1, \ldots, k^m)) = k^r J_r \ .$$

The Chern classes of CICYs can be computed from the entries in the configuration matrix. The total Chern class is

$$c = c_1^r J_r + c_2^{rs} J_r J_s + c_3^{rst} J_r J_s J_t \ ,$$

where,

$$c_1^r = 0, \ c_{2r} = \frac{1}{2} d_{rst} \left[-\delta^{st}(n_r + 1) + \sum_{j=1}^{K} q_j^s q_j^t \right], \ c_3 = \frac{1}{3} d_{rst} \left[\delta^{rst}(n_r + 1) - \sum_{j=1}^{K} q_j^r q_j^s q_j^t \right] \ . \tag{2.27}$$

The triple intersection numbers d_{rst} of a favorable CICY X can simply be obtained by integration of wedge products of the forms J_r over X.

$$d_{rst} = \int_X J_r \wedge J_s \wedge J_t \ . \tag{2.28}$$

[2]Only a minimal amount of mathematical formalism involving holomorphic vector bundles is needed in this chapter, and thus we do not review this subject here. In later chapters we will extensively use such technology and thus a review of some basic material will be provided in Chapter 4.

The Euler number is,

$$\chi(X) = \int_X c_3(X) = d_{rst} c_3^{rst} \ , \tag{2.29}$$

which is equivalent to (2.5) by the Hirzebruch-Riemann-Roch theorem [87].

The simplest CICY is described as the vanishing locus of a degree $n+2$ polynomial, p, in $\mathbb{P}^{n+1}$, given by

$$X = \left[\mathbb{P}^{n+1} | n+2\right] \ . \tag{2.30}$$

The homogeneous coordinates of $\mathbb{P}^{n+1}$ are $\{Z_0, Z_1, \ldots, Z_n\}$, as introduced in (2.12). The most general defining polynomial is

$$p = c_i m_i(\mathbf{Z})$$

where $\{m_i(\mathbf{Z})\}$ is the set of all $n+2$ degree monomials and $\{c_i\}, c_i \in \mathbb{C}$ are the coefficients. Different choices for the constants $\{c_i\}$ correspond to different choices for the complex structure of the underlying Calabi-Yau manifold. However, not all choices of the $\{c_i\}$ give rise to distinct complex structures. If two choices of the coefficients can be related by a rescaling $Z_A = \lambda Z_A$ with $\lambda \in \mathbb{C}^*$ or by a general linear transformations $Z_A = M_{AB} z_B$ with $M_{ij} \in GL(n+1, \mathbb{C})$, then they correspond to the same complex structure. For this Calabi-Yau manifold (2.30), the complex structure moduli space consists of the coefficients that gives distinct complex structures of X [3].

As an example of such a manifold, which we will use in later chapters, let us consider the quintic Calabi-Yau three-fold. It is a hypersurface given by a degree 5 homogeneous

[3] This is not true in general and a full treatment can be found in [37].

polynomial in $\mathbb{P}^4$. The configuration matrix (2.26) is

$$X = \left[\mathbb{P}^4|5\right]^{1,101}_{-200} \tag{2.31}$$

with $h^{1,1} = 1$ and $h^{2,1} = 101$. Let the homogeneous coordinates of $\mathbb{P}^4$ be $\{z_a\}, a = 0, \ldots, 4$. The defining polynomial is $P = c_i m_i(z), i = 1, \ldots, 126$, where the m_i are the degree 5 monomials in the Z_A and the c_i's are corresponding coefficients. By the general linear transformations $M_{AB} \in GL(5, \mathbb{C})$ and the overall factor in the defining polynomial above, we get $126 - (25 - 1) - 1 = 101$ independent c_i's, which agrees with the Hodge number in (2.31). From (2.27), the Chern classes are given by,

$$c_1(X) = 0, \quad c_2(X) = 10, \quad c_3(X) = -40.$$

By (2.28) and (2.29), the intersection and Euler numbers are

$$d = 5, \quad \chi = -200$$

which agrees with the stated data in (2.31).

2.2 Numerical Integration over CICYs

In this section, we will discuss how to compute numerical integrals over Calabi-Yau manifolds. This will be an essential tool in all of the algorithms appearing in this thesis. The integrals we will consider take the form

$$I = \int_X f \mu_\Omega = \int_X f \Omega \wedge \bar{\Omega} \tag{2.32}$$

where f is an arbitrary function over X and μ_Ω, as a top form (2.24), takes the role of the measure. First, we will introduce the Monte-Carlo integration. Next, we will introduce a more advanced method called adaptive integration. For clarity of exposition, we will focus on the simplest CICY, which is the vanishing locus of a degree $n+2$ polynomial in $\mathbb{P}^{n+1}$ defined in (2.30). However, the following discussion can be generalized to the any CICY without too much effort.

The homogeneous coordinates of the ambient $\mathbb{P}^{n+1}$ are again denoted by $\{Z_A\}, A = 0, \ldots, n+1$. We will then break $\mathbb{P}^{n+1}$ up into $n+2$ polydiscs [109]. More precisely we write

$$\mathbb{P}^{n+1} = \bigcup_{A=0}^{N} D_A, \qquad D_A = \left\{ [z_0 : \cdots : z_{A-1} : z_{A+1} : \cdots : z_n] \;\middle|\; |z_j| \leq 1 \right\} \simeq D^{n+1}, \tag{2.33}$$

where the $z_\alpha = Z_\alpha / Z_A$ with $\alpha = 0, \ldots, n+1$, omitting $\alpha = A$, are the local affine coordinates of the polydiscs D_A. In other words, given a specified set of homogeneous coordinates we divide all of the homogeneous coordinates by that with the largest magnitude in order to get the affine coordinates (and the number 1) for that point on the polydisc where it lives. Note that a generic point in $\mathbb{P}^{n+1}$ lies in only one polydisc, the overlaps being a set of measure zero. In addition the affine coordinates on each polydisc vary over a finite range, with the modulus being constrained to be less than or equal to one. Given these two facts we can see that this partitioning of the manifold is well suited to numerical integration techniques. Let X_A be the restriction of D_A to X. Obviously, these X_A's then cover $X = \bigcup_{A=0}^{N} X_A$. On patch X_A, the coordinates z_α must obey the defining relation of the Calabi-Yau three-fold, expressed in suitable coordinates.

$$p(z_0, \ldots, z_{A-1}, z_{A+1}, \ldots, z_{n+1}) = 0 \; . \tag{2.34}$$

Solving this equation for one variable, which we will denote as z_δ, then leaves us with n

independent coordinates on each polydisc restricted to X, the correct number for a manifold of this dimension. The remaining independent coordinates on a given patch are then denoted by $\{z_i\}, i = 0, \ldots, n-1$.

The non-where vanishing holomorphic $(n, 0)$ form Ω is known analytically. Consider a $(n+1, 0)$ form $\tau = \sum_{A=0}^{n+1} dZ_0 \wedge \ldots \wedge Z_A \wedge \ldots \wedge dZ_{n+1}$ on $\mathbb{C}^{n+2}$. By dividing the defining relation p, we have a form τ/p, which is well-defined on $\mathbb{P}^{n+1}$ except the hypersurface $p = 0$. Now, define [99, 110]

$$\Omega = \int_{\gamma_p} \frac{\tau}{p},$$

where γ_p is a small loop around $p = 0$ in $\mathbb{P}^{n+1}$. We can see that Ω is a globally defined and nowhere vanishing holomorphic $(n, 0)$-form on $p = 0$. In a coordinate patch X_A, integrating along the loop γ_p by the residue theorem, we find

$$\Omega = p_\delta^{-1} \prod_{i=0}^{N-2} dz_i \ , \tag{2.35}$$

where p_δ (p_i) is derivative of p with respect to corresponding coordinate z_δ (z_i).

2.2.1 Monte-Carlo Integration

The idea of the Monte-Carlo integration is to approximate a definite integral by evaluating the integrand at a sample of randomly chosen points on the domain [111]. Let S be a sample containing n_s points. Then the integral (2.32) becomes

$$I \approx I_{n_s} = \frac{V}{n_s} \sum_{a=1}^{n_s} f(P_a) \tag{2.36}$$

where $P_a \in S$ is a random point and $V = \int_X \mu_\Omega$ is the volume of X. The statistical error of such an approximation is of order $1/\sqrt{n_s}$ times a quantity proportional to $\langle f \rangle$, the mean of the integrand in the sample. To reduce the error in this approximation, it is useful to sample points in a manner that is uniformly distributed according to the volume form μ_Ω of X (see for example [112]). In other words, in an open set $U \in X$, the number of sample points taken in that set should be proportional to $\int_U \mu_\Omega$.

Writing out the explicit expressions for $i^n \mu_\Omega$ given (2.35), the following is found

$$i^n \mu_\Omega = |p_\delta|^{-2} \prod_{i=0}^{n} dz_i \wedge \prod_{\bar{j}=0}^{n} d\bar{z}_{\bar{j}} \ . \tag{2.37}$$

This can be rewritten in terms of ambient space quantities in the following manner

$$i^n \mu_\Omega = \delta^2(p) \prod_{\alpha=0}^{n+1} dz_\alpha \wedge \prod_{\bar{\beta}=0}^{n+1} d\bar{z}_{\bar{\beta}} \ . \tag{2.38}$$

We can approximate this by spreading out the delta function with a small parameter ϵ as follows

$$i^n \mu_\Omega \approx \frac{1}{\epsilon^2} \Theta(\epsilon - |p|) \prod_{\alpha=0}^{N-1} dz_\alpha \wedge \prod_{\bar{\beta}=0}^{N-1} d\bar{z}_{\bar{\beta}} \tag{2.39}$$

so that the volume form now has support on a slab of thickness ϵ about X. Given (2.39) one can simply do the following to obtain our set of points $\{P_a \in X_A\}_{a=1}^N$. First generate a sample set of n_s points on $\mathbb{P}^{n+2}$ evenly distributed in the coordinate measure. Second, discard any points for which $|p| > \epsilon$. Finally, for the points that remain, project them onto the Calabi-Yau manifold X using the Fubini-Study metric on $\mathbb{P}^{n+1}$. In this manner, we obtain a set of points distributed on X in a good approximation to the measure given by μ_Ω and the integral follows directly from (2.36).

2.2.2 Adaptive Integration

Adaptive integration is a combination of the higher-dimensional rectangle rule and the Monte-Carlo sampling [109]. The idea is to first change the domain from X to the ambient space $\mathbb{P}^{n+1}$. Then, a suitable cell decomposition of $\mathbb{P}^n$ is constructed with Monte-Carlo sampling. Finally, the integral I follows by the standard rectangle rule. Again, we will illustrate this algorithm with the example in (2.30).

First, consider a projection map $\pi : X \to \mathbb{P}^n$ from a n dimensional Calabi-Yau manifold to $\mathbb{P}^n$. Without loss of generality, we can choose $\{Z_0, Z_1, \ldots, Z_n\}$ to be the independent homogeneous coordinates of X and set $Z_\delta = Z_{n+1}$ to be the redundant coordinate. Then, the map is given by identifying the coordinates of $\mathbb{P}^n$ with the $n+1$ independent homogeneous coordinates. Locally any point of $\mathbb{P}^n$ has $n+2$ preimages, which implies that X is a $(n+2)$-sheeted cover of $\mathbb{P}^n$. Thus, we can use the Integration by Substitution to express the integral I in terms of an integral over $\mathbb{P}^n$

$$I = \int_X f(Z)\mu_\Omega = \int_{\mathbb{P}^n} \sum_{k=1}^{n+2} f\big(\pi_k^{-1}(Z)\big) w_k(Z), \quad w_k(Z) = \left|\frac{\partial \pi_k^{-1}}{\partial Z}\right| \mu_\Omega. \tag{2.40}$$

Here index $k = 1, \ldots, n+2$ sums over $n+2$ different sheets and $w_k(Z)$ are the weights defined by the product of the Jacobian of the coordinate transformation and the Calabi-Yau measure defined in (2.24). With the polydiscs introduced in (2.33), we can simplify the integral further as

$$I = \sum_{A=0}^{n+1} \int_{D^n} \sum_{k=1}^{n+2} f\big(\pi_k^{-1}(\mathbf{z})\big) \frac{1}{|p_\delta|^2} d^n z \wedge d^n \bar{z} \ . \tag{2.41}$$

Following the notation in (2.34), here $\mathbf{z} = \{z_i\}, i = 0, \ldots, n-1$ denotes the corresponding inhomogeneous coordinates on each patch and $d^n z = \prod_{i=0}^{n-1} dz_i$. Notice, the polydisc D^n is the Cartesian product of n individual disks D. Given (2.41) we will simply focus on the

integral over such polydiscs in later discussion.

To evaluate the integral over D^n, we need to decompose the polydisc into small cells and then apply the rectangle rule to each cell. Since the weight function (2.40) is not uniform on D^n, to reduce the numerical error, we generate these cells using an adaptive scheme. First, generate an uniform cell decomposition of D^n. To do that, we will study this problem on a single disk first. If the radius of D is R, then the disk can be divided into constant rings with width ΔR and there are $n_R = R/\Delta R$ such rings. Each ring can be divided further into constant annuli segments with central angles separated by $\Delta A_r, r = 1, \ldots, n_R$. To make sure all annuli having the same volume, we demand $\Delta A_r = \Delta A_1/(2r-1)$. In this way, we obtain a constant cell decomposition of D with volume $\Delta S = (A_1 \Delta R^2)/2$, which gives the desired cell decomposition for D^n by Cartesian product.

Next, we subdivide the initial cells adaptively according to the weight (2.40). For each cell c_l, one might define the weighted volume by $v_l = w(z_l)S_l$ where $w(z_l)$ is the weight evaluated at the middle point z_l of the cell and S_l is its Cartesian volume. Notice, however, that there are in general $(n+2)$ different weights $w_k(z_l), k = 1, \ldots, n+2$ at each point of $\mathbb{P}^n$. The definition above only works when X is a two-sheeted cover of $\mathbb{P}^n$ [109], because, in that case, one can show that the weights w_1 and w_2 are always equal to each other. To generalize this definition of weighted volume and associate a unique weight to each cell, one natural idea is to consider the mean of these weights $w(z_l) = \langle w_k(z_l) \rangle$. In what follows we will work with this choice most of the time. Sometimes, it is also useful to identify $w(z_l)$ with the maximum of them $w(z_l) = \max w_k(z_l)$. Compared with the first approach, this will lead to a finer cell decomposition of D^n. Now, we set an error bar e and compute the weighted volume v_l for each cell. If there are cells with $v_l > e$, then we recursively subdivide them by either dividing the radius or the central angle for the corresponding annuli and we can do this for each of disk in D^n. To reduce the error, the subdividing is determined randomly for each step in the

algorithm. By doing so, we can obtain a cell decomposition of D^n with $v_l < e$ for each cell.

In the end, the integral can be evaluated by the standard rectangle rule over the cells. The key step in the algorithm is how to subdivide the cells and generate a suitable cell decomposition. To see this process in detail, let's consider an example. Let X be a degree 3 hypersurface in $\mathbb{P}^2$ with complex structure

$$\begin{aligned} P &= 15Z_0^3 + 67Z_1Z_0^2 + 76Z_2Z_0^2 + 45Z_1^2Z_0 + 26Z_2^2Z_0 + 79Z_1Z_2Z_0 \\ &\quad +6Z_1^3 + 37Z_2^3 + 71Z_1Z_2^2 + 97Z_1^2Z_2 \ . \end{aligned} \tag{2.42}$$

We generate three samples with different e and plot the first coordinate (in the first patch) in Figure 2.1.

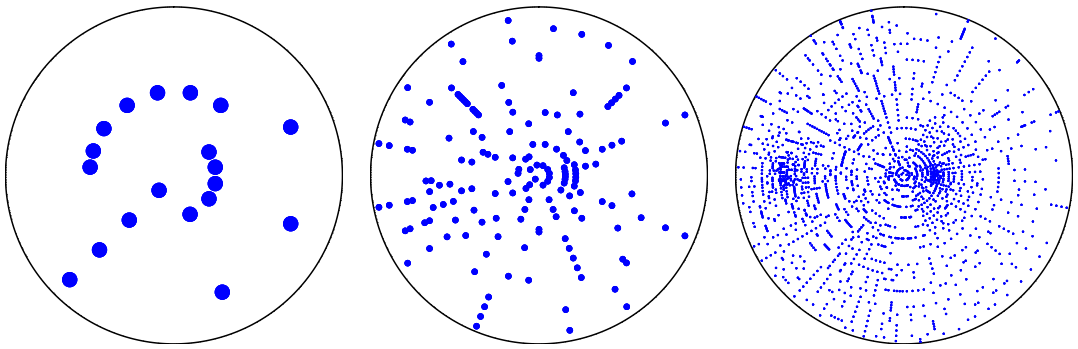

(a) $e = 5 \times 10^{-3}$ (b) $e = 5 \times 10^{-4}$ (c) $e = 5 \times 10^{-5}$

Figure 2.1: A cell decomposition with different error bars e. The manifold is a degree 3 hypersurface in $\mathbb{P}^2$ with complex structure given in (2.42). The results shown are for the patch where Z_0 is the largest coordinate.

2.3 Numerical Ricci-Flat Metrics

In this section, we will introduce some of the algorithms that are used in the literature to compute numerical Ricci-flat metrics on Calabi-Yau manifolds. We will first define the

algebraic metric, which is a useful ansatz for the metric on Kähler manifolds. This ansatz has parameters that can be tuned numerically to obtain the Ricci-flat object. We discuss two algorithms for performing this numerical tuning, Donaldson's algorithm [112, 113, 114, 115, 117, 118] and the minimization algorithm [119, 120]. The discussion will be illustrated with examples from the code that was written as part of the research work of this thesis.

2.3.1 Algebraic Metrics

Let X be a CICY with "polarization" given by $L \to X$, where L is an ample holomorphic line bundle [140]. By definition, there then exists some positive integer k_0, and, for every integer $k > k_0$, there is a projective embedding from X to $\mathbb{P}^{n_k-1}$ given by

$$i_k : \; X \to \mathbb{P}^{n_k-1}, \quad (x_0, \ldots, x_{d-1}) \mapsto \big[s_0(x) : \ldots : s_{n_k-1}(x)\big], \tag{2.43}$$

where x_i are coordinates on X, s_α is a basis of $H^0(X, L^k)$ and n_k is the dimension of $H^0(X, L^k)$. Given the polarization above, the Kähler class is fixed by $[J] = c_1(L)$ [87]. We saw in Section 2.1.2 that there exists a natural metric on complex projective spaces called the Fubini-Study metric. We remind the reader that the Kähler potential associated to this metric (2.13) was is given by

$$K_{FS} = \ln \sum_{\alpha=0}^{N} z_\alpha \bar{z}_\alpha \; . \tag{2.44}$$

The algebraic metric is associated to a simple generalization of this Kähler potential,

$$K_{h,k} = \frac{1}{k\pi} \ln \sum_{\alpha,\bar{\beta}=0}^{n_k-1} \bar{s}_{\bar{\beta}} h^{\bar{\beta}\alpha} s_\alpha, \tag{2.45}$$

where $h = h_{\alpha\bar{\beta}}$ is a constant Hermitian matrix. The corresponding metric is given by

$$g_{i\bar{j}} = \partial_i \bar{\partial}_{\bar{j}} K_{h,k}. \tag{2.46}$$

All of the metrics (2.45) corresponding to different Hermitian matrices are in the same Kähler class, as fixed by the polarization. In [121, 122] it was proven that, given a projection embedding (2.43), for a large enough integer k, any metric of X can be approximated by such algebraic metric with a suitably chosen h. Given this, our next task is to find the Hermitian matrix h that leads to the Ricci-flat metric on a Calabi-Yau manifold.

2.3.2 Donaldson's Algorithm

In this section, we will introduce Donaldson's Algorithm. The idea is that the Ricci-flat metric can be approximated by a certain "balanced metric," which can be computed by the iteration of an operator called the "T operator" [113]. We will first introduce the balanced metric and then discuss how to compute it with T operator iteration. In examples, we will make use of the adaptive numerical algorithm discussed in the proceeding section to perform the integrations over Calabi-Yau manifolds that will be required.

Balanced Metrics

The Kähler potential defined in (2.45) can be understood as giving a fiber metric of L^k. With it, or more precisely its inverse, we can define an inner product on $H^0(X, L^k)$ as follows

$$M(h)_{\alpha\bar{\beta}} = \left\langle \bar{s}_{\bar{\beta}} \middle| s_\alpha \right\rangle = i \frac{n_k}{\mathrm{Vol}_{CY}} \int_X \frac{s_\alpha \bar{s}_{\bar{\beta}}}{\sum_{\bar{\delta}\gamma} \bar{s}_{\bar{\delta}} h^{\bar{\delta}\gamma} s_\gamma} \mu_\Omega \,. \tag{2.47}$$

Here Vol_{CY} is the integral of $-i\mu_\Omega$ over X. As a function of the parameters h, this inner product $M(h)$ can again be used to define an metric on L^k via,

$$K_{M,k} = \frac{1}{k\pi} \ln \sum_{\alpha,\bar{\beta}=0}^{n_k-1} \bar{s}_{\bar{\beta}} M^{\bar{\beta}\alpha} s_\alpha = \ln ||s||^2_{M,k} \ . \tag{2.48}$$

We call this metric balanced, with parameters h^b_k when

$$M(h^b_k) = h^b_k \ . \tag{2.49}$$

In [113] it was shown that these balanced metrics have some special properties.

Theorem 2.1. *For each $k \geq 1$, there exists an unique balanced metric, with associated parameters h^b_k, of L^k. This gives a sequence of metrics $\{g^k_{i\bar{j}}\}$ on X,*

$$g^k_{i\bar{j}} = \partial_i \bar{\partial}_{\bar{j}} K_{h^b_k,k} \ . \tag{2.50}$$

For a Calabi-Yau manifold X [4] with given Kähler and complex structure moduli, this sequence approaches to the Ricci-flat metric as $k \to \infty$.

To find the parameters h^b_k corresponding to the balanced metric, we define the T operator

$$T(h)_{\alpha\bar{\beta}} = M(h)_{\alpha\bar{\beta}} = -i\frac{n_k}{\mathrm{Vol}_{CY}} \int_X \frac{s_\alpha \bar{s}_{\bar{\beta}}}{\sum_{\gamma\bar{\delta}} h^{\gamma\bar{\delta}} s_\gamma \bar{s}_{\bar{\delta}}} \mu_\Omega \ . \tag{2.51}$$

Notice that h^b_k is the fixed point of T operator. It can be shown [113] that iterating the T operator,

$$h^{i+1}_k = T(h^i_k), \tag{2.52}$$

[4] For a general Käher manifold X with $c_1(X)$ non-vanishing, the sequence will converge to the metric with constant curvature.

starting from an an arbitrary Hermitian matrix h_k^0, leads to a convergence towards the parameters h_k^b. Therefore, if we find fixed points under the iteration of the T operator for high enough k, we should obtain a good numerical approximation to the Ricci-flat metric on X.

To summarize, with Donaldson's algorithm as described here, we have a way to approximate the Ricci-flat metric on X in terms of the algebraic metric derived from the Kähler potential (2.45) constructed using the parameters h_k^b obtained by iterating the T operator.

At this point an obvious question is, if we follow the above procedure and obtain an approximation to the Ricci-flat metric on X at a given fixed k, how accurate is this result? In other words, how do we evaluate the error in the approximation to the metric?

For a given matrix of parameters h_k, the associated Kähler form ω_k is given by

$$\omega_k = \frac{i}{2}\bar{\partial}\partial K_{h,k} = \frac{i}{2\pi k}\bar{\partial}\partial \ln \sum_{\alpha,\bar{\beta}=0}^{n_k-1} h_k^{\alpha\bar{\beta}} s_\alpha \bar{s}_{\bar{\beta}}. \tag{2.53}$$

This can be used to define a top form ω_k^d on X. On the other hand, we gave another top form in (2.24). These two forms are the same everywhere (up to an overall constant) if the metric associated to (2.53) is Ricci-flat. This fact allows us to define an error function [113]

$$\sigma_k = \frac{-i}{\mathrm{Vol}_{CY}} \int_X \left| 1 - \frac{w_k^d/\mathrm{Vol}_k}{\Omega\wedge\bar{\Omega}/\mathrm{Vol}_{CY}} \right| \mu_\Omega, \tag{2.54}$$

where

$$\mathrm{Vol}_k = \frac{1}{d!}\int_X \omega_k^d \tag{2.55}$$

is the volume associated with ω_k. Clearly, this error function σ_k vanishes if and only if ω_k is the Kähler form associated to the Ricci-flat metric. Analytical estimation [131] shows that

this error scales as $\frac{1}{k^2}$ as $k \to \infty$.

To finish this subsection, we summarize Donaldson's algorithm below

1. Choose an ample line bundle L and twisting number k.
2. Compute the global sections $s_\alpha \in H^0(X, L^k)$.
3. Pick an initial Hermitian matrix h_0.
4. Compute the T operator (2.51) iteratively and find the parameters h_k^b of the balanced metric.
5. Evaluate the error function (2.54) with the resulting approximation to the Ricci-flat metric to check the accuracy of the result.

An example using the Donaldson algorithm

Let us consider the K3 surface: $X = [\mathbb{P}^3|4]$. The defining polynomial is

$$P = z_0^4 + z_1^4 + z_2^4 + z_3^4 - 2z_0z_1z_2z_3 \ . \tag{2.56}$$

We will choose the polarization $L = O(1)$. We compute the balanced metric from $k = 1, \ldots, 7$ by T operator iteration and then evaluate the error function (2.54) for each k. The integral is evaluated with the adaptive method discussed in Sec.2.2.2. The result is plotted in Figure 2.2.

The least-squares-fit curve is

$$E(k) \sim \frac{3.46}{k^2} + \frac{0.45}{k} \ . \tag{2.57}$$

We see that, with the increase of k, the error function does indeed decrease towards zero. This indicates that the balanced metric approaches the Kähler potential to the Ricci-flat

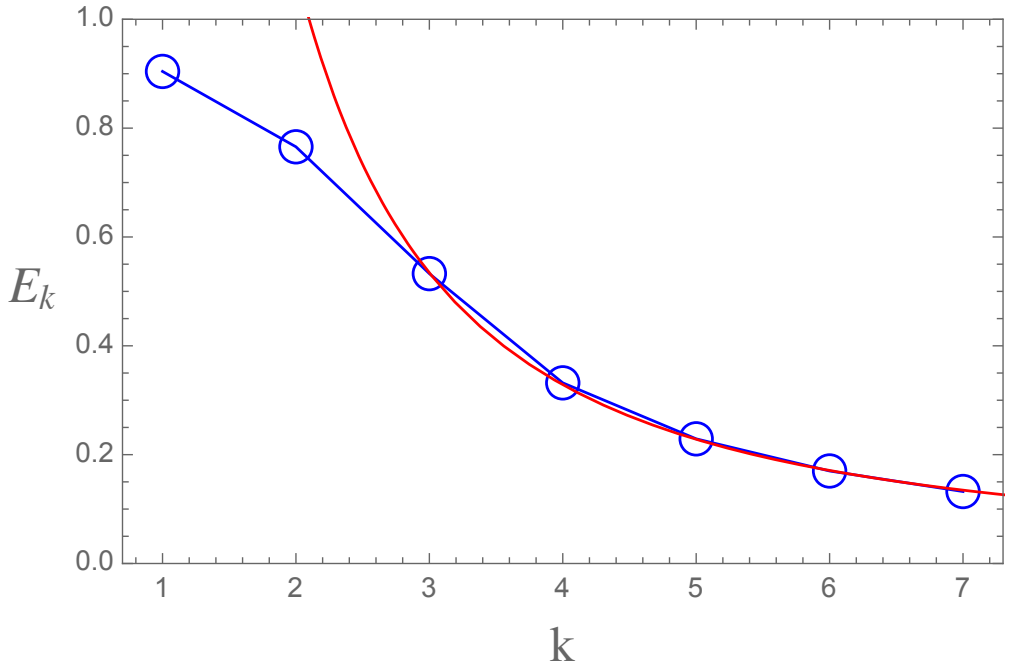

Figure 2.2: Error function of numeric metrics on a K3 surface.

metric in $O(k^{-2})$, which agrees with the above analysis. The integral was performed with the adaptive algorithm described above on a sample of 10^5 points for iteration of the T operator and 10^4 points for the computation of the error function.

2.3.3 A Minimization Algorithm

In this section, we will review the minimization algorithm developed by Headrick and Nassar [120]. In this approach, the Ricci-flat metric is approximated by the "optimal metric" which is the minimum of an appropriately constructed functional.

The functional defined in [120] is as follows

$$E(\omega) = \int_X (\eta - \langle\eta\rangle)^2 \mu_\Omega \, . \tag{2.58}$$

In this expressions μ_Ω was defined in (2.24) and η in (2.25). The idea is that, in many examples of interest, expressions for Ω are known analytically. One can then use the ansatz (2.45) to compute ω and thus η and $E(\omega)$. From there, one can perform a minimization on E, to find the choice of the parameters h that make that quantity as small as possible. In the limit $k \to \infty$ there is enough freedom in the Kähler potential ansatz to set E to zero. Given the positive semi-definite nature of the integrand in (2.58) this is a global minimum of the functional. At this minimum we have $\eta = \langle\eta\rangle$ and thus $\omega^n = (-i)^n n! \langle\eta\rangle \Omega \wedge \overline{\Omega}$. This is precisely the Monge-Ampere equation that should be solved in order to obtain a Ricci-flat metric. For any finite k we would not expect that the ansatz (2.45) embodies the flexibility necessary to achieve an exact vanishing of (2.58). Instead we obtain an approximation to the Ricci-flat Kähler potential at each finite k, called the optimal metric [120], and simply increase the value of k until a desired precision is reached.

Examples using the minimization algorithm

In this section we continue our review of the relevant pieces of [120], focussing on the setup for the particular examples we will be considering. As we have already stated, for simplicity, in this thesis we will discuss Calabi-Yau n-folds X that are constructed as simple hypersurfaces in products of projective spaces. It is certainly possible to consider examples which are more complex in their description by utilizing the same methods that we are describing here. Here, for clarity of exposition, we will specialize even further and consider the CICY defined in (2.30).

Over a space such as (2.30) a line bundle can be specified by its first Chern class, and thus the available L in constructing the ansatz (2.45) are simply given by $\mathcal{O}_X(k)$ where $c_1(\mathcal{O}_X(k)) = k\omega$. Given that the s_α are then simply elements of $H^0(X, \mathcal{O}(k))$, they are given by a basis of the set of all degree k polynomials in quotient ring associated to the defining

relation p. A basis of this space is easily obtained in terms of the ambient space coordinates Z_A. To obtain a metric from the Kähler potential (2.45), however, we must take derivatives with respect to coordinates on X itself. This is most easily achieved by using the following manipulations [120].

Taking the s_α to be a basis of representatives of the cohomology classes of the coordinate ring of the right degree, we can, given a Hermitian matrix h, write down the following metric on $\mathbb{P}^{n+1}$

$$\hat{g}_{\alpha\bar{\beta}} = \frac{1}{k\pi}\hat{\partial}_\alpha\hat{\partial}_{\bar{\beta}} \ln \sum_{\alpha,\bar{\beta}=0}^{n_k-1} h^{\alpha\bar{\beta}} s_\alpha \bar{s}_{\bar{\beta}} \ . \tag{2.59}$$

Here we have denoted ambient space quantities with hats to try and aid exposition. There is then a simple relationship between this quantity and the metric we desire on X, $g_{i\bar{j}} = \partial_i\bar{\partial}_{\bar{j}}K_{h,k}$. This is given by the following [123]

$$g_{i\bar{j}} = \hat{g}_{i\bar{j}} - \frac{p_i}{p_\delta}\hat{g}_{\delta\bar{j}} - \frac{\bar{p}_{\bar{j}}}{\bar{p}_{\bar{\delta}}}\hat{g}_{i\bar{\delta}} + \frac{p_i\bar{p}_{\bar{j}}}{|p_\delta|^2}\hat{g}_{\delta\bar{\delta}} \ . \tag{2.60}$$

A direct calculation using the standard expression for the holomorphic three form for such hypersurfaces (2.35) then shows that,

$$\eta = \frac{\mu_\omega}{\mu_\Omega} = \det(g_{i\bar{j}})|p_\delta|^2. \tag{2.61}$$

This expression can then be used to evaluate η for any given choice of the parameters h.

To compute the functional (2.58) requires the additional step of performing an integral over the Calabi-Yau manifold X. This integral can be computed as the sum of integrals over the individual X_A due to the fact that the overlap of these sets is of measure zero in the total

space

$$E = \sum_{A=0}^{N_s} E_A, \quad E_A = \int_{X_A} (\eta - 1)^2 \mu_\Omega \ . \tag{2.62}$$

We will use the Monte Carlo method introduced in Section 2.2.1 to compute each E_A above: the integrals E_A will be approximated with a sum over a randomly generated set of N points $\{P_a \in X_A\}_{a=1}^N$

$$E_A \approx \frac{V_A}{N} \sum_{a=1}^{N} (\eta(P_a) - 1)^2 \ . \tag{2.63}$$

Here $V_A = \int_{X_A} \mu_\Omega$ is the coordinate volume of the A'th restricted polydisc.

With all of the above pieces in place, we can compute the relevant integrals required to obtain the energy functional (2.58) as a function of the parameters h for fixed k. A Levenberg-Marquardt minimization procedure (for example) [124, 125] can then be run to find the values of the h's that correspond to the optimal metric [120]. This procedure can be repeated with increasing k until a metric with the desired degree of accuracy is found (for which the optimized value of the energy functional (2.58) is sufficiently small for example).

It should be mentioned that, practically, when k becomes large, the number of sections appearing in the metric ansatz, n_k, increases quickly and executing minimizing code can take a huge amount of computing resources. Since the parameters in the algebraic metric (2.45) h form a Hermitian matrix, the independent parameters is $N = n_k^2$. This is the number of parameters that must be minimized with respect to.

One way to ameliorate this problem is to consider Calabi-Yau manifolds which admit discrete symmetries. In this manner one can restrict attention to those sections s_α which are invariant with respect to a symmetry action on them induced from that of the base. It can be shown that [112], for given k, if the initial algebraic metric associated to h_0 is invariant under some discrete symmetry Γ, then the balanced metric is also invariant under Γ. Since, for high

enough k the balanced metric is a good approximation to the Kähler potential of the Ricci-flat metric, this too must be invariant under Γ. We are therefore justified in searching fora Γ invariant optimal metric by utilizing the minimization algorithm. In this way, the number of independent parameters in h is reduced dramatically to approximately $N_\Gamma \sim \frac{N}{|\Gamma|}$.

For example, if the complex structure is

$$P_{n-1}(\psi) = \sum_{i=0}^{n} Z_i^{n+1} - \psi(n+1)\prod_{i=0}^{n} Z_i, \tag{2.64}$$

then their exists a symmetry group Γ generated by permutations between $Z_i \leftrightarrow Z_j$, by multiplication by roots of unity $Z_i \to \exp(\frac{2\pi i}{n})Z_i$, and by complex conjugation $Z_i \leftrightarrow \bar{Z}_i$. The order of this symmetry group Γ is $|\Gamma| = 2(n+1)^{(n-1)}(n+1)!$ for generic values of ψ. This symmetry is enhanced even further at the point in moduli space corresponding to the Fermat type defining relation, $\psi = 0$, where $|\Gamma| = 2(n+1)^n(n+1)!$ [120]. For this case, we list the number of independent parameters for each k below:

k	1	2	3	4	5	6	7	8	9	10
N	5	15	35	70	126	210	330	495	715	1001
N_Γ	1	2	3	5	7	10	14	20	27	38

Finally, we can summarize the minimization algorithm as below, perhaps enhanced by the symmetry restrictions just described.

1. Choose a line bundle L and twisting number k.
2. Compute global sections $s_\alpha \in H^0(X, L^k)$.
3. Pick an initial Hermitian matrix h_0. For simplicity, and to preserve any discreet symmetries of X if they are being used, we always set h_0 to be associated to the restriction of the Fubini-Study metric of $\mathbb{P}^n$. This corresponds to taking h_0 to be the identity matrix.

4. Run Levenberg Marquardt algorithm to minimize Energy functional E (2.58). The minimized configuration gives the optimal metric.

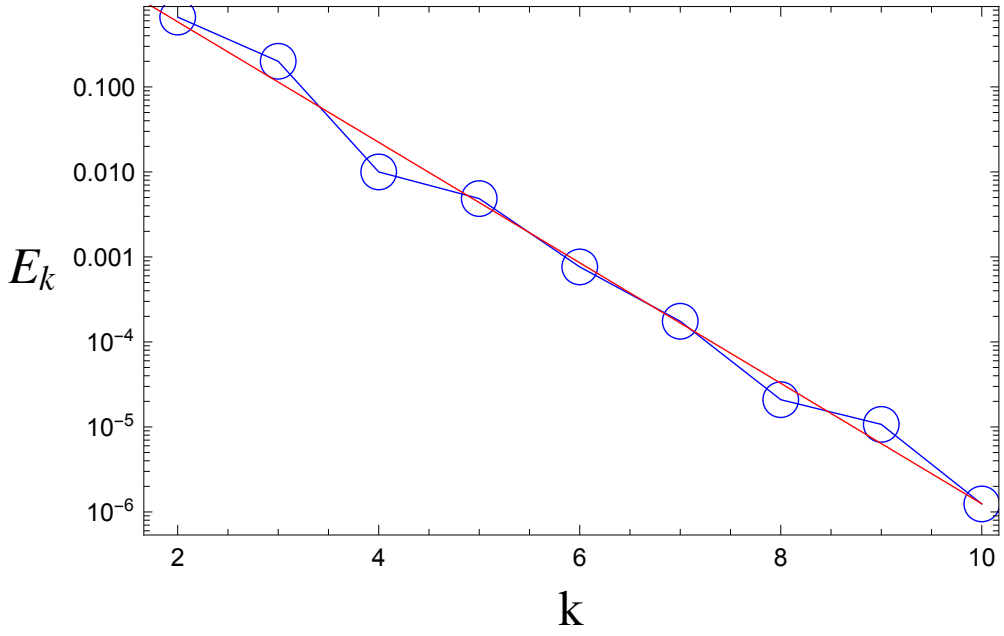

Figure 2.3: Error of numeric metric on Fermat quintic Calabi-Yau three-fold obtained with the minimization algorithm.

As an example of all of this, consider the Fermat quintic Calabi-Yau three-fold, (2.64) with $\psi = 0$ and $n = 4$. We computed the optimal metric from $k = 2$ to $k = 10$ on a sample with $n_s = 10^4$ points and $\epsilon = 0.02$. The error function for each metric is shown in the Figure 2.3, with a least-squares-fit curve given by,

$$E(k) \sim e^{2.72-1.63k}. \tag{2.65}$$

We see that, with increasing k, the error function is reduced to zero and the optimal metric approaches the Ricci-flat metric exponentially.

Chapter 3

Numeric Metrics and the Validity of Curvature Expansions

In this chapter, we will use the numerical Ricci-flat metric, together with the Monte-Carlo algorithm, to study the "large" curvature on the Calabi-Yau manifold, which determines the validity of the supergravity description of the heterotic string discussed in Chapter 1. This chapter is based on our published paper [85].

3.1 Introduction

Ricci-flat metrics on Calabi-Yau manifolds are central objects in the study of compactifications in many string theoretic settings [3, 6]. They frequently appear in a supergravity limit where curvatures are taken to be small with respect to the string scale and only a finite number of terms in an α' expansion have been kept. An assumption that is often made is that, if we are in a region of moduli space where the overall volume of the manifold is large and we are not near any singularities, then the values of curvature invariants on different points of the manifold will not become large and truncating the expansion at some finite order should be valid.

How do we know if this assumption is justified however? Could there be regions on the manifold where certain curvature invariants become large compared to the scale set by the

overall volume in a manner that one would not naively expect? There are some choices of moduli for which such an expansion clearly breaks down. For example, for Calabi-Yau manifolds constructed as complete intersections in some simple ambient space, it is often easy to compute loci in moduli space, such as a conifold locus [37, 126, 127, 128, 129, 130], where the variety becomes non-transverse. Near to such singular loci higher order curvature invariants will not be controlled by the scale set by the overall volume and one would expect the supergravity approximation to break down. Similar comments could be made in regions of parameter space where certain cycles become small but non-vanishing.

The general question that may arise, however, is somewhat more difficult to answer. Say that we have some description of a Calabi-Yau manifold as an algebraic variety with a specific choice of coefficients in the defining polynomial (perhaps with these having been determined by some moduli stabilization mechanism). How do we decide if the approximations made in truncating the α' expansion are valid in such a case? It is not clear, for example, if there could be regimes of moduli space corresponding to Calabi-Yau manifolds exhibiting regions of very high curvature which are nevertheless not near to any singularity. One might suspect that if the coefficients appearing in a defining relation are very large or very small that one might have an issue. More precisely, due to the overall scaling available in such defining relations, one might be concerned if large hierarchies in the sizes of coefficients that appeared were present. But how does one know for sure and what does one say if the coefficients are simply generic looking, seemingly innocuous, values? In this chapter we wish to show that modern numerical methods for determining Ricci-flat metrics on Calabi-Yau manifolds [109, 112, 113, 115, 116, 117, 119, 120, 131, 132] are a practical and efficient tool for deciding such questions in many cases.

The structure of the rest of this chapter is as follows. We will begin, in Section 3.2, with a review of the types of higher derivative corrections (coming from spacetime curvature)

that might appear in the low-energy effective action of string theories. We will also present our procedure for studying high curvature regions numerically and apply these methods explicitly to a number of concrete examples. In Section 3.3 we introduce some dimensionless curvature invariants and use them to study higher curvature invariants for families of Calabi-Yau manifolds. We demonstrate that we can reproduce expected hierarchies of curvature scales, associated to the presence of singularities, and describe how these methods can be used to address the issues described in this introduction. In Section 3.4 we briefly conclude and discuss possible future directions of research.

3.2 Curvature Invariants on Calabi-Yau Manifolds

In this section, we will first briefly review the low energy effective field theory appearing in heterotic compactifications and explain why high curvatures are cause for concern in using such technology. Then, we will introduce a Monte Carlo algorithm to find the high curvature regions and apply it to a variety of Calabi-Yau manifolds.

3.2.1 The Curvature Expansion in the Effective Action

As we discussed in the introduction, in considering Calabi-Yau compactification, the low energy physics is usually described using a finite number of terms in the effective action. This is valid if there are no large curvatures, compared to the string scale, in the spacetime manifold. For the $E_8 \times E_8$ heterotic string, the low-energy effective action (bosonic part) is

schematically given by the following [133, 134].

$$S = \frac{1}{2\kappa}\int d^{10}x(-G)^{1/2}e^{-2\phi}(R + 4(\partial\phi)^2 - \frac{1}{2}H^2 - \frac{\alpha'}{4}TrF^2 + \alpha' R^2 + (\alpha')^3 R^4 + (\alpha')^4 R^5 + \ldots) \,. \tag{3.1}$$

Here the first 'higher derivative correction' is R^2, by which we simply mean an invariant made out of a contraction of two copies of the Riemann tensor. Higher order corrections involving the other fields also appear. We will ignore these here and focus on terms built solely from the curvature. That these are small is therefore necessary, but not sufficient, for the effective action to be valid. The second order terms appearing in (3.1) are absent for type II string theories, whose first higher derivative correction starts from R^4 [135]. Nevertheless, a similar expansion does occur and thus the discussion of this chapter will be relevant in that context as well.

Let $r_c(X)$ be a function of position denoting the radius of curvature at points on the spacetime manifold X. Then higher order corrections (coming from the spacetime curvature) are small and can be ignored if [3]

$$\frac{l_s}{r_c(X)} \ll 1$$

for every point on the manifold X. In Calabi-Yau compactification, this implies that, compared with string scale, there is no high curvature regions on the Calabi-Yau manifold. Instead, if there exists a point with large curvature $l_s \sim r_c$, then there are infinite higher order terms in the effective action which should be included and the α' expansion breaks down. This is our motivation to study high curvature regions on Calabi-Yau manifolds.

We will now discuss the higher curvature terms $R^2, R^3, R^4, \ldots$ that we will consider. One initial point that should be mentioned is that frequently in discussions of (3.1) these are

obtained in terms of the spin connection, not the usual Levi-Civita connection in general relativity. However, when considering curvature scalars, we will briefly remind the reader that these two connections give the same set of possibilities. First, let's briefly review the construction of spin connection. Suppose X is a n dimensional spacetime X with metric g_{ab}. The vielbein $e^l_a(x)$ is a set of orthogonal spacetime vector fields that satisfy [6]

$$g_{ab} = e_a{}^l \eta_{lm} e_b{}^m \tag{3.2}$$

where η_{lm} is the Minkowski metric and l, m are spinor indices, which can be raised and lowered with η_{lm}. By definition, the inverse veilbein is

$$(e^a_l(x))^{-1} = e^l_a(x) \ . \tag{3.3}$$

Two vielbeins are equivalent if they are related by a Lorentz transformation [6]

$$\tilde{e}^l_a(x) = \Lambda^l_m(x) e^m_a(x) \tag{3.4}$$

where $\Lambda^l_m(x) \in SO(n)$. Let ω be the spin connection. The associated covariant derivative is given by

$$D_a V^l_b = \partial_a V^l_b + \omega_a{}^l{}_m V^m_b - \Gamma^c_{ba} V^l_c \tag{3.5}$$

where $V(x)$ is a vector field and Γ^c_{ba} is the Christoffel symbols. The torsion is

$$T^l_{ab} = D_a e^l_b - D_b e^l_a. \tag{3.6}$$

If we impose the torsion-free condition or the vielbein is covariantly constant

$$D_a e^l_b = 0, \tag{3.7}$$

then there is an unique spin connection given by [6]

$$\omega_a^{lm} = \frac{1}{2}e^{bl}(\partial_a e_b^m - \partial_b e_a^m) - \frac{1}{2}e^{bm}(\partial_a e_b^l - \partial_b e_a^l) - \frac{1}{2}e^{cl}e^{dm}(\partial_c e_{dn} - \partial_d e_{cn})e_a^n, \tag{3.8}$$

the indices a, b are anti-symmetric. The curvature tensor is

$$R^l_{abm} = (\partial_a \omega_b)^l_m - (\partial_b \omega_a)^l_m + [\omega_a, \omega_b]^l_m \ . \tag{3.9}$$

With the help of the vielbein, it can be related to Riemann tensor by [6]

$$R^l_{abm} = e^l_d e^c_m R^d_{abc} \ . \tag{3.10}$$

Now, it is easy to see that curvature scalars obtained from the curvature of the spin connection and Levi-Civita connection are the same. For example, the first order curvature scalar, i.e. the Ricci scalar is

$$R = g^{ab}R_{ablm}e^l_c e^m_d g^{cd} = g^{ab}R_{abcd}g^{cd} \ .$$

Similar analyses work for all other higher order scalars.

With this brief aside completed, we will consider possible curvature scalars on a Calabi-Yau manifold. By definition, these can be computed by the contractions between Riemann tensors and the Ricci-flat metric. For invariants involving a fixed number of derivatives, there is more than one way to contract these indices. Indeed, it is clear that, for an order n scalar quantity R^n, there is naively $2n!$ possible contractions. However, since there are symmetries between the indices of Riemann tensor, not all such contractions are independent. What is more, if we are working with Ricci-flat metric, the Ricci tensor vanishes. Therefore, many of the contractions leads to a vanishing scalar. With this understanding, the first thing to do is to find the curvature scalars that are non-vanishing and independent.

The possible first order curvature scalars are given by

$$R = R_{\bar{a}b\bar{c}d} g^{\bar{a}w(1)} g^{\bar{c}w(2)} \tag{3.11}$$

where $w \in S_2$ is a permutation of holomorphic index (b, d). Obviously, there are two possible contractions. These are related by symmetry and both of them lead to a vanishing scalar on the Calabi-Yau manifold. The second order curvature scalars are

$$R^2 = R_{\bar{a}_1 b_1 \bar{c}_1 d_1} R_{\bar{a}_2 b_2 \bar{c}_2 d_2} g^{\bar{a}_1 w(1)} g^{\bar{c}_1 w(2)} g^{\bar{a}_2 w(3)} g^{\bar{c}_2 w(4)} \tag{3.12}$$

where $w \in S_4$ is a permutation of holomorphic index (b_1, d_1, b_2, d_2). There are $4! = 24$ possible contractions while only one of them is non-vanishing and independent. The the non-trivial R^2 invariant can be represented by the permutation $(3, 4, 1, 2)$ in the above notation.

The third order curvature scalar is

$$R^3 = R_{\bar{a}_1 b_1 \bar{c}_1 d_1} R_{\bar{a}_2 b_2 \bar{c}_2 d_2} R_{\bar{a}_3 b_3 \bar{c}_3 d_3} g^{\bar{a}_1 w(1)} g^{\bar{c}_1 w(2)} g^{\bar{a}_2 w(3)} g^{\bar{c}_2 w(4)} g^{\bar{a}_3 w(5)} g^{\bar{c}_3 w(6)} \tag{3.13}$$

with $w \in S_6$ is a permutation of holomorphic index $(b_1, d_1, b_2, d_2, b_3, d_3)$. Now, there are $6! = 720$ contractions. After a combinatorial analysis, we find two independent non-trivial scalars given by

$$(5,\ 6,\ 1,\ 2,\ 3,\ 4) \quad (4,\ 6,\ 1,\ 5,\ 2,\ 3) \ .$$

For the fourth order curvature scalar, there are $8! = 40320$ contractions which, by a similar analysis, give 6 independent non-trivial scalars. In terms of the permutation of the holomorphic indices, they are expressed below

$$(3,\,4,\,1,\,5,\,7,\,8,\,2,\,6)\quad (3,\,4,\,5,\,6,\,7,\,8,\,1,\,2)\quad (3,\,4,\,1,\,2,\,7,\,8,\,5,\,6)$$
$$(3,\,5,\,1,\,7,\,2,\,8,\,4,\,6)\quad (3,\,5,\,1,\,7,\,4,\,8,\,2,\,6)\quad (3,\,4,\,5,\,7,\,1,\,8,\,2,\,6)\ .$$

The analysis becomes more and more complicated when the order n increases. Due to the computational limitations, we will stop here and only focus on the first four curvature scalars in later discussion. Although the Ricci scalar R is zero for the metric of interest on Calabi-Yau manifolds, the other curvature scalars are in general not. What is more, their values vary over the manifold. We will introduce a Monte-Carlo algorithm to study the maximum value that they take over a given Calabi-Yau manifold in the next section.

3.2.2 High Curvature Regions

In this section, we will present an algorithm to find high curvature regions on Calabi-Yau manifolds and then demonstrate its validity through different examples. In Chapter 2, we introduced Donaldson's algorithm and the minimization algorithm to compute the Ricci-flat metrics on Calabi-Yau manifolds. Since the Ricci-flat metrics obtained from minimization algorithm are more accurate, we will use them in the curvature computations of this section.

Once we have a numerical approximation to the Ricci-flat metric on a given Calabi-Yau manifold, we are ready to study the curvature scalars. To be specific, the different possibilities corresponding to R^2, R^3 and R^4 can be computed for any given point. However, what we are interested in is to check if there are high curvature regions on the manifold. We detail the algorithm for finding such regions below.

- Find a numerical approximation to the Ricci-flat metric with minimization algorithm, as described in the previous chapter. This metric should be computed for as high

a value of k as possible, and the error measures associated to the metric should be checked to determine its accuracy.

- Find a sample of n_R points on the Calabi-Yau manifold. Check that the Ricci-curvature is approximately zero on each of these points.

- Choose a number of derivatives n_d and compute all curvature invariants that can be formed at this order. We consider all curvature invariants rather than just those appearing in a given α' expansion in the interests of generality. In addition, a large curvature appearing in a specific invariant might be a cause for concern, even if that invariant is not the particular one that appears in a given theory. One would suspect that such structure might indicate that high curvatures will appear in the α' expansion at some order, even if it is somehow evaded at the level of the number of derivatives being considered.

- Evaluate these curvature invariants on the n_R sampled points and record the highest value they attain. Denote this maximal value by $R^m_{I\,\max}$ where $m = n_d/2$ denotes the power of curvature invariants under consideration and I runs over the different possible invariants. The index I will be dropped in the case of $m = 2$ where there is only a single non-vanishing independent invariant.

One might think that in choosing the sample points in the second step in the bulleted list above, an adaptive mesh type of selection technique should be used. While we have indeed implemented such a sampling method to ensure that we are not missing any structure, in the examples we have studied this has proven to be unnecessary. No further high curvature regions are seen in these manifolds upon utilizing such a technique beyond those already successfully detected by the point sampling method described in Section 2.2.1.

There are two main errors in our algorithm. The first one comes from the Ricci-flat metric

and it depends on the parameter k . From the analysis in Chapter 2 we know that, when k increases, the numerical curvature obtained converges to the "exact" curvature exponentially. We will see this convergence explicitly in concrete examples shortly. Therefore, if we work with a large enough k in the minimization algorithm, this error is small. The second error arises from the Monte-Carlo search. The curvature scalars found by our algorithm are large, but maybe not the very largest one for the given Calabi-Yau manifold. Therefore, our numerical results give a lower bounds on the size of the curvature invariants associated to the compactification.

In the rest of this section, we will apply the algorithm to the Calabi-Yau n-fold which is described as the vanishing locus of a degree $n+2$ polynomial, p, in $\mathbb{P}^{n+1}$, as in (2.30).

For the purposes of illustrating the methodology being proposed in this chapter, we simplify our numerical computations by working on Calabi-Yau manifolds with discrete symmetries of high degree. Two kinds of examples will be considered. The first one is the famous Fermat quintic and its generalization in different dimensions. The second one is given by a defining polynomial with two parameters. Compared to the Fermat quintic, this is a slightly more complicated example.

A first class of examples

We will begin by studying one parameter families of manifolds, in varying dimension, whose defining relation is of the form (2.64),

$$p_n(\psi) = \sum_{i=0}^{n+1} Z_i^{n+2} - (n+2)\psi \prod_{i=0}^{n+1} Z_i \ . \tag{3.14}$$

We will make use of the full symmetry group available, as discussed around (2.64).

We will focus on the $\psi = 0$ case here and leave the other cases to the next section. Using the minimization algorithm, it is possible to obtain Ricci-flat metrics on Calabi-Yau manifolds of various types to a high degree of accuracy. In Figure 3.1 we illustrate this, in the case of the Fermat quartic and quintic Calabi-Yau two and three-folds respectively, by plotting the value of the functional (2.58), as a measure of the deviation from Ricci-flatness, as a function of k (note that one of these plots is a repeat of Figure 2.3 presented here for ease of exposition). We will not show such plots for all of the examples presented in this chapter as the all look extremely similar to Figure 3.1, with exponential convergence of the energy functional to zero to a high degree of accuracy. For many of the examples considered in this chapter, the freely available code found here [136] could be used to obtain the desired results. We have written our own code as a complement to this work, however, which has been especially useful in studying cases not covered by [136] such as the two parameter example of Section 3.3.4, or in considering the effectiveness of adaptive mesh style point selection techniques [109].

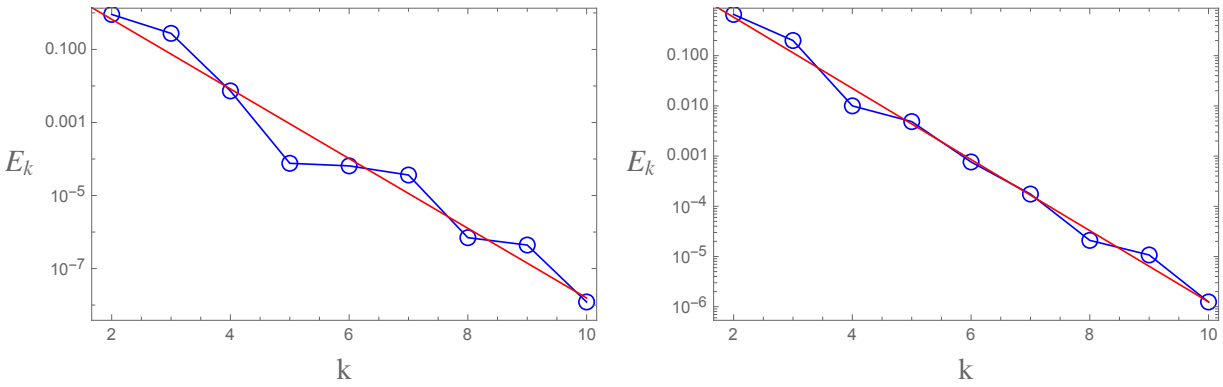

Figure 3.1: The error measure E_k is simply the value of the functional (2.58) computed for the optimized metric at a given k for the Fermat quartic (left) and quintic (left). We see that the error measure approaches zero exponentially.

We begin by considering quartic $p_2(0)$ in $\mathbb{P}^3$. In this example we utilize $N = 10^4$ points and an accuracy of $\epsilon = 0.02$ in terms of the parameters defined in Section 2.3.3. We follow the

procedure outlined at the start of this section for second order invariants in the curvature tensor with a number of points $n_R = 10^5$. To demonstrate that we have good numerical control of the higher curvature invariants being computed, we present some results as a function of k in Figure 3.2. We see that the maximum value of the Ricci scalar found

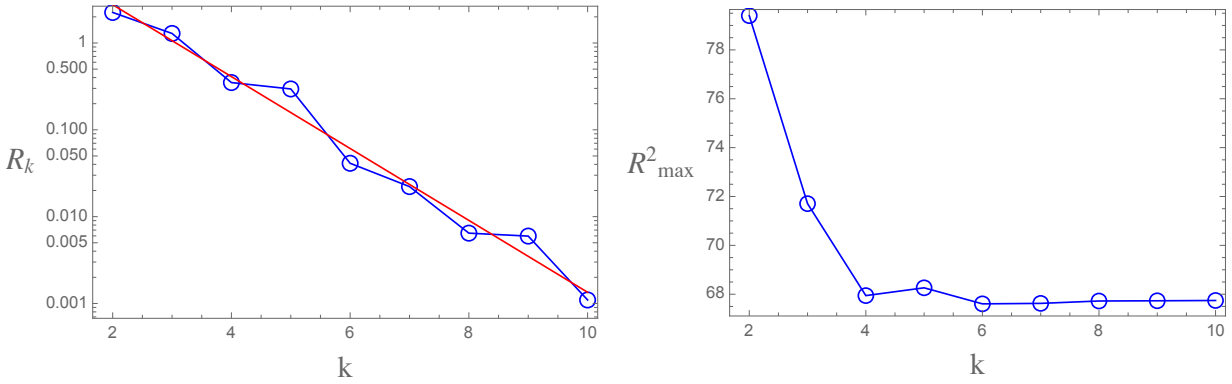

Figure 3.2: The maximum Ricci scalar (left) and magnitude of the curvature squared invariant (right) on the points sampled for the Fermat K3 in $\mathbb{P}^3$ as a function of k. The Ricci scalar approaches zero exponentially as k is increased while the higher curvature invariant approaches a fixed value.

rapidly approaches zero as we increase the accuracy of the numeric metric by increasing k. The maximum value of the higher order curvature invariant, by contrast, exponentially approaches a constant value - indicating that our accuracy is sufficient to trust the numerical result for this quantity. On the high curvature region where R^2 is large, we also compute the third and fourth order curvature scalars. The results (from large to small) are listed below:

$$R^2_{\max} \approx 67.74 \,,$$
$$R^3_{I\,\max} \approx (2.28 \times 10^2, -2.28 \times 10^2) \,,$$
$$R^4_{I\,\max} \approx (4.59 \times 10^3, 2.32 \times 10^3, 2.32 \times 10^3, 2.29 \times 10^3, -0.08, -0.16) \,.$$

Notice that the first term in $R^4_{I\,\max}$ equals $(R^2_{\max})^2$ and is the maximal one in the list. These results are as expected. If one higher curvature invariant becomes large then we would

typically expect the others to follow suit.

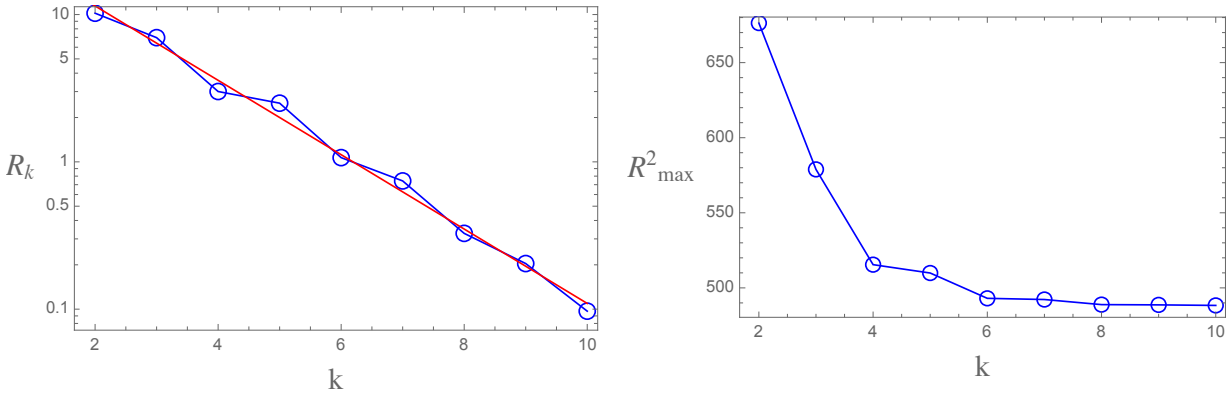

Figure 3.3: The maximum Ricci scalar (left) and magnitude of the curvature squared invariant (right) on the points sampled for the Fermat quintic three-fold in $\mathbb{P}^4$ as a function of k. The Ricci scalar approaches zero exponentially as k is increased while the higher curvature invariant approaches a fixed value.

Now, let's consider the Fermat quintic. Following the algorithm outlined in (3.2.2), the Ricci-flat metric is computed with parameters $L = \mathcal{O}(1)$, $N = 10^4$, and $\epsilon = 0.02$. Then, we perform the Monte-Carlo search over $n_R = 10^5$ points and identify the highest curvature region where the R^2 attains its maximum value in the sample. To measure the accuracy of the numerical curvature, we computed the R and R^2 for different k. The result is shown in Fig 3.3, which again indicates that the error of the numerical Ricci curvature decreases exponentially with k and our numerical results are trustable. We also compute the third and fourth order curvature scalars. The results (from large to small) are listed below:

$$R^2_{\text{max}} \approx 4.87 \times 10^2 \ ,$$

$$R^3_{I\,\text{max}} \approx (1.95 \times 10^3, -7.86 \times 10^3) \ ,$$

$$R^4_{I\,\text{max}} \approx (2.38 \times 10^6, 1.67 \times 10^6, 7.92 \times 10^5, 3.76 \times 10^5, -2.00 \times 10^4, -1.18 \times 10^5) \ .$$

Again, we find that the largest R^4 is given by the $(R^2_{\text{max}})^2$.

By the same procedure, we also applied our algorithm to the Fermat Calabi-Yau fourfold and fivefold. The Monte-Carlo search is performed over a sample with $n_R = 10^5$ points for the invariant R^2. The numeric metric used here is computed at $k = 5$ in the minimization algorithm. Once again, for the point of highest curvature, we computed the Ricci scalar and R^2_{max} for different k. The results are in Fig 3.4 and Fig 3.5. Once again, we find that the numerical curvature converges exponentially with k and our numerical results are reliable.

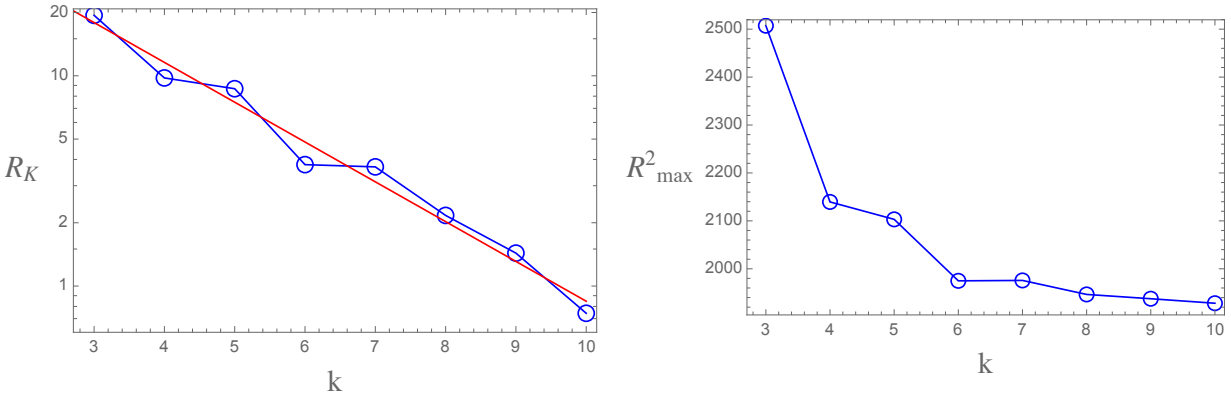

Figure 3.4: The maximum Ricci scalar (left) and magnitude of the curvature squared invariant (right) on the points sampled for the Fermat Calabi-Yau fourfold in $\mathbb{P}^5$ as a function of k. The Ricci scalar approaches zero exponentially as k is increased while the higher curvature invariant approaches a fixed value.

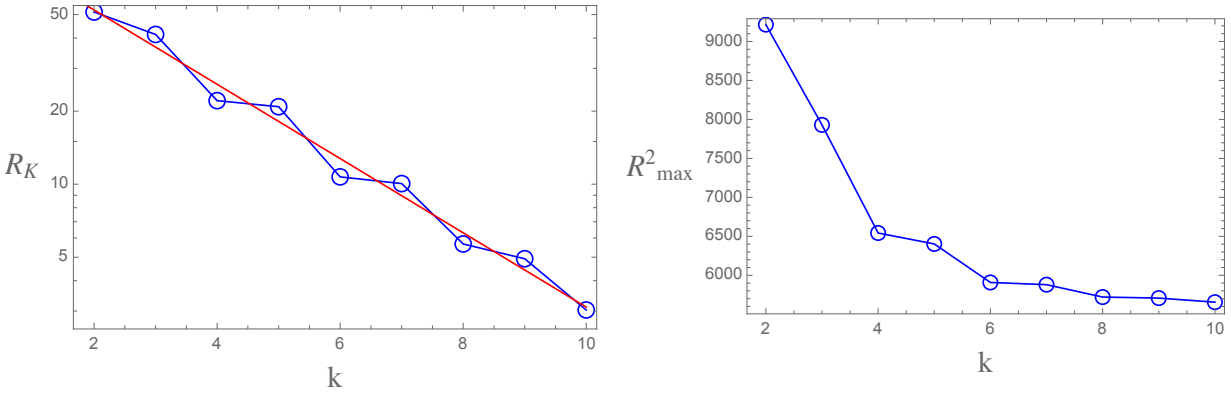

Figure 3.5: The maximum Ricci scalar (left) and magnitude of the curvature squared invariant (right) on the points sampled for the Fermat Calabi-Yau fivefold in $\mathbb{P}^6$ as a function of k. The Ricci scalar approaches zero exponentially as k is increased while the higher curvature invariant approaches a fixed value.

An example of non-Fermat type

In order to provide one final example which is not of the "ψ deformed Fermat" type we will consider a $K3$ surface embedded inside $\mathbb{P}^3$ with a defining relation depending upon two parameters of the following form

$$P_2(\psi_1, \psi_2) = Z_0^4 + Z_1^4 + \psi_1(Z_2^4 + Z_3^4) + \psi_2 Z_0^2 Z_1^2 \ . \tag{3.15}$$

In this case, the order of the discrete symmetry that is available to simplify our computations is only $|\Gamma| = 16$. This leads to a number of technical complications in completing the analysis of this example. For example, one can not use symmetry relationships between patches on the manifold to reduce the number of separate polydiscs that need to be considered. One also needs to consider more sections of L^k at each given k. With our code, we compute the numeric metric of the K3 surface with $\psi_1 = 1$ and $\psi_2 = 8$. The parameters used in the minimization algorithm are $L = \mathcal{O}(1)$, $\epsilon = 0.02$ and $N = 10^4$. The result in Fig 3.6 shows that the error function decreases exponentially with k.

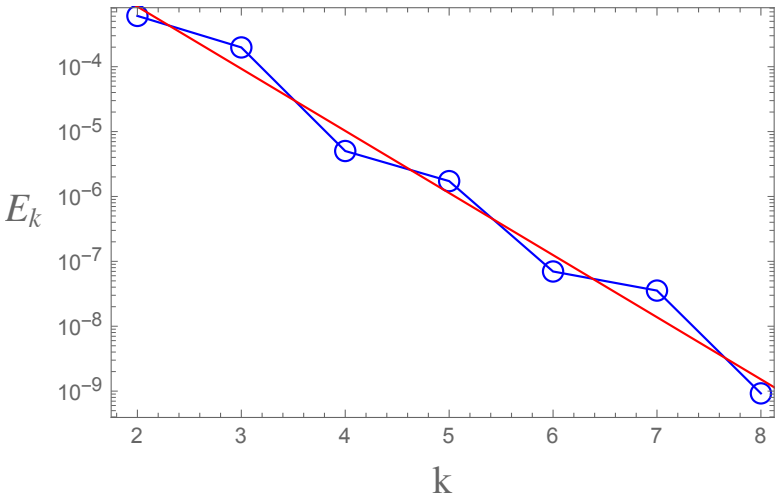

Figure 3.6: The error measure E_k is simply the value of the functional (2.58) computed for the optimized metric at a given k for the Fermat quartic (left) and quintic (left). We see that the error measure approaches zero exponentially.

Next, we run the Monte-Carlo search over $n_R = 5 \times 10^5$ points and plot the second order curvature scalars in Figure 3.7. The maximum value of the Ricci scalar once more goes exponentially to zero with increasing k while the maximum value of the higher curvature invariant approaches a constant value. This shows that our numerical results are accurate enough to be used to study the high curvature region of Calabi-Yau manifolds.

In conclusion, we have introduce a numerical method to find high curvature regions on

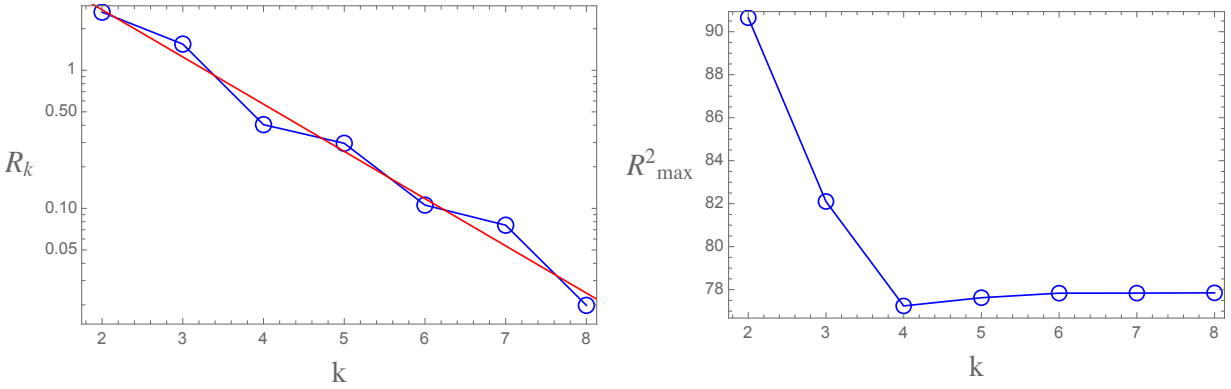

Figure 3.7: The maximum Ricci scalar (left) and magnitude of the curvature squared invariant (right) on the points sampled for the quartic in $\mathbb{P}^4$ given in (3.15), with $\psi_1 = 1$ and $\psi_2 = 8$, as a function of k. The Ricci scalar approaches zero exponentially as k is increased while the higher curvature invariant approaches a fixed value.

Calabi-Yau manifolds. The reliability of our method has been shown explicitly in different examples. Next, we will apply this technique to families of Calabi-Yau manifolds and study how these curvature scales vary across complex structure moduli space.

3.3 Curvature Hierarchies in Complex Structure Moduli Space

In this section, we will apply the numerical methods developed so far to study curvature hierarchies in the complex structure moduli space.

3.3.1 Expected High Curvature Regions

Not all choices of defining polynomials, or equivalently complex structure, give rise to smooth Calabi-Yau manifolds. Specifically, if the defining relation is such that the following equations can be satisfied [126, 127, 129, 130]

$$p(Z) = 0, \quad \partial_i p(Z) = 0, \tag{3.16}$$

then the space given by the vanishing locus of p is singular[1]. The curvature close to these singularities can be very "large."

As an example, consider the one parameter family defined in (2.64). For $n = 2$, the defining polynomial becomes

$$p_2(\psi) = Z_0^4 + Z_1^4 + Z_2^4 + Z_3^4 - 4\psi Z_0 Z_1 Z_2 Z_3 \tag{3.17}$$

where $\psi \in \mathbb{C}$ constitutes an one dimensional subspace of the complex structure moduli space. Notice that ψ and $\alpha\psi$ with $\alpha^4 = 1$ gives the same complex structure because since we can find that $p_2(\psi)$ and $p_2(\alpha\psi)$ become the same if a non-degenerate coordinate transformation is performed

$$Z_0 \to \alpha^{-1} Z_0 \ , \ \ Z_i \to Z_i \ , \ i = 1, 2, 3 \ . \tag{3.18}$$

Therefore, the good coordinate is ψ^4. A simple computation using (3.16) reveals that the following singularities [128].

- Conifold singularity: $\psi^4 = 1$.
- Large complex structure limit (LCSL): $\psi^4 = \infty$.

[1] The singularities, if they are point-like, can sometimes be resolved by the "splitting transitions" [55, 126, 137, 138, 139].

The conifold singularities are at the locations $\psi = (1, i, -1, -i)$ on the complex plane.

For $n = 3$, we have the one-parameter family of Calabi-Yau three-folds

$$p_3(\psi) = Z_0^5 + Z_1^5 + Z_2^5 + Z_3^5 + Z_4^5 - 5\psi Z_0 Z_1 Z_2 Z_3 Z_4 \, . \tag{3.19}$$

By the same analysis, the good coordinate on the complex structure moduli space is ψ^5 and the singularities are as follows

- Conifold singularity: $\psi^5 = 1$.
- Large complex structure limit: $\psi^5 = \infty$.

The conifold singularities are at $\psi = (1, e^{\frac{2\pi i}{5}}, e^{\frac{4\pi i}{5}}, e^{\frac{-4\pi i}{5}}, e^{\frac{-2\pi i}{5}})$ in the complex plane. The location of these singularities is plotted for later use in Figure 3.8.

At the singular points we have been discussing, it is well known that the curvature diverges. Therefore, we expect that there are large curvature scalars on the singular loci of the complex structure moduli space. If we consider the real axis on the complex plane, there will be very large curvature at $\psi = (-1, 1, \infty)$ for the $K3$ surface and at $\psi = (1, \infty)$ for the Calabi-Yau three-folds. We will see this structure reproduced explicitly with our numerical methods in next subsection.

3.3.2 Scanning Complex Structure Moduli Space Numerically for High Curvature Regions

Now, we wish to address the central question of this chapter. Given a set of defining relations for a Calabi-Yau variety can we determine if the Ricci-flat metric exhibits curvature scales

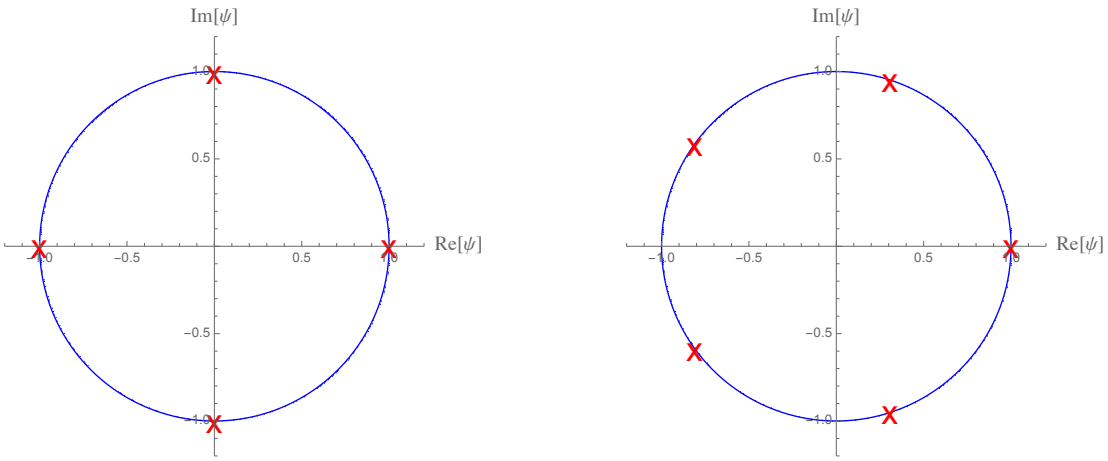

Figure 3.8: The conifold singularities of the one parameter family of $K3$ surfaces (left) and Calabi-Yau three-folds (right) on the complex plane.

that are wildly different from that set by the overall volume? To do this, we will compute the following dimensionless quantities

$$\tau_I^m = (R_{I\,\max}^m)^{\frac{1}{2m}} V_\omega^{1/2n} \,. \tag{3.20}$$

This is the dimensionless ratio of the mass scale set by the curvature invariant to the mass scale set by the overall volume of X (i.e. the compactification scale). The quantities $R_{I\,\max}^m$ are, of course, rather meaningless in isolation as the metric can be multiplied by an arbitrary overall scale while maintaining a Ricci-flat solution, adjusting the curvature invariants in a correlated manner. This dimensionless quantity encapsulates whether there is a region of anomalously high curvature compared to the scale set by the size of the manifold. Once more, the index I will be dropped in the case of $m = 2$ where there is only a single non-vanishing independent invariant.

In computing the volume of the Calabi-Yau manifold we will obtain slightly different values for different choices of complex structure. This is because the minimization algorithm presented in Section 2.3.3, allows the code to choose the overall normalization which is assigned

to the metric via the parameters h. The algorithms converge to slightly different volumes even if the Calabi-Yau manifolds are in the same family. For example, with the adaptive numerical integration introduced in Section 2.2.2, we computed the volume of Calabi-Yau manifolds in the families defined in (3.17) and (3.19). The results are plotted in Figure 3.9. We will use these volumes to compute the dimensionless quantity τ_I^m.

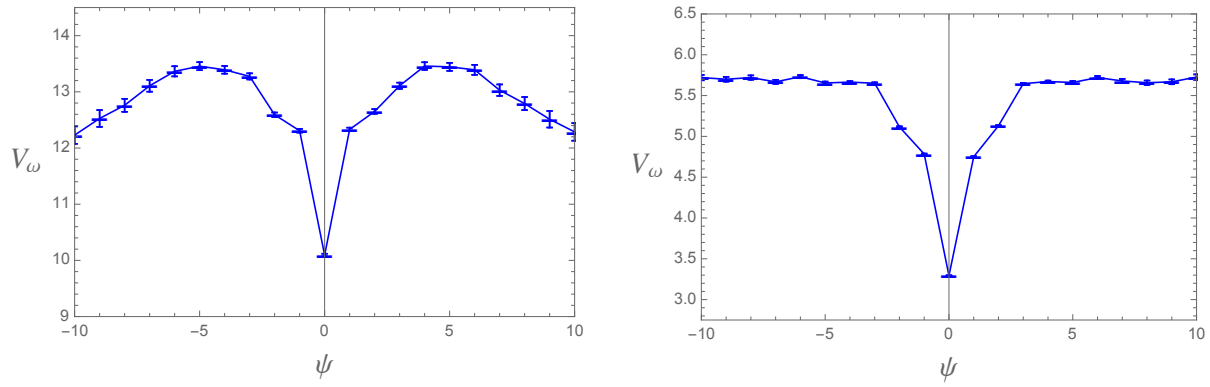

Figure 3.9: The volume V_ω of the Calabi-Yau manifolds as a function of ψ for the one parameter family of $K3$ surfaces (3.17) (left) and quintic three-folds (3.19) (right).

We perform all of the steps of our algorithm at some fixed k which, following the discussion of the previous chapter, is high enough to give a good approximation to the metric. We then repeat the computations at a much higher k value to check the results do not change. The small differences between the results obtained in this manner give us a measure of the error in our results due to the numerical nature of the metric being used. In order to highlight the errors coming from the accuracy of the numerical metrics that are being used, we have included error bars associated to this source of uncertainty in the plots of results that will be presented throughout this section. The error of the numerical metrics is large as one nears curvature singularities in moduli space [120]. This can be seen in Figure 3.10, where we plot the energy functional (2.58) of numerical metric ($k = 8$) for the one parameter family and two parameter family of Calabi-Yau manifolds.

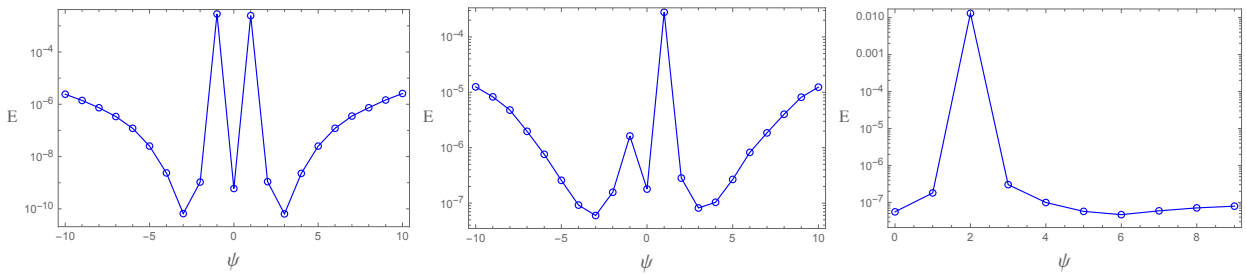

Figure 3.10: The energy functional E of the numeric metric ($k = 8$) as a function of ψ for the one parameter family of $K3$ surfaces (left), quintic three-folds (middle) and two parameter family of $K3$ surfaces (right).

In order to demonstrate that with this procedure can indeed isolate regimes in moduli space where the α' expansion is breaking down, we apply our methodology to regions where the existence of high curvature, associated to singularity structure, is well understood. In particular we show we can detect the appearance of high curvatures near both conifold points and large complex structure limits. Given these results we expect that this methodology can act as a useful probe in finding such high curvature regions more generally.

3.3.3 Examples 1: One Parameter Families

We begin by considering the one parameter family of quartics $p_2(\psi)$ in $\mathbb{P}^3$. To demonstrate that we have good numerical control of the higher curvature invariants being computed, we presented, in Figure 3.2, some plots for the example of the Fermat quartic $\psi = 0$. Obtaining such results for a variety of values of ψ and plotting the invariant τ^2 to obtain a appropriately normalized measure of the size of the higher order curvature terms, we arrive at Figure 3.11. In compiling this plot we computed initially with $k = 5$ and $L = \mathcal{O}(1)$ and have checked the level of numerical error in our results by repeating the calculations at $k = 10$. The plot in Figure 3.11 has several features that demonstrate that we can indeed isolate regimes of moduli space leading to higher curvature corrections correctly using numerical methods. First, the $K3$ of the form we are discussing has conifold singularities at $\psi = \pm 1$. The

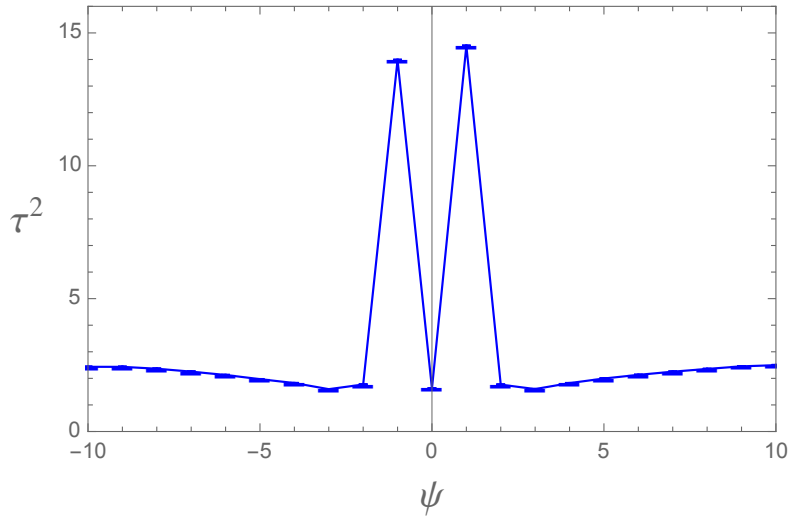

Figure 3.11: The dimensionless measure of the maximum value of second order curvature invariants on the sampled points, τ^2 from (3.20), as a function of ψ for the one parameter family of quartics in $\mathbb{P}^3$ (2.64). The expected features in this plot, given the known location in moduli space of curvature singularities, are correctly reproduced.

associated spikes in τ^2, which are not infinite because a finite sampling of points will not land exactly on a singular point in the manifold, can clearly be seen in Figure 3.11. In addition to this obvious feature, one can also see that τ^2 tends to increase as $|\psi|$ gets larger. This can be seen more clearly in a plot omitting the large features due to the conifold points, as in Figure 3.12. This corresponds to the increase in curvature scales appearing in the Ricci-flat metric as the manifold approaches the large complex structure limit.

Although the above analysis was for an algebraic $K3$ surface, very similar results can be obtained for three-folds and indeed higher dimensional varieties. Here we will content ourselves with presenting analogous results for the quintic Calabi-Yau three-fold, using $L = \mathcal{O}(1)$, $N = 10^4$, $n_R = 10^5$ and $\epsilon = 0.02$.

In Figure 3.13, we present the analogous plots to those presented above in the $K3$ case for quintic Calabi-Yau three-folds in $\mathbb{P}^4$ of the form (2.64). It is important to note that there is only one conifold point in moduli space in these quintic examples, at $\psi = 1$. Nevertheless,

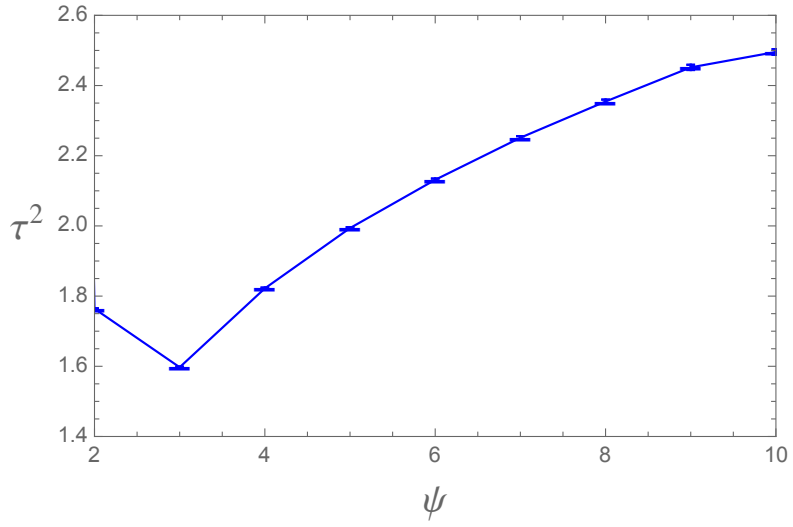

Figure 3.12: The same data as presented in Figure 3.11 with the large features associated to the conifold points omitted from the plot range. The tendency towards a hierarchy of scales between that set by the overall volume and that by highest value of the second order curvature invariant as the large complex structure limit is approached can clearly be seen.

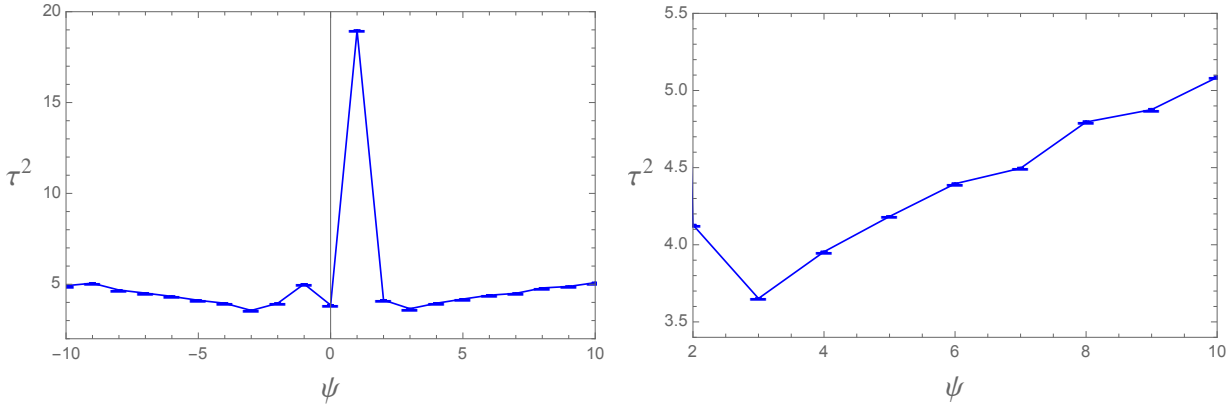

Figure 3.13: The measure of second order curvature invariants τ^2, as a function of ψ for the one parameter family of quintics in $\mathbb{P}^4$ (2.64). The expected features can be seen in the left hand plot, given the known location in moduli space of curvature singularities, are correctly reproduced. An additional small feature is also seen at $\psi = -1$. The same data is presented in the right hand plot with the large features associated to the conifold points omitted from the plot range. The tendency of τ^2 to increase as we approach the large complex structure limit can clearly be seen.

in Figure 3.13 a definite, albeit smaller, peak can be seen in the plot of τ^2 against complex structure at $\psi = -1$. The variety is completely smooth at this point. To check that this is

a real effect one can repeat the computation, at both $\psi = -1$ and $\psi = 1$, with an increased number of points $n_R = 10^7$. The result at $\psi = 1$ changes dramatically when we do this with τ^2 changing from 11.2 to 19.0 (recall the error bars in the plots here represent the uncertainty due to the numerical nature of the metric and do not include errors due to point sampling in computing curvatures - which are negligible except at the singular points in moduli space). This is because as we compute the curvature on more and more points, we will randomly pick out curvatures that are closer and closer to the singularity, where τ^2 diverges. The result at $\psi = -1$, however, hardly changes at all in changing n_R by two orders of magnitude, with τ^2 simply varying from 4.96 to 5.01. In this case we already have a good approximation to the maximum value of the finite range of values of τ^2 at various points in this smooth manifold.

Although it does not lead to a particularly large hierarchy of scales in this case, this is naively a feature of the type we were looking to find. The increase in τ^2 at $\psi = -1$ is corresponds to a Ricci-flat metric which exhibits rather large variations in curvature compared to nearby metrics in complex structure moduli space. Nevertheless, this point is not near to any singularity in the slice of moduli space obtained by varying ψ over real values. In [120] a discussion of a potential explanation for an avatar of this structure, albeit not directly linked to computing higher curvatures, at the point $\psi = -1$ was given[2]. Those authors point out that this point in moduli space is relatively close to two conifold points, at $\psi = e^{\frac{4\pi I}{5}}$ and $\psi = e^{\frac{6\pi I}{5}}$, as shown in Figure 3.8, which do not appear in the slice through moduli space encompassed by the plot in Figure 3.13. We can check if this explanation is correct in our context, simply by performing a similar plot along a line through moduli space that does include those singularities. This plot is presented in Figure 3.14

We see from Figure 3.14 that the slight bump at $\psi = -1$ is indeed due to the nearby conifold points. We see that τ^2 varies smoothly between the two peaks due to the conifold points just

[2]We would like to thank the referee of our paper and Matthew Headrick for suggesting that we pursue this explanation explicitly in this context

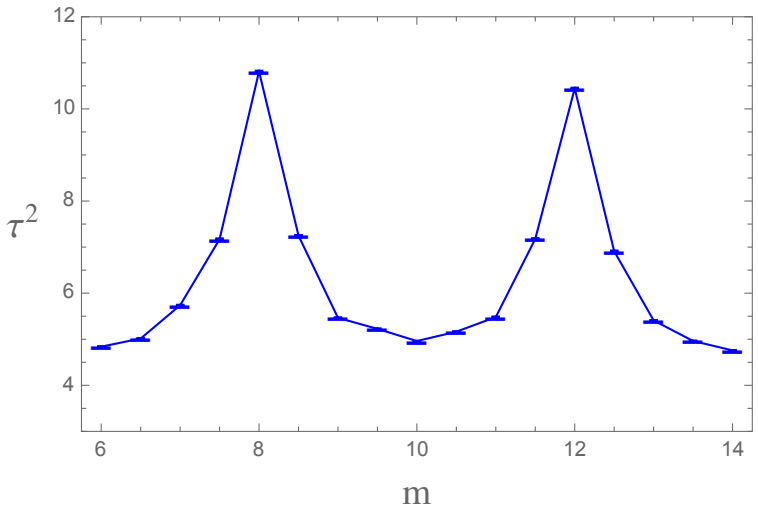

Figure 3.14: The measure of second order curvature invariants τ^2, as a function of m for the one parameter family of quintics in $\mathbb{P}^4$ (2.64) with $\psi = e^{i\frac{\pi m}{10}}$. The expected features due to the conifold singularities at $m = 8$ and $m = 12$ can clearly be seen in the plot. Note that $m = 10$ corresponds to $\psi = -1$, the value where a small feature was see in Figure 3.8. We can clearly see from this point of view that there is nothing special about $\psi = -1$. The value of τ^2 at this point is part of a smooth variation interpolating between the two curvature singularities. This demonstrates that the slight bump seen in Figure 3.8 is indeed due to the proximity of $\psi = -1$ to conifold points in parts of the complex structure moduli space that are not covered by that plot.

mentioned, with the value obtained at $m = 10$, corresponding to $\psi = -1$, agreeing with the height of the small bump in Figure 3.13. In [120] relatively poor convergence of numerical methods was seen at this same point in moduli space. We can see that this is probably indeed due to the relatively high curvatures that appear on the manifold at that locus in complex structure moduli space.

Despite the fact that the feature we have observed here has a simple explanation, this example gives a good demonstration of the utility of these methods. In cases where such effects are more pronounced, and no explanation of its origins could be found, knowledge of this type would be vital in understanding where the α' expansions of string theories are valid. In addition, in any given case one might not know from analytical methods how close to a singularity one would have to be in order to see an effect of this type. The numerical

methods being used here can straightforwardly answer such questions.

Note that, in addition to the features described above, it is just as important that elsewhere in the space of possible ψ we are *not* seeing hierarchies of higher curvature scales. Confirming this result, while consistent with naive expectations, was one of the goals of this research.

3.3.4 Examples 2: A Two Parameter Family

As with previous examples we can now explore the parameter space of the defining relation (3.15) and show how the normalized measure of the maximum value of the second order curvature invariant τ^2 varies with parameters. Since this example does not yield any surprises, we will content ourselves with showing a single plot, given in Figure 3.15, that illustrates that our numerical results reproduce the expected structure. The defining relation (3.15)

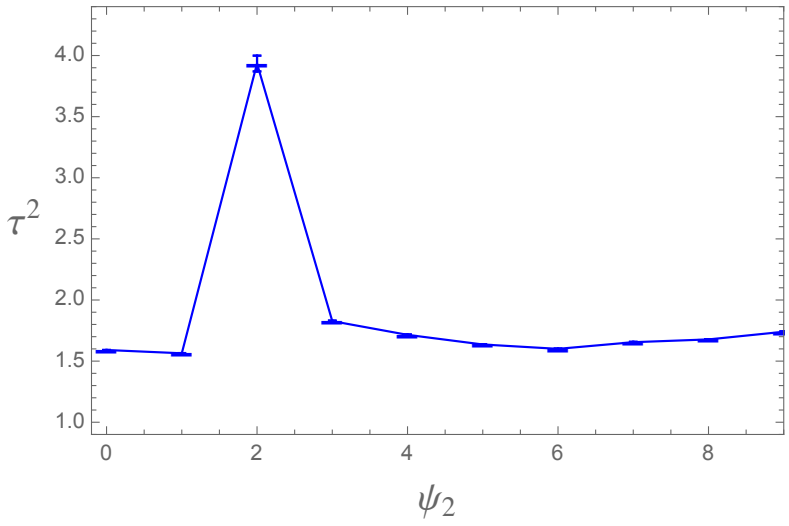

Figure 3.15: The dimensionless measure of the maximum value of second order curvature invariants on the sampled points, τ^2 from (3.20), as a function of ψ_2 with $\psi_1 = 1$ for the two parameter family of quartics in $\mathbb{P}^3$ (2.64). The expected features in this plot, given the known location in moduli space of curvature singularities, are correctly reproduced.

exhibits singularities at $\psi_1 = 1$, $\psi_2 = 2$ and as $\psi_2 \to \infty$ at constant ψ_1. The singularity at

finite parameters is clearly visible just as in previous examples and a steady increase in τ_2 as ψ_2 approaches large values is also present as expected.

3.4 Conclusions and Future Directions

In this chapter we have studied to what extent numerical methods can be utilized to detect hierarchies of curvature scales appearing in Ricci-flat metrics on Calabi-Yau manifolds at different locations in moduli space. These hierarchies concern a comparison of the scale set by the volume of the Calabi-Yau manifold to those determined by higher order curvature invariants. By illustrating that we can reproduce the expected behavior of such quantities as the system approaches singular points in complex structure moduli space, we have demonstrated that such techniques are rather effective in deciding this issue. Indeed, this is true even if simple point finding strategies for performing numerical integrations on the Calabi-Yau manifold are used: one does not necessarily need to adopt adaptive mesh procedures as one might suspect.

These techniques are a useful tool in deciding where in moduli space α' expansions, that are commonly used in constructing effective theories describing string compactifications, are valid. Already in the case of points in moduli space close to known singularities, the methods described here can be useful. While it is well known that hierarchies of curvature scales diverge at the singular points themselves, information about the size of these quantities at a given distance in moduli space from such loci can be more difficult to obtain analytically. The size of such hierarchies can easily be obtained in many examples using the methods presented here. The utility of these methods is only likely to increase as advances are made in techniques for computing Ricci-flat metrics numerically.

Many future extensions of the type of work carried out here could be envisioned. One could

use numerical approximations to the gauge connection in heterotic theories [109, 131, 132], for example, to study similar issues in the validity of α' expansions in those contexts. One could also study not just the complex structure dependence of hierarchies of curvature scales, but also their variation with Kähler moduli. In particular, in principle numerical methods could be used to delineate the boundaries of the Kähler cones of Calabi-Yau geometries: information which is often quite difficult to obtain (see [93] for just one recent study where such considerations were the key limiting factor). However, we suspect that such a study would require an improvement in the currently known numerical techniques for finding approximations to Ricci-flat metrics. To divide the Kähler cone finely enough to detect the desired structure, one would have to consider polarizations including rather large numbers. This would lead to issues with computational complexity as the number of parameters appearing in the standard ansatz for the Kähler potential (2.45) would become large very quickly as one tried to obtain an accurate approximation to the metric.

Chapter 4

Numerical Hermitian Yang-Mills Connections

In this chapter, we will review the basic proprieties of poly-stable holomorphic vector bundles, especially the Hermitian Yang-Mills connection and the numerical algorithm to compute it. Next, we will review how to apply this algorithm to study bundle stability. In the end, we will show the effectiveness of this numerical method with a non-trivial example.

4.1 Holomorphic Vector Bundles

In the work that will be described in this and the next chapter we will require some technical constructions from the mathematics of holomorphic vector bundles. We present the necessary background in this section.

A holomorphic vector bundle V over a variety X is a complex vector bundle satisfying the following conditions [87]:

- The projection map $\pi : V \to X$ is a holomorphic map.
- Let $\{U_\alpha\}$ be an open cover of X. The trivialization map over any open set U_α

$$\psi_\alpha : \pi^{-1}(U_\alpha) \to U_\alpha \times \mathbb{C}^n \tag{4.1}$$

is biholomorphic.

With this definition, for two open sets U_α and U_β with $U_\alpha \cap U_\beta \neq \emptyset$, the transition function $t_{\alpha\beta} : U_\alpha \cap U_\beta \to GL_n(\mathbb{C})$ is holomorphic and is given by the following,

$$t_{\alpha\beta} = \psi_\alpha \circ \psi_\beta^{-1} \ . \tag{4.2}$$

Let V_x be the fiber of V at $x \in X$, which is a n dimensional complex vector space. The dual bundle V^* is constructed by replacing each fiber with its dual $V_x^* = (V_x)^*$ and by taking the transition functions to be $t^*_{\alpha\beta} = (t^{\mathrm{T}}_{\alpha\beta})^{-1}$. On a open set U_α, a section σ is a map $\sigma : U_\alpha \to V$ such that $\pi \circ \sigma = \mathrm{id}$. A frame is a collection of sections $e = \{e_1, \ldots, e_n\}$ on U_α, which spans the fiber V_x for each $x \in U_\alpha$ [1]. The corresponding frame for the dual bundle V^* is $e_* = (e^1_*, \ldots, e^n_*)$ with the relations $e^i_*(e_j) = \delta^i_j$. Denote the space of holomorphic global sections to be $H^0(X, V)$. A holomorphic vector bundle V is globally generated [140] if there exist global holomorphic sections $s_1, \ldots, s_n \in H^0(X, V)$ such that for any $x \in X$ the collection $s_1(x), \ldots, s_n(x)$ generates the fiber V_x.

The set of V-valued (p, q) forms on X is denoted by $\mathcal{A}^{p,q}(V)$. The operator $\bar\partial : \mathcal{A}^{p,q} \to \mathcal{A}^{p,q+1}$ for differential forms can be generalised to V-valued forms [140]

$$\bar\partial_V : \mathcal{A}^{p,q}(V) \to \mathcal{A}^{p,q+1}(V) \tag{4.3}$$

mapping bundle-valued (p, q)-forms to bundle-valued $(p, q + 1)$-forms. For a frame $e = (e_1, e_2, \ldots, e_n)$ of V we can write a vector bundle-valued (p, q)-form $\sigma \in \mathcal{A}^{p,q}(V)$ as $\sigma =$

[1] A frame for V over U_α is essentially the same thing as a trivialization of V over U_α.

$\sum_{i=1}^{n} \sigma^i \otimes e_i$, where $\sigma^i \in \mathcal{A}^{p,q}$ are regular (p,q)-forms. Then $\bar{\partial}_V$ acts as

$$\bar{\partial}_V \sigma = \sum_{i=1}^{n} \bar{\partial}\sigma^i \otimes e_i \,. \tag{4.4}$$

It is straightforward to show from this definition that $\bar{\partial}_V^2 = 0$ and that the Leibniz rule

$$\bar{\partial}_V(f\sigma) = \bar{\partial}(f) \wedge \sigma + f \otimes \bar{\partial}_V(\sigma)$$

holds. Here, f is a differentiable function on X.

4.1.1 Connections and Curvature

A Hermitian structure on a vector bundle V is defined by a Hermitian inner product on each fibre V_x. Let σ and ρ be two sections of V, which, in terms of the frame introduced above, can be written as $\sigma = \sum_{i=1}^{n} \sigma^i e_i$ and $\rho = \sum_{i=1}^{n} \rho^i e_i$. Then, the Hermitian structure G, acting on σ and ρ, can be expressed as [87, 140]

$$G(\sigma, \rho) = G_{ij} \sigma^i \bar{\rho}^j \,, \quad G_{ij} = G(e_i, e_j) \,. \tag{4.5}$$

Locally, the Hermitian structure is described by a Hermitian $n \times n$ matrix G. The Hermitian structure η can also be understood as an isomorphism between the vector bundle V and its dual V^*, so $\eta : V \xrightarrow{\simeq} V^*$. Let the inverse map of η be $\eta^* : V^* \xrightarrow{\simeq} V$ then we have [140]

$$G(\sigma_i) = G_{ji} \sigma_*^j \,, \qquad G^*(\sigma_*^i) = \bar{G}^{ji} \sigma_j \,, \qquad G^{ij} G_{jk} = \delta_k^i \,. \tag{4.6}$$

A connection, ∇, on V is a linear map $\nabla : \mathcal{A}^0(V) \to \mathcal{A}^1(V)$ which satisfies the Leibniz rule

[87, 140]

$$\nabla(f\sigma) = d(f) \otimes \sigma + f\nabla(\sigma) \tag{4.7}$$

for local sections σ and local functions f. Writing the section $\sigma = \sum_{i=1}^{r} \sigma^i e_i$ with respect to a local frame $e = (e_1, \ldots, e_r)$, the map can be explicitly given by

$$\nabla(\sigma) = (d\sigma^i + A^i{}_j \sigma^j) \otimes e_i \,, \quad \nabla(e_j) = A^i{}_j e_i \tag{4.8}$$

where the second expression defines A, the gauge field.

The curvature of a connection ∇ is defined by

$$F_\nabla = \nabla \circ \nabla : \mathcal{A}^0(V) \to \mathcal{A}^1(V) \to \mathcal{A}^2(V) \,. \tag{4.9}$$

This satisfies,

$$F_\nabla(f\sigma) = f F_\nabla \sigma \tag{4.10}$$

for a section σ and a function f which implies that $F_\nabla \in \mathcal{A}^2(\mathrm{End}(V))$. In terms of a local frame we can write the curvature of a connection as $\nabla \circ \nabla(e_i) = \sum F_{ij} \otimes e_j$. The relation between the local form of the curvature and the gauge field is then easy to derive

$$F = dA - A \wedge A \,. \tag{4.11}$$

For a different local frame $e' = (e'_1, e'_2, \ldots, e'_n)$ related to the original one by $e'_i = \sum h^j{}_i e_j$ the hermitian metric transforms as [87]

$$G' = hGh^+ \,. \tag{4.12}$$

while the connection and curvature transform as

$$A' = dhh^{-1} + hAh^{-1} \,, \tag{4.13}$$

and

$$F = hFh^{-1} \,. \tag{4.14}$$

These transformation properties will be important to us going forward.

Mathematical Gauge and Physical Gauge

Consider decomposing the connection as $\nabla = \nabla^{(1,0)} + \nabla^{(0,1)}$ where $\nabla^{(1,0)} : \mathcal{A}^{0,0}(V) \to \mathcal{A}^{1,0}(V)$ and $\nabla^{(0,1)} : \mathcal{A}^{0,0}(V) \to \mathcal{A}^{0,1}(V)$ where the superscripts denote holomorphic/anti-holomorphic index structure. We say a connection is compatible with the complex structure if $\nabla^{(0,1)} = \bar{\partial}_V$, as defined in Equation (4.3). A connection is compatible with the fiber metric if the following expression

$$d(\sigma_1, \sigma_2) = (\nabla\sigma_1, \sigma_2) + (\sigma_1, \nabla\sigma_2) \tag{4.15}$$

holds for any two sections σ_1 and σ_2 [87]. For holomorphic vector bundles with hermitian metrics, there exists an unique connection which is compatible with both the complex structure and metric structure, called the Chern connection. In a holomorphic frame, it is given by [87]

$$A^{(1,0)} = (\partial G)G^{-1} \quad A^{(0,1)} = 0 \,. \tag{4.16}$$

The corresponding curvature is

$$F^{(1,1)} = \bar{\partial} A^{(1,0)}, \quad F^{(2,0)} = F^{(0,2)} = 0 \,. \tag{4.17}$$

In the holomorphic frame (sometimes called in "mathematical" gauge [131]), the gauge field is of type $(1,0)$ and the curvature is of type $(1,1)$, and both of them are uniquely determined by the hermitian metric G.

A frame $e = \{e_1, e_2, \ldots, e_r\}$ is called an unitary frame ("physical" gauge [131]) if it gives an orthonormal $G(e_i, e_j) = \delta_{ij}$ basis for each fiber of V. The unitary frames always exist locally, since we can take any frame and apply the Gram-Schmidt process. By Equation (4.15), it is straightforward to show that the metric compatible connection has a gauge field associated to such a frame which is anti-hermitian.

$$A = -A^+ \tag{4.18}$$

where it will not cause confusion we will use the word 'connection' to refer to both a connection and the collections of gauge fields to which it corresponds. We will call a connection of the type (4.18) a physical connection.

To go from an holomorphic frame to an unitary frame we need to perform a (complex) gauge transformation h. For a $SU(n)$ bundle, this gauge transformation on V should be an element of $SU(n)_{\mathbb{C}} = SL(n, \mathbb{C})$. By Equation (4.12), it satisfies $hGh^+ = I$ and can be calculated from G [131]. Consider the decomposition of the inverse hermitian metric in mathematical gauge $G^{-1} = U\Lambda U^+$ where Λ is a real diagonal matrix consisting of the eigenvalues of G^{-1} and U is the unitary matrix consisting of the corresponding eigenvectors. The complex gauge transformation is given by

$$h = U\sqrt{\Lambda}U^+ \,. \tag{4.19}$$

It is easy to check that $G^{-1} = h \cdot h^+$ and $\det h = 1$. Indeed, we have $\det h = \det U \det(\sqrt{\Lambda})$ $\det U^+ = \det(\sqrt{\Lambda}) = 1$. The last equality is due to the fact that the fiber metric of a $SU(n)$ holomorphic vector bundle is a $SL(n, \mathbb{C})$ matrix, leading to $\det(G^{-1}) = 1$ and $\det(\sqrt{\Lambda}) = 1$.

Also, by the matrix exponential, h can be written as $h = e^{\frac{1}{2}U(ln\Lambda)U^+}$. Here the exponent is a hermitian and traceless matrix, which is an element of $sl(3,\mathbb{C})$. Thus, we have seen that h in (4.19) is the gauge transformation that we are looking for.

Performing the gauge transformation (4.19) according to (4.13), the connection becomes [131]

$$A^{(1,0)} = (\partial h^{-1})h, \quad A^{(0,1)} = (\bar{\partial} h)h^{-1} \, . \tag{4.20}$$

It is straightforward to check that the anti-hermitian condition (4.18) is obeyed and this is the physical connection. The corresponding curvature is given by

$$\begin{aligned} F^{(2,0)}_{ab} &= (\partial_a A^{(1,0)}_b - \partial_b A^{(1,0)}_a) + [A^{(1,0)}_a, A^{(1,0)}_b] \, , \\ F^{(1,1)}_{a\bar{b}} &= (\partial_a A^{(0,1)}_{\bar{b}} - \bar{\partial}_{\bar{b}} A^{(1,0)}_a) + [A^{(1,0)}_a, A^{(0,1)}_{\bar{b}}] \, , \\ F^{(0,2)}_{\bar{a}\bar{b}} &= (\bar{\partial}_{\bar{a}} A^{(0,1)}_{\bar{b}} - \bar{\partial}_{\bar{b}} A^{(0,1)}_{\bar{a}}) + [A^{(0,1)}_{\bar{a}}, A^{(0,1)}_{\bar{b}}] \, . \end{aligned}$$

We will use this procedure in a computation of a physical Hermitian Yang-Mills connection in the next chapter.

Bundle-Valued Cohomology

Given the generalized Dolbeault operator defined in (4.3), we have the complex of bundle-valued forms

$$0 \xrightarrow{\bar{\partial}_V} \mathcal{A}^{p,0}(V) \xrightarrow{\bar{\partial}_V} \mathcal{A}^{p,1}(V) \xrightarrow{\bar{\partial}_V} \ldots \xrightarrow{\bar{\partial}_V} \mathcal{A}^{p,n-1}(V) \xrightarrow{\bar{\partial}_V} \mathcal{A}^{p,n}(V) \xrightarrow{\bar{\partial}_V} 0 \, .$$

In analogy to the usual forms, a V-valued form $\sigma \in \mathcal{A}^{p,q}(V)$ is closed if $\bar{\partial}_V \sigma = 0$ and is exact if it can be expressed as $\sigma = \bar{\partial}_V \rho$ with $\rho \in \mathcal{A}^{p,q-1}(V)$. The V-valued cohomology is defined

to be [140]

$$H^{p,q}(V) = \frac{\ker \bar{\partial}_V}{\mathrm{im}\, \bar{\partial}_V} \tag{4.21}$$

where $H^{p,q}(V) = H^q(X, V \otimes \Omega^{p,0})$. This definition reduces to the former definition of Dolbeault cohomology groups when $V = \mathcal{O}$.

As in the usual Dolbeault cohomology, there exists V-valued harmonic forms associated to each cohomology class in $H^{p,q}(V)$. With Hermitian structure, one can define a generalisation of the Hodge dual operation $\bar{\star}_V : \mathcal{A}^{p,q}(V) \to \mathcal{A}^{n-p,n-q}(V^*)$ by setting [140]

$$\bar{\star}_V(\alpha \otimes s) = \star(\bar{\alpha}) \otimes G(s)\,, \tag{4.22}$$

where $\star$ the the regular Hodge star operation on forms, s is a local section of V and α is a (p, q) form. It follows that $\bar{\star}_V \circ \bar{\star}_V = (-1)^{p+q}$, in analogy with the properties for the regular Hodge star. The adjoint operator $\bar{\partial}_V^\dagger : \mathcal{A}^{p,q}(V) \to \mathcal{A}^{p,q-1}(V)$ of $\bar{\partial}_V$ relative to this inner product satisfies

$$(\bar{\partial}_V \alpha, \beta) = (\alpha, \bar{\partial}_V^\dagger \beta)\,, \tag{4.23}$$

and takes the form $\bar{\partial}_V^\dagger = -\bar{\star}_V \circ \bar{\partial}_{V^*} \circ \bar{\star}_V$. Furthermore, one can define the generalised Laplacian

$$\Delta_V = \bar{\partial}_V^\dagger \bar{\partial}_V + \bar{\partial}_V \bar{\partial}_V^\dagger\,. \tag{4.24}$$

It is self-adjoint under the inner product above. Bundle-valued forms $\alpha \in \mathcal{A}^{p,q}(V)$ are called harmonic with respect to the Hermitian structure h if they satisfy $\Delta_V \alpha = 0$. On a compact manifold, it indicates that α should be both closed and co-closed,

$$\bar{\partial}_V \alpha = 0\,, \qquad \bar{\partial}_V^\dagger \alpha = 0\,. \tag{4.25}$$

The harmonic forms are in one-to-one correspondence with the cohomology groups $H^{p,q}(M,E) \cong H^q(M, V \otimes \Omega_X^{(p,0)})$. This can be seen from the generalized Hodge decomposition, i.e. every form $\alpha \in \mathcal{A}^{p,q}(V)$ can be expressed as $\alpha = \eta + \bar{\partial}_V \beta + \bar{\partial}_V^\dagger \gamma$, where η is harmonic.

Finally, the Hodge star $\bar{\star}_V : \mathcal{A}^{p,q}(V) \to \mathcal{A}^{p,q}(V)$ to $\mathcal{A}^{n-p,n-q}(V^*)$ defined in (4.22) induces a complex linear isomorphism to the cohomology

$$H^{p,q}(V) \cong H^{n-p,n-q}(V^*)^* \ . \tag{4.26}$$

This is the famous Serre's duality and we will use it extensively in the computations of bundle cohomology.

Chern Classes

Chern classes are subsets of cohomology classes in the base manifold which are one measure of the non-triviality of a bundle. The total Chern class of V is defined by $c(V) = [\det(1 + \frac{i}{2\pi}F)]$ where F is the curvature of some connection and the square brackets denote that the cohomology class should be taken. It can be shown that the total Chern class is independent of the choice of the connection [140]. We define the Chern classes $c_k(V) \in H^{2k}(X, \mathbb{R})$ by the expansion of $c(V) = 1 + c_1(V) + c_2(V) + \ldots$ with

$$\begin{aligned} c_0(V) &= [1] \ , \\ c_1(V) &= \left[\left(\frac{i}{2\pi} \right) \mathrm{tr}\, F \right] \ , \\ c_2(V) &= \left[\frac{1}{2} \left(\frac{i}{2\pi} \right)^2 (\mathrm{tr}\, F \wedge \mathrm{tr}\, F - \mathrm{tr}(F \wedge F)) \right] \ , \\ &\vdots \end{aligned} \tag{4.27}$$

Since F is a two-form, on an d-dimensional complex manifold the Chern classes $c_j(V)$ for $2j > d$ vanish identically. Also, irrespective of the dimension of X, $c_j(V) = 0$ for $j > n$ where n is the rank of the bundle V.

The total Chern character is defined by $ch(V) = \mathrm{tr}\exp\left(\frac{iF}{2\pi}\right)$. Expanding this expression, we define the jth Chern character to be

$$ch_j(V) = \frac{1}{j!}\,\mathrm{tr}\left(\frac{iF}{2\pi}\right)^j \tag{4.28}$$

and the series terminates when $2j > d$. The index of V (or the Euler characteristic) is related to the top Chern class by

$$\mathrm{ind}(\bar{\partial}_V) = \sum_{i=0}^{d}(-1)^i h^i(X,V) = \int_X ch(V)\wedge \mathrm{Td}(X)\ , \tag{4.29}$$

where $\mathrm{Td}(X)$ is the Todd class for the tangent bundle of X. This result is known as the Hirzebruch-Riemann-Roch formula [140]. For a Calabi-Yau d-fold X and an $SU(n)$ bundle V it is easy to show that,

$$\int_X ch(V)\wedge \mathrm{Td}(X) = \frac{1}{2}\int_X c_d(V)\ . \tag{4.30}$$

4.1.2 Hermitian Yang-Mills connections

As discussed earlier, to preserve supersymmetry, we ask the internal space to be a Calabi-Yau manifold while the gauge field should satisfy the Hermitian Yang-Mills equation [10]

$$F_{ab} = F_{\bar{a}\bar{b}} = 0\ , \tag{4.31}$$

$$g^{\bar{b}a}F_{a\bar{b}} = 0\ . \tag{4.32}$$

Here $F_{a\bar{b}}$ is the field strength of A_a and $g^{\bar{b}a}$ is the Ricci-flat metric on X. Solving the Hermitian Yang-Mills equations is equivalent to find a connection on a vector bundle satisfying certain algebraic conditions [65, 66]. Let X be a Calabi-Yau three-fold and V be a vector bundle with rank n. The first condition (4.31) is equivalent to the vector bundle V being holomorphic. The second one (4.32) implies that V is slope poly-stable and slope zero. The slope of a sheaf F is defined as,

$$\mu(F) \equiv \frac{1}{\mathrm{rk}(F)} \int_X c_1(F) \wedge \wedge J \wedge J \ , \tag{4.33}$$

where J is the Kähler form on X. Sheaves are a generalization of the concept of vector bundles that we will require in this section. In particular, the slope of the vector bundle V is obtained from (4.33) simply by substituting V for F. A holomorphic vector bundle V is stable (semi-stable) if for all sub-sheaves $F \subset V$, we have $\mu(F) < \mu(V)$ ($\mu(F) \leq \mu(V)$). Otherwise, V is unstable. V is called poly-stable if it is a direct sum of stable bundles $\mathcal{V} = \bigoplus_n V_n$ with same slope. Obviously, we have stable $\subset$ poly-stable $\subset$ semi-stable.

Given a vector bundle V, it can be very difficult to decide if it is stable or not. Such a computation would require the enumeration all of its (infinite number of) sub-sheaves and calculation of their slopes which would then be compared with $\mu(V)$. In more detail, a sheaf F is a sub-sheaf of V if $0 < \mathrm{rk}(F) < \mathrm{rk}(V)$ and there exists an injective morphism $i : F \to V$. The space of homomorphisms between F and V, denoted $\mathrm{Hom}_X(F, V)$, is isomorphic to the space of global holomorphic sections $H^0(X, F^* \otimes V)$. So, a necessary condition for F to be a sub-sheaf of V is

$$0 < \mathrm{rk}(F) < \mathrm{rk}(V) \text{ and } H^0(X, F^* \otimes V) \neq 0 \ . \tag{4.34}$$

For a $SU(n)$ vector bundle, it can be shown [67] that it is sufficient to instead demand that the slope of all sub-line bundles $\mathcal{L} \subset \wedge^k V$, for all k with $0 < k < n$, is negative. Since line

bundles are classified by their first Chern class on a Riemannian manifold, this is a dramatic simplification of the problem.

Given how difficult it is to check stability, it is useful to note that there is a simpler necessary condition that a bundle must satisfy in order to be stable. If an $SU(n)$ bundle V is stable then $H^0(X,V) = H^0(X,V^*) = 0$. Indeed, if $H^0(X,V)$ were non-vanishing, then it is clear that $\mathrm{Hom}_X(O,V) \cong H^0(X, O^* \otimes V) = H^0(X,V) \neq 0$ and, hence, that the trivial sheaf O would de-stabilize V for any choice of Kähler moduli. A similar argument holds for V^* which is stable exactly if V is. This fact is also useful in the analysis of bundle-valued cohomology associated to stable bundles.

For a poly-stable bundle V with fiber metric G, then the Hermitian Yang-Mills equation (4.32) in "mathematical" gauge is given by [109, 131, 132]

$$g^{\bar{b}a} F_{a\bar{b}} = g^{\bar{b}a} \bar{\partial}_{\bar{b}} A_a = g^{\bar{b}a} \bar{\partial}_{\bar{b}} (G^{-1} \partial_a G) = 0. \tag{4.35}$$

The fiber metric is called a Hermite-Einstein bundle metric if it obeys the equation above. Thus, to compute the Hermitian Yang-Mills connection, it is sufficient to study the Hermite-Einstein bundle metric. As a (poly-) stable bundle, V does not have global sections. Given this, it turns out to be convenient to study a twisted bundle $\mathcal{V} = V \otimes L^k$ where L is an ample line bundle and k is some integer. For such an $U(n)$ bundle, the corresponding Hermitian Yang-Mills equation is

$$F_{ab} = F_{\bar{a}\bar{b}} = 0, \qquad g^{a\bar{b}} F_{a\bar{b}} = \mu(\mathcal{V}) \cdot \mathbf{1}_{n\times n} \, . \tag{4.36}$$

In the case of an $SU(n)$ bundle, the first Chern class $c_1(V)$, and thus the slope, vanishes and the equation (4.36) reduces to the Hermitian Yang-Mills equation in (4.32) correctly.

4.1.3 Holomorphic Vector Bundles Over Calabi-Yau Manifolds

A variety of constructions of holomorphic vector bundles are utilized in the physics literature, for example the spectral cover construction [141, 142, 143], extensions [15] and the monad construction [36, 144, 145, 146]. In this section, we will first discuss line bundles over complete intersections in products of projective spaces as a prerequisite to then focus on the case of monad bundles over the same spaces.

Line bundles on CICYs

Line bundles can be used in the construction of higher rank monad bundles, so we will study their proprieties first. For an ambient space A with m projective factors, we consider a favorable complete intersection Calabi-Yau three-fold X. Let $J_r, r = 1, \ldots, m$ be a basis of the Kähler cone. We can define a line bundle $L = O_X(\mathbf{k})$ on X, where $\mathbf{k} = (k^1, \ldots, k^m)$ is an m-dimensional integer vector via its first Chern class. The line bundle is uniquely defined to be that for which $c_1(L) = k^r J_r$ with $r = 1, \ldots, m$. The dual of the line bundle L is simply given by $L^* = O_X(-\mathbf{k})$.

Now, we will study the cohomology of line bundles over X. By the Serre's duality, the cohomology of L over X has the property that

$$h^0(X, L) = h^3(X, L^\vee), \quad h^1(X, L) = h^2(X, L^\vee) \, . \tag{4.37}$$

The index (4.29) of L can be written as

$$ind(L) \equiv \sum_{q=0}^{3} (-1)^q h^q(X, L) = \frac{1}{6} \left(d_{rst} k^r k^s k^t + \frac{1}{2} k^r c_{2r}(TX) \right) \tag{4.38}$$

with implicit summation in $r, s, t = 1, \ldots, m$. The d_{rst} and $c_{2r}(TX)$ are the intersection numbers and the coefficient of the second Chern classes of X, contracted with the intersection numbers, respectively. A special class of line bundles called positive line bundles are the ones given by $L = O_X(\mathbf{k})$ with all $k^r > 0$. With the help of the Kodaira vanishing theorem, the cohomology of such bundles are

$$H^q(X, L \otimes K_X) = 0 \ , \quad \forall \ q > 0 \ , \tag{4.39}$$

where K_X is the canonical bundle of X and it is trivial here. Thus, the only non-vanishing cohomology of positive line bundles is $H^0(X, L)$, which is determined by the index $h^0(X, L) = ind(L)$ (4.38). The situation is similar for negative line bundles L, i.e. $L = O_X(\mathbf{k})$ with all $k^r < 0$. By Serre's duality, the only non-vanishing cohomology of a negative line bundle is $h^3(X, L)$. Again, it can be computed from the index using $h^3(X, L) = -\text{ind}(L)$.

For a line bundles $L = O(\mathbf{k})$ with "mixed" or zero entries k^r, the cohomology cannot be easily determined. In general, the computation contains two steps. First, compute the cohomology of line-bundles over the ambient space. In our cases, the ambient spaces will be products of projective spaces, and the associated cohomology is given by the Bott formula [36],

$$h^q(\mathbb{P}^n, O(k)) = \begin{cases} \binom{k+n}{n} & q = 0 \qquad k \geq 0, \\ \binom{-k-1}{n} & q = n \qquad k \leq -n-1, \\ 0 & \text{otherwise}, \end{cases} \tag{4.40}$$

together with the Künneth formula

$$H^n(\mathbb{P}^{n_1} \times \ldots \times \mathbb{P}^{n_m}, O(q_1, \ldots, q_m)) = \bigoplus_{k_1 + \ldots + k_m = n} H^{k_1}(\mathbb{P}^{n_1}, O(q_i)) \times \ldots \times H^{k_m}(\mathbb{P}^{n_m}, O(q_m)) \ . \tag{4.41}$$

The second step is computing the cohomology of a vector bundle $V = V|_X$ on X. If X is a smooth co-dimension K hypersurface in the ambient space, which, according to the configuration matrix, can be regarded as the zero locus of a holomorphic section s of the bundle N, then the following, "Koszul," exact sequence exists [36, 139, 147]:

$$0 \to V \otimes \wedge^K N_X^* \to V \otimes \wedge^{K-1} N_X^* \to \ldots \to V \otimes N_X^* \to V \to V|_X \to 0 \ . \tag{4.42}$$

Here, N_X^* is the dual to the normal bundle. So, if we know the cohomology of the bundles $\wedge^j N^* \otimes V$ on the ambient space, then the cohomology of $V|_X$ can be determined by the Koszul sequence. It is easy to see that for higher co-dimensional spaces, this computation can be very tedious. To simplify it, we can use the Leray spectral sequences [36, 139] for which computer implementations are available [148]. Recently, with the help of such tools, analytical formulae for line bundle cohomology on several different Calabi-Yau three-folds was found [149]. The formula for the quintic $X = [\mathbb{P}^4|5]$ is [150]

$$H^0(X, O(k)) = \text{Max}\left(\delta_{k0} + \frac{5}{6}k^3 + \frac{25}{6}k, 0\right) \ .$$

This is a simple expression. However, for manifold with $h^{1,1} > 1$, the formula looks different on the different regions in the Picard lattice and thus becomes more complex. For example, for this manifold with $h^{1,1} = 2$,

$$X = \left[\begin{array}{c|c} \mathbb{P}^1 & 2 \\ \mathbb{P}^3 & 4 \end{array}\right]^{2,86}_{-168} \ . \tag{4.43}$$

the cohomology of line bundle $L = O(k_1, k_2)$ is [149]

$$h^0(X,L) = \begin{cases} k_1 + 1\ , & k_1 \geq 0,\ k_2 = 0 \\ \mathrm{ind}(L), & k_1 \geq 0,\ k_2 > 0 \\ -k_1 + 1, & k_1 < 0\ , k_2 = -4k_1 \\ \frac{32}{3}k_1(1-k_1^2) + \mathrm{ind}(L), & k_1 < 0\ , k_2 > -4k_1 \\ 0 & \text{otherwise} \end{cases}$$

$$h^1(X,L) = \begin{cases} -(k_1+1)\ , & k_1 < 0,\ k_2 = 0 \\ -\mathrm{ind}(L), & k_1 < -1,\ \ -4k1 > k_2 > 0 \\ -k_1 + 1 - \mathrm{ind}(L)\ , & k_1 \leq -1,\ k_2 = -4k_1 \\ \frac{32}{3}k_1(1-k_1^2)\ , & k_1 \leq -1,\ k_2 > -4k_1 \\ 0 & \text{otherwise} \end{cases}$$

where $\mathrm{ind}(L) = \left(6k_1(1+k_2^2) + k_2(11+k_2^2)\right)/3$.

Now, we will introduce some special line bundles which will be used in the coming sections. The determinental line bundle $\wedge^n V$ is that whose fiber is the top exterior power of the fiber of V at each point on the manifold. When $V = \Omega$ the cotangent bundle, it defines the canonical bundle $K_X = \wedge^r \Omega$ [87]. The dual of K_X is called anticanonical bundle denoted by K_X^{-1}. We say a line bundle L is ample (or of positivity properties) if there is a positive integer P such that the tensor power $L^{\otimes P}$ has enough sections to give an embedding of X

into projective space [87]. A variety is Fano if its anticanonical bundle is ample [147]. The simplest example of a Fano variety is the complex projective space $\mathbb{P}^n$. Its anticanonical bundle is $O(n+1)$, which is ample.

Monad Bundle on CICYs

With our discussion of line bundles in place, we are ready to introduce monad bundles. Monad bundles can be defined in more generality than we will require here, and thus we will restrict ourselves to the special case in which they are defined in terms of line bundles through the short exact sequence below.

$$0 \to V \to B \xrightarrow{\mathbf{f}} C \to 0 \quad . \tag{4.44}$$

Here,

$$B = \bigoplus_{i=1}^{r_B} O_X(\mathbf{b}_i) \ , \quad C = \bigoplus_{j=1}^{r_C} O_X(\mathbf{c}_j) \ .$$

are sums of line bundles with ranks r_B and r_C respectively and $\mathbf{f}$ is a r_C by r_B matrix with elements

$$f_{ij} \in H^0(X, O(c_j - b_i)).$$

In general, the monad (4.44) defines a coherent sheaf $V = \ker(\mathbf{f})$. It is a holomorphic vector bundle when the bundle morphisms as matrix satisfies the condition

$$\mathrm{rk}(\mathbf{f}) = r_B - r_C \tag{4.45}$$

everywhere over the Calabi-Yau manifold X. This constant $n = r_B - r_C$ is the rank of V. Thus, a monad bundle is specified by two sets of sets of integers $\{b_i\}$ and $\{c_j\}$ satisfying (4.45). We will ask that any integer set appearing in $\{b_i\}$ does not also appear in $\{c_j\}$.

Suppose a monad bundle V' is defined by the short exact sequence

$$0 \to V' \to B \oplus R \xrightarrow{\mathbf{f}'} C \oplus R \to 0 \ ,$$

where the repeated summand R is a line bundle or direct sum of line bundles. Then, the bundle V' is equivalent to V defined in (4.44), thus the common summand R is, in fact, redundant.

The dual bundle V^* is given by the short exact sequence

$$0 \to C^* \xrightarrow{\mathbf{f^T}} B^* \to V^* \to 0 \ , \tag{4.46}$$

with $V^* = \text{coker}(\mathbf{f^T})$. In terms of the basis of the Kähler cone $\{J_r\}, r = 1, \ldots, m$, the Chern classes of V are given by

$$\begin{aligned} c_1^r(V) &= \sum_{i=1}^{r_B} b_i^r - \sum_{j=1}^{r_C} c_j^r \ , \\ c_{2r}(V) &= \frac{1}{2} d_{rst} \left(\sum_{j=1}^{r_C} c_j^s c_j^t - \sum_{i=1}^{r_B} b_i^s b_i^t \right) \ , \\ c_3(V) &= \frac{1}{3} d_{rst} \left(\sum_{i=1}^{r_B} b_i^r b_i^s b_i^t - \sum_{j=1}^{r_C} c_j^r c_j^s c_j^t \right) \ , \end{aligned} \tag{4.47}$$

where d_{rst} are the triple intersection numbers on X. The cohomology of V is computed through the associated long exact sequence

$$\begin{aligned} 0 \ &\to \ H^0(X,V) \to H^0(X,B) \to H^0(X,C) \\ &\to \ H^1(X,V) \to H^1(X,B) \to H^1(X,C) \\ &\to \ H^2(X,V) \to H^2(X,B) \to H^2(X,C) \\ &\to \ H^3(X,V) \to H^3(X,B) \to H^3(X,C) \to 0 \ . \end{aligned} \tag{4.48}$$

If the bundle V is poly-stable, then $h^0(X,V) = h^3(X,V) = 0$. So, the other cohomologies are $h^1(X,V)$ and $h^2(X,V)$. We only need to compute one of them from (4.48) and the other one follows by the index $ind(V) = -h^1(X,V) + h^2(X,V)$.

A monad bundle V can act as the gauge bundle in a supersymmetric vacuum of heterotic string theory, if it satisfies the following constraints:

- V is poly-stable somewhere in the Kähler cone, i.e. there exist Kähler moduli of X such that V is (poly-) stable [67]. For spaces with $h^{1,1} > 1$, the vector bundle splits its Kähler cone into "chambers" where V is stable and the chambers where it is not. These different areas are separated by the stability walls, which have important applications in the model building and the moduli stabilization [35, 57, 58, 59].

- The structure group is SU(n), i.e. $c_1(V) = 0$. From (4.47), this is the requirement that

$$\sum_{i=1}^{r_B} b_i^r = \sum_{j=1}^{r_C} c_j^r \ , \quad \forall r = 1, \ldots, m \ . \tag{4.49}$$

- Anomaly cancellation imposes a topological constraint $c_2(TX) - c_2(V) = W$ where $W \in H_2(X,\mathbb{Z})$ is a effective divisor in X wrapped by a five brane. Demanding that a supersymmetry preserving five brane exists then leads to the condition [151]

$$c_{2r}(V) = \frac{1}{2} d_{rst} \left(\sum_{j=1}^{r_C} c_j^s c_j^t - \sum_{i=1}^{r_B} b_i^s b_i^t \right) \leq c_{2r}(TX) \qquad \forall r \ . \tag{4.50}$$

Notice that unlike the last two constraints, which can be simply studied in terms of the properties of the line bundles in B and C, there is no simple expression for the stability constraint and in fact, as we have already described, it is very difficult to study. We will discuss this in detail in next sub-section.

Stability

Given a monad bundle V over a Calabi-Yau three-fold X, we will describe in more detail how to determine if this vacuum satisfies the stability constraint (4.1.3). To begin with, let's expand the Kähler form as $J = t^r J_r$ with the t^r being the Kähler moduli. Substituting this into the definition of slope in (4.33), we have

$$\mu(F) = \frac{1}{\mathrm{rk}(F)} d_{ruv} c_1^r(F) t^u t^v \ ,$$

where the $d_{ruv} = \int_X J_r \wedge J_u \wedge J_v$ are the triple intersection numbers of X, and $c_1(F) = c_1^r(F) J_r$. Introduce the "dual Kähler moduli," s_r, by $s_r \equiv d_{ruv} t^u t^v$. The slope then becomes

$$\mu(F) = \frac{1}{\mathrm{rk}(F)} s_r c_1^r(F) \ . \tag{4.51}$$

Compared with the Equation (4.33), this is a much simpler expression for the slope and will be used when studying stability.

For a general $SU(n)$ bundle V, it is difficult to check its stability. However, if the base manifold is cyclic, that is if $Pic(X) = \mathbb{Z}$, Hoppe's criterion provides a sufficient condition for stability. It is stated as follows [67, 150, 152, 153].

Theorem 4.1 (Hoppe's criterion)**.** *Over a projective manifold X with Picard group $Pic(X) = \mathbb{Z}$, let V be a vector bundle with $c_1(V) = 0$. If*

$$H^0(X, \wedge^p V) = 0, \quad \forall p = 1, 2, \ldots, n-1 \ ,$$

then V is stable.

For the favorable CICYs considered here, the cyclic ones are just those with $h^{1,1} = 1$, i.e. the

Kähler cone has dimensional one admitting an unique polarization. While for the general CICYs with $h^{1,1} > 1$, the situation become more complicated since the Kähler cone admits infinite many different polarizations, the vector bundles can be stable with respect to any of them. The Hoppe's criterion for the general manifolds (generalized Hoppe's criterion) is necessary, but no longer sufficient condition to determine the bundle stability [67, 153]. Nonetheless, it still provides an important necessary check of stability.

To study the bundle stability over more general manifolds, as discussed in section 4.1.2, it is sufficient to consider the sub-line bundles of $\wedge^p V, p = 1, 2, \ldots, \mathrm{rk}\, V - 1$. All of these sub-line bundles have the potential to make the bundle unstable and will be called potential destabilizing line bundles. For a line bundle L to be potentially destabilizing there must exist a nontrivial morphism from L to one of the $\wedge^p V$ for $p = 1, 2, \ldots, \mathrm{rk}\, V - 1$, i.e. $\mathrm{Hom}(L, \wedge^p V) = H^0(X, \wedge^p V \otimes L^*) \neq 0$. Also, if these morphisms are injective, then $H^0(X, L) = 0$. Since an injection $L \to \wedge^p V$ gives an injection $H^0(X, L) \to H_0(X, \wedge^p V)$, from the generalized Hoppe's criterion, we have $H_0(X, \wedge^p V) = 0$, thus we have $H^0(X, L) = 0$. Finally, one has to search for a polarization in the Kähler cone such that the stability condition

$$\mu(L) < \mu(V) = 0, \quad \text{for all potentially destabilizing line bundles} \tag{4.52}$$

holds. The vector bundle V is stable if there exists such a polarization and V is unstable if it does not. This systematic strategy is summarized below:

1. **Check if the generalized Hoppe's criteria hold.**

$$H^0(X, \wedge^p V) = 0, \quad p = 1, 2, \ldots, n - 1\ . \tag{4.53}$$

2. **Find all the possible potentially destabilizing line bundles.**

A line bundle L is potentially destabilizing line bundle if

$$H^0(X, L) = 0 \quad \text{and} \quad H^0(X, \wedge^p V \otimes L^*) \neq 0, \quad p = 1, 2, \ldots, n-1 \,. \tag{4.54}$$

Note that the morphism implied by these conditions is not necessarily injective. Thus the conditions here are sufficient to show stability but necessary.

3. **Search for the polarization in the Kähler cone such that the stability condition (4.52) holds.**

   V is stable if there exists a such polarization.

Now, we will give some examples of stable bundles. First, all line bundles are stable. Second, the sum of line bundles $V = \bigoplus L_i = \bigoplus O(k_i)$ are poly-stable (and slope zero) if there exists an polarization such that

$$\mu(L_i) = 0, \quad k_i^r s_r = 0 \quad \text{for each} \quad i = 1, 2, \ldots n. \tag{4.55}$$

Due to this simple expression, the stability of the sum of line bundles is easy to study. Third, consider the monad bundles which are defined using positive line bundles, i.e. all $b_i > 0$ and $c_j > 0$ in the definition of monad (4.44). The positive monad bundles are stable on cyclic CICYs [67, 150]. They are believed to be stable on non-cyclic CICYs [67, 153]. Monads with all negative line bundle components are unstable. On the other hand, monads bundles containing line bundles with entries that are vanishing or of mixed sign can still be stable [17]. In this case, however, there is no general argument and stability has to be studied case by case with the algorithm described in (4.1.3).

We now give an example of a stability analysis. This example will form the basis of some novel numerical work at the end of this chapter in Section 4.2.3. There, numerical methods

will be used to analyze the stability of this case, which has qualitatively different properties from those that have appeared in the literature to date [109, 131, 132]. Part of this novelty comes from the interplay between complex structure and stability for this bundle. Related to this, in the following analysis a rather special choice of complex structure is implicitly being made for the Calabi-Yau three-fold. The exact nature of this choice, and its relevance to stability, will be discussed in detail in Section 4.2.3 where it will be described in the context of the numerical analysis.

Let X be the Calabi-Yau three-fold defined in (4.43). Define the bundle V by the following monad

$$0 \to V \to O(2,-1) \oplus O(0,2) \oplus O(-1,1)^{\oplus 2} \xrightarrow{f} O(0,3) \to 0, \tag{4.56}$$

where $f = (f_1, f_2, f_3, f_4)$ is the bundle morphism. Since $h^{1,1} = 2$, the Kähler form of X can be expanded as $J = t_1 J_1 + t_2 J_2$. As usual, t_1 and t_2 are the Kähler moduli. The dual Kähler moduli is given by

$$s_1 = 4t_2^2, \quad s_2 = 8t_1 t_2 + 2t_2^2 \,. \tag{4.57}$$

Substituting into (4.51), the slope of a line bundle L is

$$\mu(L) = c_1^1(L) s_1 + c_1^2(L) s_2 \tag{4.58}$$

where $c_1(L) = c_1^1(L) J_1 + c_1^2(L) J_2$ is the first Chern class of L.

To begin with, it is straightforward to check that $H^0(X, V) = 0$ and $H^0(X, V^*) = 0$ from the long exact sequence (4.48). Next, we will find all the possible line bundles that satisfies the condition (4.54), i.e. the potentially destabilizing line bundles. First, consider $L = O(a, b)$ with $a, b \geq 0$. Clearly, for these line bundles $H^0(X, L) \neq 0$. Therefore by (4.54), such L can be ignored. Second, note that all $L = O(a, b)$ with $a, b \leq 0$ cannot be destabilizing line

bundles. That is, (4.52) is satisfied for all such line bundles. Therefore, the only potentially destabilizing line bundles that could concern us are those of the form $L = O(a, b)$ with $ab < 0$. After a long cohomology computation with the methods introduced in sub-section 4.1.3, we find that the sub-line bundles of V are of the form

$$O(2, -b_1), \quad b_1 \geq 2 \quad \text{and} \quad O(3, -b_2), \quad b_2 \geq 5, \quad \text{and} \quad O(4, -b_3), \quad b_3 \geq 5 \, . \tag{4.59}$$

The bundle V is stable if for all these line bundles $\mu(L) < 0$. According to Equation (4.58), the dual Kähler moduli has to be

$$\frac{s_2}{s_1} < \frac{c_1^1(L)}{c_1^2(L)}$$

for each L in (4.59). To guarantee that $\mu(L) < 0$ for all of them, we find that $\frac{s_2}{s_1} > 1$, which can be determined by the line bundle $O(2, -2)$ called the "maximally" destabilizing line bundle [67, 153]. On the other hand, since V is a $SU(3)$ bundle, one also needs to consider the sub-line bundles of $\wedge^2 V = V^*$. One can find that the sub-line bundle of V^* is of the form

$$O(-a, 1), \quad a \geq 2 \, . \tag{4.60}$$

By a similar analysis, the "maximally" destabilizing line bundle is $O(-2, 1)$, which imposes another constraint $\frac{s_2}{s_1} < 2$. Combining these two together, we find that the V is stable if $1 < \frac{s_2}{s_1} < 2$. Using (4.57) we find that the bundle is stable if $\frac{4}{3} < \frac{t_2}{t_1} < 4$ in the Kähler cone, and is unstable otherwise. The result is plotted in Figure 4.1. Notice that the different areas are separated by two 'stability walls' which are determined by the maximally destabilizing line bundles $O(2, -2)$ and $O(-2, 1)$. In summary, checking the stability of a monad bundle analytically is laborious. There is an alternative, numerical, way to obtain the same results using the generalized Donaldson's algorithm [109]. We will discuss this in the next Section.

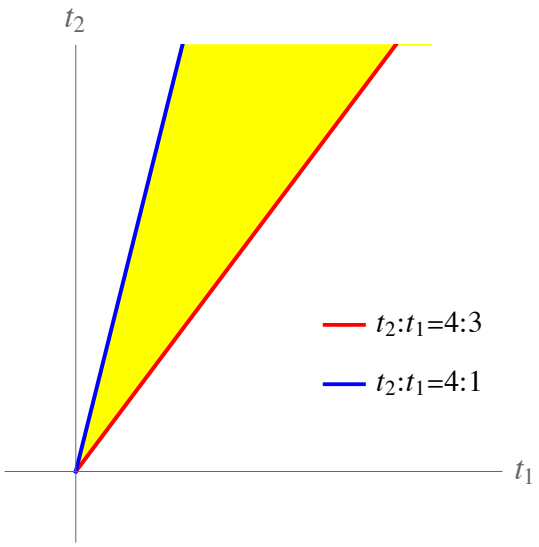

Figure 4.1: The stable chamber of the Kähler cone of X defined in (4.43) in the presence of the vector bundle V defined in (4.56). The stability walls are determined by the "maximally" destabilizing line bundle $O(2,-2)$ (red line) and $O(-2,1)$ (blue line). The bundle V is stable in the subspace (yellow) between two walls and unstable in other area.

4.2 Numerical Hermitian Yang-Mills Connections

In this section, we will introduce the generalized Donaldson's algorithm and then use it to study the Hermitian Yang-Mills connection of a simple example.

4.2.1 The Generalized Donaldson's Algorithm

In this section we will describe the generalization of Donaldson's Algorithm, introduced in Chapter 2, to study Hermitian Yang-Mills connections on a vector bundle V with rank $n > 1$. For a poly-stable bundle, $H^0(X,V) = 0$, i.e. there are no global sections. This prevents us from applying an analogue of Donaldson's algorithm directly. Instead, consider a twisting by some positive integer power k of an ample line bundle L to obtain $V \otimes L^k$. If k is sufficiently large then $H^0(X, V \otimes L^k) \neq 0$. Let $\{S^a_\alpha\}$ be a basis of $H^0(X, V \otimes L^k)$ with $a = 1, \cdots, n$ labeling the vector space directions of the fiber and $\alpha = 1, \cdots, N_k = h^0(X, V \otimes L^k)$. This

basis defines an embedding from X to a Grassmannian $G(n, N_k)$ [131].

$$x \longmapsto \left[\begin{pmatrix} S_0^1(x) \\ \vdots \\ S_0^n(x) \end{pmatrix} : \cdots : \begin{pmatrix} S_{N_k-1}^1(x) \\ \vdots \\ S_{N_k-1}^n(x) \end{pmatrix} \right]. \tag{4.61}$$

With these global sections S_α^i, we can define a bundle metric $\tilde{G}$ of $V \otimes L^k$ as [109, 131, 132]

$$(\tilde{G}^{-1})^{\bar{j}i} = \sum_{\alpha,\beta=0}^{N_k-1} (\bar{S})_{\bar{\beta}}^{\bar{j}} H^{\bar{\beta}\alpha} S_\alpha^i, \tag{4.62}$$

where $H = H_{\alpha\bar{\beta}}$ is, as in Chapter 2, a constant hermitian matrix with dimension N_k.

Now, by the logic of Donaldson's algorithm, we define T operator [131, 132]

$$T(H)_{\alpha\bar{\beta}} = \frac{N_k}{n \operatorname{Vol}_{CY}} \int_X S_\alpha^i (\bar{S}_{\bar{\delta}}^{\bar{j}} H^{\bar{\delta}\gamma} S_\gamma^i)^{-1} \bar{S}_{\bar{\beta}}^{\bar{j}} \, \mathrm{dVol}, \tag{4.63}$$

where n is the rank of V. Notice that we introduce an extra normalization n in the definition of T operator to make it converging smoothly. The balanced metric is determined by the fixed point of T operator defined below

$$T(H_k^b) = H_k^b. \tag{4.64}$$

In [154, 155] it was shown that the balanced metric has good curvature properties and will be summarized below.

Theorem 4.2 (Wang, Seyyedali)**.** *If V is a Gieseker stable bundle with rank r, then there exists an unique balanced metric associated to H_k^b for each twist of V, i.e. $V \otimes L^k$. After untwisting, H_k^b gives a sequence of bundle metrics $\{G_k\}$ of V. When $k \to \infty$, the metric G_∞*

solves the "weak Hermite-Einstein equation"

$$g^{a\bar{b}}F_{a\bar{b}} = \Big(\mu + \frac{\bar{R} - R}{2}\Big)\mathbf{1}_{n\times n}$$

where

- *R is the scalar curvature.*
- *$\overline{R} = \int R\sqrt{\det g}\; d^{2d}x$ is the averaged scalar curvature.*

When X is Calabi-Yau manifold and V is a $SU(n)$ bundle, R, $\overline{R}$ and μ vanish in Theorem 4.2. The "weak Hermite-Einstein equation" then reduces to the Hermitian Yang-Mills equation. Since all poly-stable bundles are Gieseker stable, this theorem implies that Hermitian-Einstein bundle metrics on poly-stable bundles can be approximated by a series of balanced metrics with $k \to \infty$. If the bundle V is not Gieseker stable, then the balanced metric of twisted bundle $V \otimes L^k$ does not exist and the corresponding bundle metric of V after untwisting does not solve the Hermitian Yang-Mills equations.

The parameters giving the balanced metric H_k^b can be computed iteratively by

$$(H_{m+1})^{\bar{\beta}\alpha} = (T(H_m)_{\alpha\bar{\beta}})^{-1} \tag{4.65}$$

where H_{m+1} and H_m are two matrix denoting the the mth and $(m+1)$th iteration of T operator. The initial matrix H_0 can be chosen to be any hermitian matrix. To compare H_m and H_{m+1}, it is sufficient to consider their eigenvalues. Let $v^{max}(m)$ be the maximum eigenvalue of H_m. Then, define an function [109]

$$r_{max}(m) = \frac{v^{max}(m+1)}{v^{max}(m)} - 1. \tag{4.66}$$

Obviously, if as $m \to \infty$ the quantity $r_{max}(m)$ approaches to zero, then balanced metric H_k^b exists and the bundle V is poly-stable. While if $r_{max}(m)$ do not approach zero, then H_k^b does not exist and V is not Gieseker stable. This observation provide us a way to distinguish poly-stability of bundles by studying the existence of balanced metrics.

Now, suppose we have balanced bundle metric $\tilde{G}$ of $V \otimes L^k$ by (4.64). To obtain a bundle metric G on V, we need to 'untwist' it by the bundle metric G_L of L. In general, G_L can be computed using Donaldson's algorithm again with some twist k_L. The larger k_L is, the more accurate is the G_L. However, if we consider two Donaldson's algorithms together, the total error depends on both k and k_L. In [132] a systematic study was performed on how the choice of k_L effects the total error of the algorithm. They find that the most efficient choice is to take $k_L = nk$. Then $\wedge^n(V \otimes L^k) = L^{nk}$, which is just the determinant line bundle. The fiber metric becomes $(G_L)^{nk} = \wedge^n \tilde{G} = \det(\tilde{G})$. In this case, we don't need to run Donaldson's algorithm again for fiber metric on L and so we can decrease the total error in the algorithm. Considering this untwisting, the bundle metric on V becomes

$$G^{-1} = \frac{\tilde{G}^{-1}}{(\det \tilde{G}^{-1})^{\frac{1}{n}}} = \frac{S^+ H S}{(\det(S^+ H S))^{\frac{1}{n}}} \,. \tag{4.67}$$

It is easy to check that $\det(G^{-1}) = 1$ as expected. Substituting this result into the Hermitian Yang-Mills equation (4.32), we have

$$g^{a\bar{b}} F_{a\bar{b}} = g^{a\bar{b}} \partial_{\bar{b}} (\tilde{G}^{-1} \partial_a \tilde{G}) - \frac{1}{n} \operatorname{tr}(g^{a\bar{b}} \partial_{\bar{b}} (\tilde{G}^{-1} \partial_a \tilde{G})) 1_{n \times n} \,. \tag{4.68}$$

Here, $g^{a\bar{b}} F_{a\bar{b}}$ is a $n \times n$ matrix and will approach to zero matrix with $k \to \infty$ if the bundle under consideration is stable. This allows us to define an error function [132]

$$\tau(A_\mathcal{V}) = \frac{1}{n} \int_X \Big(\sum |\lambda_i| \Big) \, \mathrm{dVol}_{CY}, \tag{4.69}$$

where λ_i, $i = 1, \ldots, n$ are the eigenvalues of $g^{a\bar{b}} F_{a\bar{b}}$. Obviously, it approaches zero if $\{G_k\}$ converges to Hermitian-Einstein bundle metric.

The Hermitian Yang-Mills connection in the "mathematical" gauge is [131, 132]

$$A^{(1,0)}_{\bar{b}} = \bar{\partial}_{\bar{b}} G \cdot G^{-1} = \bar{\partial}_{\bar{b}} \tilde{G} \cdot \tilde{G}^{-1} - \frac{1}{n} \operatorname{tr}(\bar{\partial}_{\bar{b}} \tilde{G} \tilde{G}^{-1}) \tag{4.70}$$

where $\tilde{G}^{-1}$ is the fiber metric (4.5). To obtain the physical Hermitian Yang-Mills connection, we need to perform a complex gauge transformation h, which is related to the fiber metric by $G^{-1} = h \cdot h^{+}$. It is convenient to write it as

$$h = \frac{\tilde{h}}{(\det \tilde{G}^{-1})^{\frac{1}{2n}}} \tag{4.71}$$

where $\tilde{h}$ is the analogy gauge transformation for the twisted bundle with $\tilde{G}^{-1} = \tilde{h} \cdot \tilde{h}^{+}$. From (4.19), this quantity is given by

$$\tilde{h} = U \sqrt{\tilde{\Lambda}} U^{+} \tag{4.72}$$

where U and $\tilde{\Lambda}$ consist of the eigenvectors and eigenvalues of $\tilde{G}^{-1}$ respectively. Substituting this quantity into (4.71), it is easy to check that $\det h = 1$, i.e. $h \in SL(n, \mathbb{C})$ is a complexified $SU(n)$ gauge transformation. By (4.20), the Hermitian Yang-Mills connection in "physical" gauge is

$$A^{(0,1)}_{\bar{b}} = \bar{\partial}_{\bar{b}} h \cdot h^{-1} = \bar{\partial}_{\bar{b}} \tilde{h} \cdot \tilde{h}^{-1} - \frac{1}{2n} \operatorname{tr}(\tilde{G} \bar{\partial}_{\bar{b}} \tilde{G}^{-1}) \tag{4.73}$$

and the $A^{(1,0)}$ component is obtained by the anti-hermitian property (4.18).

4.2.2 Example: A $SU(2)$ Vector Bundle on a K3 Surface

Now, we will demonstrate the Generalized Donaldson's Algorithm in an example. The manifold will be taken to be a K3 surface $X = [\mathbb{P}^3|4]$ with defining polynomial

$$Z_0^4 + Z_1^4 + Z_2^4 + Z_3^4 - 2Z_0Z_1Z_2Z_3 = 0\ . \tag{4.74}$$

Since the Picard group of this manifold is rank 1, the polarization is fixed by $L = O(1)$. The $SU(2)$ vector bundle V will be taken to be the dual monad

$$0 \to O(-3) \xrightarrow{f} O(-1)^{\oplus 3} \to V \to 0, \tag{4.75}$$

where the bundle morphisms are $f = (x_0^2, x_1^2, x_2^2)$. Now, we will use Donaldson's algorithm to study the Hermitian Yang-Mills connection of V. The detail of this algorithm is summarized below

1. Find the embedding (4.61) for the twist $k > 0$.

   The twisted bundle $V \otimes L^k$ is given by

   $$0 \to O(-3+k) \longrightarrow fO(-1+k)^{\oplus 3} \to V \otimes L^k \to 0. \tag{4.76}$$

   The space of global sections is

   $$H^0(X, V \otimes L^{\otimes k}) = \frac{H^0(X, O(-1+k)^{\oplus 3})}{f(H^0(X, O(-3+k)))}. \tag{4.77}$$

   Let $\{\hat{e}_i\}, i = 1, \ldots, 3$ to be a frame of $O(-1+k)^{\oplus 3}$. Then a basis of $H^0(X, V \otimes L^{\otimes k})$

can be written as

$$S_\alpha = \sum_{i=1}^{3} S_\alpha^i \hat{e}_i. \tag{4.78}$$

However, these four frames are not independent. The exactness of (4.76) implies that $\sum_{i=1}^{3} f_i \hat{e}_i = 0$. If we treat the $\hat{e}_3$ to be a redundant frame, then

$$\hat{e}_3 = \frac{f_1 \hat{e}_1 + f_2 \hat{e}_2}{(-f_3)} \ . \tag{4.79}$$

With this in mind, the basis in (4.78), can be written as

$$S_\alpha = \sum_{i=1}^{2} \left(S_\alpha^i - \frac{S_\alpha^3}{f_3} \right) \hat{e}_i \ . \tag{4.80}$$

These sections gives the desired embedding (4.61).

2. Find the parameters H_k^b leading to the balanced metric via (4.64). Let H_0 be identity matrix with dimension N_k and apply the T operator (4.63) on it iteratively. The computation will converge and the fixed point is H_k^b. With it, we can get a bundle metric $\tilde{G}^k$ on $V \otimes L^k$ using (4.62). We then obtain the bundle metric G_k on V by untwisting as in (4.67).

3. Assuming the Ricci-flat metric $g^{a\bar{b}}$ of X has been computed with the algorithms discussed in Chapter 2, compute the error function τ (4.69) for each G_k. Check it is approaching a small value.

4. Compute the Hermitian Yang-Mills connection in (4.70) with the fiber metric G_k. Then, transform it to the "physical" gauge by the gauge transformation (4.73).

Following this algorithm we can compute the Hermitian Yang-Mills connection of the example above. The error function is plotted in Figure 4.2. We find that, with increasing k, the error

function decreases with a rate of order $O(k^{-2})$, which agrees with the analytic analysis [131] performed for this bundle. The bundle is stable and this can be detected numerically.

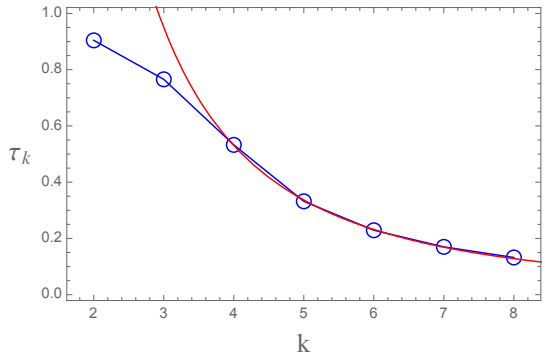

Figure 4.2: The error function (4.69) of the numerical approximation to the Hermitian Yang-Mills connection on the bundle V given in (4.75) over the K3 surface given in (4.74). The least-squares-fit curve is $8.76/k^2 - 0.07/k$.

4.2.3 Example: A $SU(3)$ Vector Bundle on a Calabi-Yau three-fold

In this subsection, we return to the example discussed in Section 4.1.3, equation (4.56). We will first describe how the poly-stability of this bundle depends crucially on the complex structure of the base Calabi-Yau three-fold. We will then show that we can decide the stability of this bundle numerically, using the methods discussed in this Chapter. In some ways this work can be seen as the 'complex structure dependence' analogue of the numerical investigation of Kähler moduli dependence of stability, as carried out in [109]. The complex structure dependence of such computations is built in to the numerical methods in a much more explicit manner than the dependence on the Kähler form. Nevertheless, it is non-trivial to show that numerical stability analyses work for such bundles. These constructions are infinitesimally close to being in a non-stable regime of moduli space and, as such, it is not completely obvious that an approximate numerical approach will be able to resolve the necessary structure. Given this, the results of this section constitute a novel example of a

type which has not appeared in the literature prior to this work.

The Calabi-Yau three-fold X we will consider is a degree $(2,4)$ hypersurface, with defining relation P, in the ambient space $\mathbb{P}^1 \times \mathbb{P}^3$, as defined in (4.43). The holomorphic vector bundle V is defined by the monad (4.56), which we reproduce here for convenience

$$0 \to V \to O(2,-1) \oplus O(0,2) \oplus O(-1,1)^{\oplus 2} \xrightarrow{f} O(0,3) \to 0 \ . \tag{4.81}$$

The bundle map $f = (f_1, f_2, f_3, f_4)^T$ takes values in

$$f_1 \in H^0(X, O(-2,4)), \quad f_2 \in H^0(X, O(0,1)), \quad f_3, f_4 \in H^0(X, O(1,2)). \tag{4.82}$$

By the techniques developed in Sec. 4.1.2, it is straightforward to show that $h^0(X, O(0,1)) = 4$ and $h^0(X, O(1,2)) = 20$. We will choose the f_2, f_3, f_4 to be the generic elements in the corresponding cohomologies.

However, from the long exact sequence associated with Koszul sequence (4.42),

$$0 \to H^0(X, O(-2,4)) \to H^1(A, O(-4,0)) \xrightarrow{P} H^1(A, O(-2,4)) \to \cdots \ , \tag{4.83}$$

we find that the dimension of $H^0(X, O(-2,4))$ depends on the choice of complex structure P. A direct calculation utilizing the Bott-Borel-Weil Theorem (4.40), shows that,

$$h^0(B, O(-2,4)) = \begin{cases} 0, & P \quad \text{generic} \\ 1, & P = x_1^2 P_1(y) + x_2^2 P_2(y) \end{cases} \tag{4.84}$$

where $P_1(y)$ and $P_2(y)$ are arbitrary homogeneous polynomials in y of degree 4.

When P takes the special form given in (4.84), the relevant piece of the bundle map can be

shown to be given by $f_1 = \frac{P_2(\mathbf{y})}{x_1^2}$ using the technology introduced in [105]. For a generic P, by contrast, $f_1 = 0$. Thus, only a restricted sub-locus of complex structure moduli space can an irreducible holomorphic monad of the form (4.56) be defined. That the complex structure of X was restricted to this locus was being implicitly assumed in Section 4.1.3.

As discussed in Section 4.1.3, when the irreducible monad V can be defined, it is stable for the choice of polarization $L = O(1,2)$. On the other hand, when P takes the generic form in (4.84), then the bundle map $f_1 = 0$ and the $SU(3)$ bundle V becomes

$$V' = O(2,-1) \oplus V", \tag{4.85}$$

$$0 \to V" \to O(0,2) \oplus O(1,1)^{\oplus 2} \xrightarrow{f'} O(0,3) \to 0\ . \tag{4.86}$$

This is an $S(U(1) \times SU(2))$ bundle and is not poly-stable for the choice of polarization $L = O(1,2)$.

Let us see is we can detect the stability properties of V and V' with numerical methods. First, we compute the Ricci-flat metric of X with Donaldson's algorithm. The computational details have been discussed in Section 2.3.2. Next, we apply the numerical methods described in this Chapter to the stable bundle V, on the special locus in complex structure moduli space, and the unstable bundle V', given a generic defining relation. Following the same procedure to that used in Section 4.2.2, we compute the numerical connection by iteration of the T operator from $k = 1$ to $k = 3$. For each iteration, the measure of convergence (4.66) is evaluated for both V and V'. The results are plotted in Figure 4.3. As can clearly be seen, the stable bundle V converges nicely, with the plots assymptoting to zero. The same is not true for the unstable bundle V'. These results clearly indicate that their exists a Hermitian Yang-Mills connection on V, but not on V', in agreement with the algebraic

analysis. We also compute the error functional (4.69) for the numerical connections from $k = 2$ to $k = 4$. The results, as presented in Figure 4.4, again indicate the the existence of Hermitian Yang-Mills connection for stable bundle V and not for the unstable bundle V'.

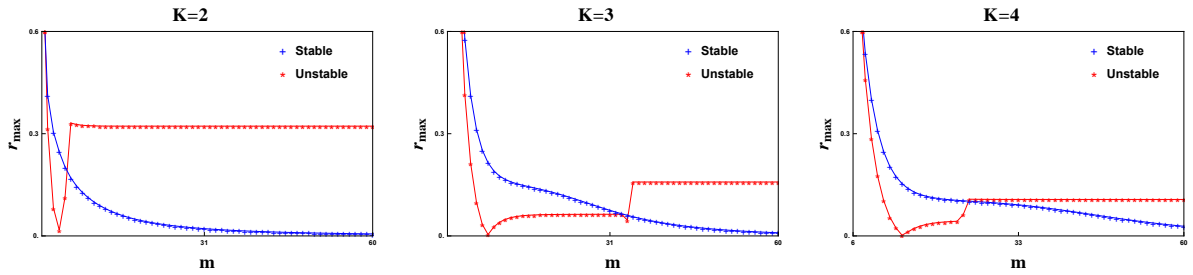

Figure 4.3: The measure of convergence r_{max} for the stable bundle V (blue) and the unstable bundle V' (red) as a function of the iteration m of the T operator for $k = 2, 3, 4$. It can clearly be seen that measure approaches zero for V, but not for V', in the large m limit.

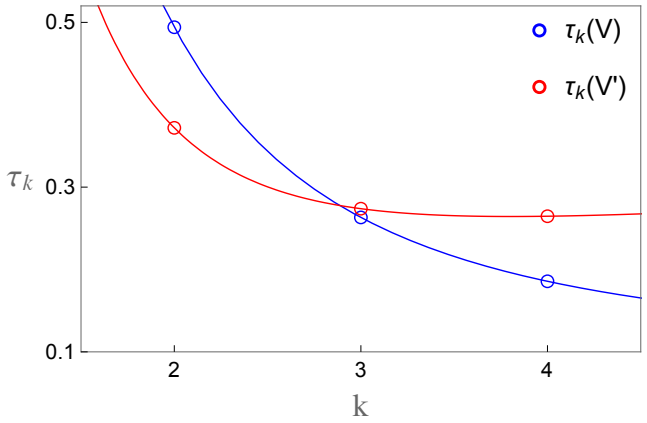

Figure 4.4: The error function τ as a function of the twist k for both V (Blue) and V' (Red). The error function can be seen to be decreasing with the twist for the stable bundle V but not for the unstable object V'.

In conclusion, we have proven that numerical methods can be used to establish the stability of bundles, even if they are only stable at higher codimension loci in complex structure moduli space. As mentioned above, this work complements the analysis of [109], which demonstrated that numerical methods could account for Kähler moduli dependence of stability as embodied

by the phenomenon of stability walls.

In this chapter we have already seen some applications of the numerical methods we have reviewed for solving the Hermitian Yang-Mills equations. In the next chapter we will describe a further use of these methods, in a situation where analytic results are not available to us.

Chapter 5

Numerics and Chern-Simons Superpotentials

We will apply the generalized Donaldson's algorithm to compute the holomorphic Chern-Simons invariant in Calabi-Yau compactification. As part of the superpotential in the low-energy effective theory, this invariant is important for our understanding of problems like moduli stabilization. This chapter is based on an ongoing project.

5.1 Introduction

In [60], methods were introduced to compute contributions to the superpotential of heterotic string compactifications that arise from Chern-Simons invariants associated to the gauge and tangent bundles. Those methods were rather complete but did suffer from one non-explicit step. The computations were performed with the E_8 gauge fields and the spin connection in a gauge commonly used in mathematics where they are of $(1,0)$ index type. Many computations in the physics literature are carried out instead in gauges where these connections are real. Changing between the two gauges involves a non-trivial gauge transformation which can modify the result of the computations. This step in the computations was omitted as it requires detailed knowledge of gauge fields, associated to bundles over Calabi-Yau three-folds, that solve the Hermitian Yang-Mills equations. Although, due to the complexity of

the situation and the fact that the Donaldson Uhlenbeck Yau theorem is non constructive [65, 66], analytic expressions for such gauge fields are not available, numerical expressions for these objects can be obtained [85, 109, 131, 132]. In this work we will use these numerical techniques to complete this last step in the computations of [60].

Chern-Simons invariants appear in several key places in the description of heterotic compactifications. Consider a compactification of the heterotic string on a smooth Calabi-Yau three-fold X with a gauge bundle V. The Gukov-Vafa-Witten superpotential [69] in the four dimensional theory is as follows

$$W = \int_X (H + idJ) \wedge \Omega \, . \tag{5.1}$$

Locally the Neveu-Schwarz threeform field strength can be written as

$$H = H_0 + \alpha'(\omega_3(\omega) - \omega_3(A)) \;\; \text{where} \;\; \omega_3(A) = \frac{1}{8\pi^2} \operatorname{tr}(dA \wedge A + \frac{2}{3} A^3) \tag{5.2}$$

and a similar expression holds for $\omega_3(\omega)$. In (5.2) H_0 is a closed contribution to H, A is the connection on the gauge bundle and ω is the spin connection. Given this, we see that the superpotential (5.1) contains a term

$$W_{\text{CS}} = \alpha' \int_X (\omega_3(\omega) - \omega_3(A)) \wedge \Omega \tag{5.3}$$

This is the form of the holomorphic Chern-Simons invariant that is frequently given in the physics literature.

The ordinary Chern-Simons invariants also appear in such compactifications of heterotic string theory. The field strength (5.2) obeys a quantization condition which is frequently

written as follows

$$\frac{1}{\alpha'}\int_C H - \int_C (\omega_3(\omega) - \omega_3(A)) \in \mathbb{Z}\ . \tag{5.4}$$

Here, C is any three-cycle in X. This condition essentially says that H_0 in (5.2) is integrally quantized. The second term in (5.4), a three dimensional integral, is the form in which ordinary Chern-Simons invariants are frequently written in the physics literature.

The ordinary and holomorphic Chern-Simons invariants that appear in (5.3) and (5.4) above are, in fact, not well defined in isolation. The integrands that appear are gauge dependent, and as such it is not possible to construct a well defined integral over X or C in the usual manner. The result would depend on the partition of unity used in constructing the integral over the manifold from those over coordinate patches.

For the superpotential expression this issue is solved in the physical situation by noting that the superpotential as a whole includes H and not simply $\mathrm{tr}(\omega_3(A) - \omega_3(\omega))$. The Neveu-Schwarz field strength is gauge invariant, and as such the superpotenial (5.1) is well defined. Nevertheless, in terms of computations, it is inconvenient that the Chern-Simons contribution to the superpotential is not separately well defined. For the flux quantization condition (5.4), the situation is more serious. The equation (5.4) is simply not well defined as written and we must be more careful in defining this aspect of heterotic theories.

To account for these issues, the authors of [60] pointed out that the correct definitions to use for the Chern-Simons invariants above are those taken from the mathematics literature [156, 157]. Consider two connections, A and A_0, on the same vector bundle $\mathcal{V}$. The holomorphic Chern-Simons invariant is then defined as follows [156].

$$CS_{A_0}(A) = \int_X \frac{1}{8\pi^2}\,\mathrm{tr}\left(\overline{\partial}_{A_0} a \wedge a + \frac{2}{3} a \wedge a \wedge a + 2a \wedge F_0\right) \wedge \Omega\ . \tag{5.5}$$

In this expression A is the argument of the Chern-Simons invariant and A_0 is referred to as the reference connection. The adjoint valued one form $a = A - A_0$ and F_0 is the field strength of the reference connection. Finally the derivative operator appearing is defined as $\overline{\partial}_{A_0} a = da + A_0 \wedge a + a \wedge A_0$. In a similar fashion the ordinary Chern-Simons invariants found in the mathematics literature are defined as follows [157].

$$OCS_{A_0}(A, C) = \int_C \frac{1}{8\pi^2} \operatorname{tr} \left(\overline{\partial}_{A_0} a \wedge a + \frac{2}{3} a \wedge a \wedge a + 2a \wedge F_0 \right) . \tag{5.6}$$

Note that both (5.5) and (5.6) are manifestly well defined. The integrands in these cases are gauge invariant and thus the problems which were discussed above with regard to the definitions of (5.3) and (5.4) simply do not appear.

How does one relate the well defined quantities (5.5) and (5.6) to the quantities appearing in heterotic physics? To make such a connection it is useful to rewrite (5.5) as follows

$$CS_{A_0}(A) = \int_X \frac{1}{8\pi^2} \operatorname{tr}(\omega_3(A) - \omega_3(A_0) - d(A \wedge A_0)) \wedge \Omega \, . \tag{5.7}$$

A similar expression can be obtained by rewriting (5.6). This rewriting makes the mathematical definition of the holomorphic Chern-Simons invariant look more like (5.3) if we set $A_0 = \omega$, that is if we identify the reference connection with the spin connection. but there are still a number of differences. The first issue to be addressed is that the definition (5.7) is given in terms of two connections on a single bundle, whereas the physical quantities appearing in (5.3) and (5.4) seemingly involve two different bundles, V and TX. In [60] it was pointed out that this is easily resolved by noting that, in a consistent heterotic compactification $\mathrm{Ch}_2(TX) = \mathrm{Ch}_2(V)$, at least in the absence of five-branes. A long standing result [158, 159] then says that the bundles V and TX are the same in terms of smooth structure, even if they differ at the holomorphic level. The quantity H is gauge invariant under both

diffeomorphisms and gauge transformations. We are therefore free to choose gauges where ω and A are written with respect to the same trivialization. Further, we can choose a gauge where at least one of the connections is $(1,0)$ in terms of index structure in the trivialization chosen. Such a choice sets the term involving $d(A \wedge A_0)$ in (5.7) to zero. If we make both of these choices, it turns out that (5.7) and (5.5) become the same - thus relating the physics to the well defined mathematical quantity.

For the ordinary Chern-Simons terms appearing in (5.4) the situation is different. Equation (5.4) is simply not well defined as stands, and the Chern-Simons term appearing should be replaced by (5.6) once the above gauge choices have been made.

It is worth noting that the different types of Chern-Simons terms appearing in the heterotic theory are not unrelated. As explained in [60], we have that

$$W_{\text{CS}} = \alpha' \left(b_i \mathcal{Z}^i - a^i \mathcal{G}_i) \right) \tag{5.8}$$

where

$$a^i = \text{OCS}_\omega(A, \mathcal{A}^i) \;\text{ and }\; b_i = \text{OCS}_\omega(A, \mathcal{B}_i) \; . \tag{5.9}$$

Here $\mathcal{A}^i$ and $\mathcal{B}_i$ are the usual symplectic cycle basis of special geometry, $\mathcal{Z}^i$ is the associated homogeneous coordinates on complex structure moduli space and $\mathcal{G}_i$ is the derivative, with respect to those coordinates, of the pre-potential.

In [60], methods were given to compute Chern-Simons invariants such as (5.5) in cases of physical interest for the heterotic string. The key technical ingredient in these computations is a real bundle morphism between the gauge and tangent bundles, which allows us to write A and ω with respect to the same local trivialization of the underlying smooth bundle. As

mentioned above, the implementation of these methods as presented in [60] does have one incomplete step, however, and, as we will discuss in the next section, it is this gap that we will fill by using numerical methods.

5.2 Computing Chern Simons Invariants

To compute a Chern-Simons invariant of the form (5.7) we consider starting with two bundles $V \to X$ and $V' \to X$ over the Calabi-Yau three-fold X. Since we require these two bundles to be real isomorphic there is a (possibly non-holomorphic) bundle isomorphism $f : V' \to V$. Given connections ∇_0 on V and ∇' on V', together with local frames s_i and s'_i associated to V and V', we can write down the associated gauge fields,

$$\nabla_0 s_i = A^j_{0i} s_j \quad , \quad \nabla' s'_i = A'^j_i s'_j \quad . \tag{5.10}$$

To compute (5.7), we need to describe the gauge fields in terms of the same local trivialization. To do this, we can transport the connection ∇' on V' to a connection ∇ on V using the bundle morphism f. We define,

$$\nabla(s) = f \circ \nabla'(f^{-1} \circ s), \tag{5.11}$$

where s is any section of V. We can also map across the frame s'_i of V' to a frame $\tilde{s}_i$ on V via $\tilde{s}_i = f \circ s'_i$. Given that both $\tilde{s}_i$ and s_i are frames on V we have,

$$s_i = P^j_i \tilde{s}_j \tag{5.12}$$

for some gauge transformation P. We can write the gauge fields associated to ∇ corresponding to the same frame which is used to describe A_0 in (5.10). One finds,

$$\nabla(s_i) = A^j_i s_j \quad \text{where} \quad A = P^{-1}A'P + P^{-1}dP. \tag{5.13}$$

Now if we assume that A_0 is of $(1,0)$ index structure (for example is a Chern-connection) then we can ignore the $d(A \wedge A_0)$ term in (5.7). For the remaining terms in the integrand we find the following

$$\omega_3(A) - \omega_3(A_0) = \omega_3(A') - \omega_3(A_0) + \mathrm{tr}\left(dPP^{-1}dA' - A'(dPP^{-1})^2 - \frac{1}{3}(dPP^{-1})^3\right). \tag{5.14}$$

Now if we take both A' and A_0 to be $(1,0)$ in index structure, for example taking them to be Chern-connections, then we arrive at the following expression for the Chern-Simons invariant

$$CS_{A_0}(A) = -\frac{1}{3}\frac{1}{8\pi^2}\int_X \mathrm{tr}(\theta_P)^3 \wedge \Omega \quad \text{where} \quad \theta_P = P^{-1}dP. \tag{5.15}$$

The point of the index structure assumptions made above, which minimally reduce to taking A_0 and A' to be $(1,0)$, is that they render this result dependent only on the real bundle morphism through P. We do not need to know the exact form of any of the gauge fields to compute (5.15).

In a heterotic context the above calculational procedure can be applied by, for example, taking $A_0 = \omega$ and A' to be the gauge connection. Since the solutions of both the Hermitian-Yang-Mills equations and the equations defining the spin connection result in Chern-connections in appropriate gauges, the index structure requirements above can be satisfied. However, most physical analyses of these compactifications are carried out in

gauges where the gauge field is real - in distinction to gauges where components of one index type vanishes.

To regain a physical gauge it is important to note that we would need different gauge transformations on A and A_0. Since (5.5) and (5.6) are only invariant under transformations that act on both A and A_0 in the same fashion, the transition to physical gauge will change the answer obtained for the physical quantity of interest. As discussed in [60, 156, 157], this change will be by an integral multiple of a period. We review the argument briefly here.

Consider constructing two bundles $\mathbb{V}$ and $\mathbb{V}_0$ on $C \times S^1$. We describe the circle as the interval $[0, 1]$ with the ends identified. We then construct $\mathbb{V}$ from V by using a large gauge transformation g to glue $V|_{C\times\{0\}}$ to $V|_{C\times\{1\}}$. We construct $\mathbb{V}_0$ in an analagous fashion but use the identity, rather than g, in performing the gluing. Let us define $\mathbb{A}$ to be some connection on $\mathbb{V}$ that restricts to A on the bundle over $C \times \{0\}$, and thus $g(A)$ on $C \times \{1\}$. Similarly we specify a connection $\mathbb{A}_0$ on $\mathbb{V}_0$ that restricts to A_0 on both $C \times \{0\}$ and $C \times \{1\}$. Given this situation we can view the manifold and associated bundles in two manners. Viewing the construction as a bundle over a direct product of C and a line interval, we can use Stokes' theorem to write the following

$$\mathrm{OCS}_{A_0}(g(A), C) - \mathrm{OCS}_{A_0}(A, C) = \int_{C\times S^1} \frac{1}{8\pi^2} \left(\mathrm{tr}(\mathbb{F} \wedge \mathbb{F}) - \mathrm{tr}(\mathbb{F}_0 \wedge \mathbb{F}_0)\right). \tag{5.16}$$

Viewing the construction instead as described in the proceeding paragraph, as a set of non-trivial bundles over $C \times S^1$ we can identify the right hand side of (5.16) as an integer. Thus the ordinary Chern-Simons invariants change under large gauge transformations by integers. Given (5.8), this makes it clear that holomorphic Chern-Simons invariants change under separate large gauge transformations of their argument or reference connection by an integer multiple of a period.

The goal of the current work, then, is to show that the contribution to the Chern-Simons invariant appearing in heterotic superpotentials, arising from converting the connections into a physical gauge, can be efficiently computed using numerical techniques. In other words, we wish to consider the case where we compute the superpotential in a situation where the gauge fields are in physical gauge and $H_0 = 0$.

Let us start by putting A in physical gauge. We envisage doing this as a final step, after transforming A' to A, using the real bundle morphism. We define the resulting physical gauge connection A_r and associated gauge transformation h by

$$A_r = h^{-1}Ah + h^{-1}dh. \tag{5.17}$$

Given the gauge transformation properties of the terms in (5.7), and the fact that A_0 is $(1,0)$, transforming A to physical gauge induces the following contribution to the Chern-Simons invariant

$$\mathrm{CS}_{A_0}(A_r) - \mathrm{CS}_{A_0}(A) = -\frac{1}{8\pi^2}\,\mathrm{tr}\int_X (\theta_P^2\theta_h + \theta_P\theta_h^2)\wedge\Omega - \frac{1}{3}\frac{1}{8\pi^2}\int_X \mathrm{tr}\,\theta_h^3\wedge\Omega. \tag{5.18}$$

Here we have defined $\theta_h = dhh^{-1}$. The second term on the right hand side of (5.18) is determined purely in terms of h. This is the quantity we will compute in the next section. Note that finding h requires explicit knowledge of the gauge connection - hence our recourse to numerical methods. The first term on the right hand side of (5.18) involves both the gauge transformation h and the transformation P associated to the real bundle morphism f. In any given case of interest, this real bundle morphism would have to be known already, so that the rest of the computation outlined in this section can be completed. There is then no impediment to evaluating this term if one can demonstrate one has adequate control over h. Thus, we will simply focus on the term that is an integral of θ_h^3 in what follows. It should

be noted that finding bundle morphisms such as f is another bottleneck to progress in these computations. It would be interesting to ask if numerical methods could aid in finding P as well.

Having put A in physical gauge we can then repeat the process to transform A_0 to a real gauge field A_{0r}

$$A_{0r} = g^{-1}A_0 g + g^{-1}dg. \tag{5.19}$$

This results in a further change to the holomorphic Chern-Simons invariant,

$$\begin{aligned} \mathrm{CS}_{A_{0r}}(A_r) - \mathrm{CS}_{A_0}(A_r) &= \frac{1}{3}\frac{1}{8\pi^2}\int_X \mathrm{tr}\,\theta_g^3 \wedge \Omega \\ &+ \frac{1}{8\pi^2}\int_X \mathrm{tr}\left(\theta_P^2\theta_{gh} + \theta_h^2\theta_{gh} - \theta_P\theta_{gh}^2 - \theta_h\theta_{gh}^2\right) \wedge \Omega, \end{aligned} \tag{5.20}$$

where $\theta_{gh} = hg^{-1}dgh^{-1}$. Clearly, if it can be demonstrated that numerical methods are capable of finding h and computing the necessary integrals in (5.18) a similar process could be carried out for g and the integrals appearing in (5.20).

As a final note we will mention that the bundle we will consider in the next section does not have the same second Chern-character as the tangent bundle. This example has been chosen to give a simple case on which the methodology can be demonstrated. We are envisaging it as part of a larger, direct sum of bundles in the complete heterotic compactification which is real isomorphic to TX. A similar computation would then have to be performed for all of the other components of the E_8 gauge bundle of the theory in order to put all of the gauge fields appearing in the reduction ansatz in physical gauge.

5.3 Numerical Method

In this section we will describe in detail how to explicitly compute the gauge transformation h in (5.17) and use it to compute the second term in the right hand side of (5.18). To strip away some of the pre-factors from (5.18) we will define the integral,

$$I = \int_X \mathrm{tr}(\theta_h)^3 \wedge \Omega, \quad \theta_h = (\bar{\partial} h) h^{-1} \,, \tag{5.21}$$

and will compute this quantity in what follows.

As discussed in Chapter 4, for a given fiber metric of vector bundle V, the transformation h can be determined by (4.19). In our case, the fiber metric should be the Hermitian-Einstein metric G (the Chern connection of which is the Hermitian Yang-Mills connection). Although an analytic form of G is yet unknown, we can get a well controlled numerical approximation to it by utilizing Donaldson's algorithm as in Chapter 4. However, in such a numerical procedure, instead of working with the metric on V, it is convenient to express everything in terms of the (inverse) metric $\tilde{G}^{-1}$ on the twisted bundle $V \otimes L^k$. We will therefore express the integral (5.21) in terms of the quantities associated to the twisted bundle, in particular the $\tilde{G}^{-1}$. We will then finally compute the integral via numerical integration.

Recall, in Donaldson's algorithm, that the fiber metric $\tilde{G}^{-1}$, parameterized by a hermitian matrix H, is given by equation (4.62). The Hermitian-Einstein metric is derived from $\tilde{G}^{-1}$ by untwisting as in (4.67) and the corresponding gauge transformation h satisfying $G^{-1} = hh^+$ is given in equation (4.19). We can introduce an analogous gauge transformation $\tilde{h}$ for the twisted bundle as in (4.72) with $\tilde{G}^{-1} = \tilde{h} \cdot \tilde{h}^+$ and, as shown in (4.71), h can be recovered from the $\tilde{h}$ by untwisting. Given all of this, in terms of the quantities $\tilde{h}$ and $\tilde{G}^{-1}$, the function

θ_h appearing in (5.21) becomes

$$\theta_h = \bar{\partial}\tilde{h} \cdot \tilde{h}^{-1} - \frac{1}{2n} \operatorname{tr}(\tilde{G}\bar{\partial}\tilde{G}^{-1}) \ . \tag{5.22}$$

From Donaldson's algorithm, the explicit expression of $\tilde{G}^{-1}$ is given by equation (4.62) and $\bar{\partial}\tilde{G}^{-1}$ can be computed via a straightforward derivative. However, to compute the integral, we also need the $\tilde{h}$ and $\bar{\partial}\tilde{h}$. Thus our next task is to provide a practical procedure by which these quantities can be derived from $\tilde{G}^{-1}$. Unfortunately we can not simply solve $\tilde{G}^{-1} = \tilde{h} \cdot \tilde{h}^{+}$ and take derivatives to find these quantities given our numerical knowledge of $\tilde{G}^{-1}$. The reason for this is that the expression for the inverse fiber metric is extremely complicated. While directly taking a single derivative of it is computationally feasible, the same is not true for finding expressions for $\tilde{h}$ and $\bar{\partial}\tilde{h}$. Therefore in what follows we outline a procedure that can be used to compute these quantities at any given point on a numerical sample covering the Calabi-Yau manifold, without reference to data from any other point. This can then be used to compute the quantities of interest in a practically tractable fashion.

First, as can be seen from (4.72), the transformation $\tilde{h}$ can be constructed from the eigenvalues λ_i and eigenvectors v_i of $\tilde{G}^{-1}$ satisfying

$$(\tilde{G}^{-1})v_i = \lambda_i v_i, \quad i = 1, 2, \ldots, n \ . \tag{5.23}$$

Next, the derivative of $\tilde{h}$ is given by [160],

$$\bar{\partial}\tilde{h} = (\bar{\partial}U)\sqrt{\tilde{\Lambda}}U^{+} + U(\bar{\partial}\sqrt{\tilde{\Lambda}})U^{+} + U\sqrt{\tilde{\Lambda}}(\bar{\partial}U^{+}) \ , \tag{5.24}$$

where $\bar{\partial}\tilde{G}^{-1}$ is known, and $\bar{\partial}U$ and $\bar{\partial}\tilde{\Lambda}$ can be obtained from the derivative of the corresponding λ_i and v_i. By taking a derivative of $v_i^{+}\tilde{G}^{-1}v_i$, using (5.23), and with the understanding

that $\{v_i\}$ is an orthonormal set, the derivative of the eigenvalue can be shown to be given by the following.

$$\bar{\partial}\lambda_i = v_i^+(\bar{\partial}\hat{G}^{-1})v_i \tag{5.25}$$

A quick computation, also following from (5.23) shows that the derivative of the eigenvector ∂v_i satisfies,

$$-(\bar{\partial}A_i)v_i = A_i\bar{\partial}v_i, \quad A_i = \tilde{G}^{-1} - \lambda_i I_{n\times n}\ . \tag{5.26}$$

It is easy to observe that A is a singular matrix with rank $(n-1)$. After imposing the normalization upon the v_i, we find that the $\bar{\partial}v_i$ consist of $(n-1)$ unknowns. Then, solving the linear system (5.26) for $\bar{\partial}v_i$, we get the derivative of the eigenvector. Now, with the $\bar{\partial}\lambda_i$ and ∂v_i, we can compute the quantity $\bar{\partial}\tilde{h}$ by equation (5.24).

Finally then, we have shown how θ_h can be computed directly from the metric $\tilde{G}^{-1}$, which is the output of Donaldson's algorithm. Our workflow to compute the integral (5.21) is thus as follows. First, we apply Donaldson's algorithm to obtain the metric $\tilde{G}^{-1}$ and we take its derivative. Then, we use (4.72) to construct $\tilde{h}$ and (5.25), (5.26) and (5.24) to compute $\bar{\partial}\tilde{h}$. We combine these results using (5.22) to compute θ_h. As a last step, numerical integration is used to evaluate the integral (5.21). In the next subsection we illustrate this procedure with a concrete example.

5.3.1 Example: A $SU(3)$ Monad Bundle on the Quintic

We will consider the following $SU(3)$ vector bundle V over the Fermat quintic Calabi-Yau three-fold X, defined as the dual of a two-term monad,

$$0 \to O(-2)\oplus O(-3) \xrightarrow{F} O(-1)^{\oplus 5} \to V \to 0\ . \tag{5.27}$$

Here, the bundle morphism $F = \{f_i, g_i\}, i = 1, \ldots, 5$ is such that f_i and g_i are taken to be the generic elements in $H^0(X, O(1))$ and $H^0(X, O(2))$. With the help of the equation (2.27) and (4.27), the second Chern class of the TX and V are $c_2(TX) = 10$ and $c_2(V) = 4$. Since $0 \leq c_2(V) \leq c_2(TX)$, the anomaly cancellation condition can be satisfied by the addition of supersymmetry preserving M5-branes or additional visible or hidden sector bundles. Also, notice that the dual monad above is defined with the negative line bundles over a cyclic manifold. Thus, as discussed in Chapter 4, the bundle V is poly-stable and by construction holomorphic. Thus, this example gives a well-defined supersymmetric vacuum in heterotic Calabi-Yau compactification.

Now we compute the integral (5.21). First, following Donaldson's algorithm, as reviewed in Section 4.2.1, we compute the Hermitian Yang-Mills connection of V from $k = 1$ to $k = 6$, which is given in terms of the (inverse) metric $\tilde{G}^{-1}$ of the twisted bundle $V \otimes L^k$. The error in the numerical connection is evaluated for each k according to an error function given in (4.69). The result is plotted in Figure 5.1. The figure shows that these connections are converging well to the unique Hermitian Yang-Mills one with a dependence of $O(k^{-2})$ as expected. The integration is performed numerically over a sample with $n_s = 813025$ points. These points are chosen adaptively according to the weight $w = |\Omega|^2$.

For each k we now have a fiber metric $\tilde{G}^{-1}$ of the twisted bundle $V \otimes L^k$. Following the discussion at the end of the previous sub-section, we can use this to compute θ_h from (5.22). Given that the nowhere-vanishing $(3, 0)$ form is known, and indeed can be found in (2.35), we have everything we need to evaluate the integral (5.21).

The numerical integration, which we perform over the same set of $n_s = 813025$ points which

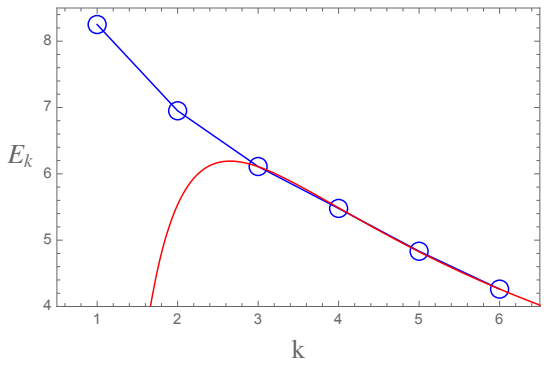

Figure 5.1: The error function (4.69) of the numerical approximation to the Hermitian Yang-Mills connection on the bundle V given in (5.27) over the Fermat quintic three-fold. The least-squares-fit curve is $\sim \frac{-43.51}{k^2} + \frac{32.83}{k}$.

were used to implement Donaldson's algorithm, can be written as,

$$I_{\text{approx}} = \sum_{i=1}^{n_s} \frac{\text{tr}(\theta_h)^3}{\bar{\Omega}} w_i \ . \tag{5.28}$$

Here w_i is $|\Omega|^2$ evaluated at the i'th point. We evaluated (5.28) with the Hermitian Yang-Mills connections from $k = 1$ to $k = 5$. The result is in general a complex number. We plot the real part of the result in Figure 5.2[1]. We can clearly see that the answer is starting to smoothly converge to an asymptotic value, which might in fact be vanishing. Code is currently running to evaluate these results to higher k and we will have thus have a clearer idea of the exact asymptotic value soon.

[1]The imaginary part of the integral has not yet smoothly converged to such a nice degree and the code to run this analysis to higher k is running as this thesis is being completed. We expect to have this result, together with the additional quantities that we wish to compute, as described at the end of this section, shortly.

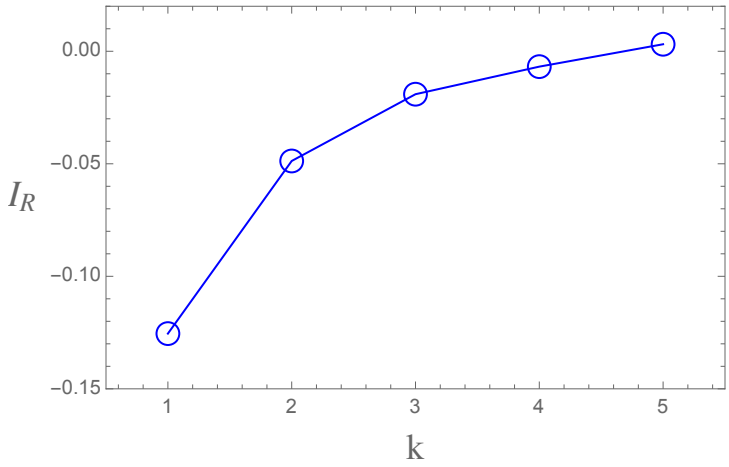

Figure 5.2: The real part of the the approximation to the integral (5.21) as defined in (5.28) as a function of the twist k in the Donaldson algorithm. The approximation to the integral can be seen to be converging to an asymptotic value as k increases

.

5.4 Conclusions

The work described in this chapter is an ongoing program of research. Although the method is fully developed, the numerical runs, which are required to complete the work to a higher degree of accuracy are still in the process of completing. Nevertheless, the results shown in this chapter are enough to demonstrate that the numerical methods we have presented can indeed calculate the desired quantities. They enable us to compute the final contributions to the Chern-Simons invariants appearing in the superpotential of heterotic compactifications, arising from converting the connections involved in to a physical gauge.

In addition to refining the results described in the previous section, we are currently performing computational runs to determine the changes in the ordinary Chern-Simons invariants (5.9) that arise due to the change to physical gauge. Since no results are yet available for these quantities we have not mentioned them in the main body of this chapter. Nevertheless, two points should be stated. First, there is a technical subtlety that arises in performing the integrals over special Lagrangian cycles that are required to compute these invariants. The

monad map in (5.27) is frequently taken to be a polynomial with coefficients in the real numbers, simply for computational ease. This leads to serious computational issues in evaluating the ordinary Chern-Simons invariants however, essentially because these are associated to real manifolds. It turns out that such map choices are too special and lead to pathologies. Thus we generalize the maps used to accommodate complex coefficients. Second, the integer valued results obtained from the gauge transformation of these quantities, as described in (5.16), will provide us with an excellent further test of our methods. An integer result for such a numerical integral is unlikely to be obtained by pure chance if an error were to be present.

The final goal of this research is to compute both h in (5.17) and g in (5.19) in a case where P associated to the real bundle morphism (5.12) is known. In such a case all of these objects could be combined according to equations (5.15), (5.18) and (5.20) to compute the full holomorphic Chern-Simons invariant of a heterotic compactification, in physical gauge, for the first time.

Chapter 6

Conclusion and Outlook

In this thesis, we have explored the application of techniques in numerical differential geometry to the physics of heterotic Calabi-Yau compactifications. The work was divided into two parts. These were numerical techniques for finding Ricci-flat metrics and their applications and numerical techniques for finding solutions to the Hermitian Yang-Mills equations and their utilization. In the following, we will summarize some of the topics we covered and discuss a few future directions.

We began Chapter 2 with a short review of the mathematics of Calabi-Yau manifolds. We then introduced two numerical methods for finding Ricci-flat metrics, Donaldson's algorithm and the Minimization algorithm, in detail. In Chapter 3, the second of these algorithms was used to study hierarchies of curvature scales on Calabi-Yau manifolds as a function of complex structure moduli. This work is of physical importance because it is crucial to know when large curvatures are developing on such a space if the approximations made in deriving string low energy effective theories are to be well controlled. We showed that the algorithm successfully found regions of large curvature which were expected on analytic grounds. Further more, the methods could provide us with useful information about curvature hierarchies in regions far from any singularities.

Due to issues of computational complexity, the current algorithms for finding Ricci-flat metrics on Calabi-Yau three-folds are only really practical for polarizations set by small

integers. An important direction of future work will be to develop more efficient algorithms in a variety of regards, in particular allowing for computations with arbitrary polarizations. Such an advance would allow us to study the Kähler moduli dependence of hierarchies in curvature scales. In particular such numerical techniques could be used to isolate the boundaries of the Kähler cone, something that can prove to be rather difficult analytically in many examples. In addition, all of the examples considered so far are Complete Intersection Calabi-Yau manifolds. It would be interesting to generalize the application of the algorithms to other large sets of Calabi-Yau manifolds, such as those realized as hypersurfaces in toric varieties.

In Chapter 4, we discussed numerical methods for obtaining Hermitian Yang-Mills connections and their application to bundle stability. We started with a brief review of the basic proprieties of holomorphic vector bundles. In particular we described, given a vector bundle, how to analytically check its stability under a fixed polarization and how to determine the stability walls that determine its Kähler cone substructure. We then introduced the generalized Donaldson's algorithm and applied it to check the stability of some vector bundles over Calabi-Yau manifolds numerically.

In particular, the last example that we presented in Chapter 4 was of a type that differed qualitatively from any that has appeared in the literature to date. The case we considered is a bundle that is only stable on a higher codimension locus in complex structure moduli space. Despite this rather delicate structure, we showed that numerical methods are effective in deciding the stability of such bundles, in work which complements existing literature concentrating on the dependence on Kähler moduli [109].

In Chapter 5 we applied the numerical methods described in Chapter 4 to fill a gap in recent work concerning the computation of holomorphic Chern-Simons invariants in heterotic

compactifications. These invariants contribute in an important manner to the superpotential of the four dimensional effective theory of such models. Recent work [60] has shown how to render the computation of these quantities tractable. However, a final step in the analysis of these superpotential contributions requires explicit knowledge of the Hermitian Yang-Mills connection and is thus prohibitively difficult to address analytically. Nevertheless, we were able to show numerical methods will be effective in completing such analyses. We presented the complete underlying methodology, together with some initial results from this on-going research project. Further results are the subject of continuing computational runs and will provide a variety of additional data. These will include some ancillary quantities that appear, that should be integer valued, as a further check that these numerical methods are functioning correctly in a situation where analytic verification is impossible.

There are a number of future directions of research involving numerical approximations to Hermitian Yang-Mills connections over Calabi-Yau manifolds that it would be interesting to explore. Similarly to the situation with numerical computations of Ricci-flat metrics, the computational complexity of the generalized Donaldson's algorithm greatly constrains the cases to which it can be practically applied. Thus the development of more efficient methods would be a crucial line of investigation. In particular, we expect that there is an analogous technique to the Minimization algorithm for the Hermitian Yang-Mills connection, which would be interesting to develop in future work. Once such algorithms have been sufficiently developed, one ultimate goal of this research would be to explicitly compute the harmonic bundle valued one forms associated to matter fields in heterotic compactifications. Access to these quantities would allow us to compute the matter field Kähler potential and physically normalized Yukawa couplings in realistic heterotic compactifications for the first time.

Bibliography

[1] J. Polchinski, *String theory. Vol. 1: An introduction to the bosonic string*, doi:10.1017/CBO9780511816079

[2] M. B. Green, J. Schwarz and E. Witten, *Superstring theory. Vol. 1: Introduction*,

[3] J. Polchinski, *String theory. Vol. 2: Superstring theory and beyond*, doi:10.1017/CBO9780511618123

[4] F. Quevedo, "Lectures on superstring phenomenology," AIP Conf. Proc. **359**, 202-242 (1996) doi:10.1063/1.49735 [arXiv:hep-th/9603074 [hep-th]].

[5] S. Dimopoulos and H. Georgi, "Softly Broken Supersymmetry and SU(5)," Nucl. Phys. B **193**, 150-162 (1981) doi:10.1016/0550-3213(81)90522-8

[6] M. B. Green, J. Schwarz and E. Witten, *Superstring theory. Vol. 2: Loop amplitudes, anomalies and phenomenology*,

[7] A. Strominger, "Superstrings with Torsion," Nucl. Phys. B **274**, 253 (1986) doi:10.1016/0550-3213(86)90286-5

[8] C. Hull, "Compactifications of the Heterotic Superstring," Phys. Lett. B **178**, 357-364 (1986) doi:10.1016/0370-2693(86)91393-6

[9] G. Lopes Cardoso, G. Curio, G. Dall'Agata, D. Lust, P. Manousselis and G. Zoupanos, "Non-Kähler string backgrounds and their five torsion classes," Nucl. Phys. B **652**, 5-34 (2003) doi:10.1016/S0550-3213(03)00049-X [arXiv:hep-th/0211118 [hep-th]].

[10] P. Candelas, G. T. Horowitz, A. Strominger and E. Witten, "Vacuum Configurations for Superstrings," Nucl. Phys. B **258** (1985) 46.

[11] B. R. Greene, K. H. Kirklin, P. J. Miron and G. G. Ross, "A Three Generation Superstring Model. 1. Compactification and Discrete Symmetries," Nucl. Phys. B **278**, 667-693 (1986) doi:10.1016/0550-3213(86)90057-X

[12] B. R. Greene, K. H. Kirklin, P. J. Miron and G. G. Ross, "A Three Generation Superstring Model. 2. Symmetry Breaking and the Low-Energy Theory," Nucl. Phys. B **292**, 606-652 (1987) doi:10.1016/0550-3213(87)90662-6

[13] V. Braun, Y. H. He, B. A. Ovrut and T. Pantev, "A Heterotic standard model," Phys. Lett. B **618**, 252-258 (2005) doi:10.1016/j.physletb.2005.05.007 [arXiv:hep-th/0501070 [hep-th]].

[14] V. Braun, Y. H. He, B. A. Ovrut and T. Pantev, "A Standard model from the E(8) x E(8) heterotic superstring," JHEP **06**, 039 (2005) doi:10.1088/1126-6708/2005/06/039 [arXiv:hep-th/0502155 [hep-th]].

[15] V. Braun, Y. H. He, B. A. Ovrut and T. Pantev, "Vector bundle extensions, sheaf cohomology, and the heterotic standard model," Adv. Theor. Math. Phys. **10**, no.4, 525-589 (2006) doi:10.4310/ATMP.2006.v10.n4.a3 [arXiv:hep-th/0505041 [hep-th]].

[16] V. Bouchard and R. Donagi, "An SU(5) heterotic standard model," Phys. Lett. B **633**, 783-791 (2006) doi:10.1016/j.physletb.2005.12.042 [arXiv:hep-th/0512149 [hep-th]].

[17] L. B. Anderson, J. Gray, Y. H. He and A. Lukas, "Exploring Positive Monad Bundles And A New Heterotic Standard Model," JHEP **02**, 054 (2010) doi:10.1007/JHEP02(2010)054 [arXiv:0911.1569 [hep-th]].

[18] V. Braun, P. Candelas, R. Davies and R. Donagi, "The MSSM Spectrum from (0,2)-Deformations of the Heterotic Standard Embedding," JHEP **05**, 127 (2012) doi:10.1007/JHEP05(2012)127 [arXiv:1112.1097 [hep-th]].

[19] L. B. Anderson, J. Gray, A. Lukas and E. Palti, "Two Hundred Heterotic Standard Models on Smooth Calabi-Yau three-folds," Phys. Rev. D **84**, 106005 (2011) doi:10.1103/PhysRevD.84.106005 [arXiv:1106.4804 [hep-th]].

[20] L. B. Anderson, J. Gray, A. Lukas and E. Palti, "Heterotic Line Bundle Standard Models," JHEP **06**, 113 (2012) doi:10.1007/JHEP06(2012)113 [arXiv:1202.1757 [hep-th]].

[21] L. B. Anderson, A. Constantin, J. Gray, A. Lukas and E. Palti, "A Comprehensive Scan for Heterotic SU(5) GUT models," JHEP **01**, 047 (2014) doi:10.1007/JHEP01(2014)047 [arXiv:1307.4787 [hep-th]].

[22] A. Strominger, "Yukawa Couplings in Superstring Compactification," Phys. Rev. Lett. **55**, 2547 (1985). doi:10.1103/PhysRevLett.55.2547

[23] P. Candelas, "Yukawa Couplings Between (2,1) Forms," Nucl. Phys. B **298**, 458 (1988). doi:10.1016/0550-3213(88)90351-3

[24] P. Candelas and S. Kalara, "Yukawa Couplings for a Three Generation Superstring Compactification," Nucl. Phys. B **298**, 357-368 (1988) doi:10.1016/0550-3213(88)90271-4

[25] B. R. Greene, K. Kirklin, P. Miron and G. G. Ross, "27**3 Yukawa Couplings for a Three Generation Superstring Model," Phys. Lett. B **192**, 111-118 (1987) doi:10.1016/0370-2693(87)91151-8

[26] J. Distler, B. R. Greene, K. Kirklin and P. Miron, "Evaluation of 27-bar**3 Yukawa Couplings in a Three Generation Superstring Model," Phys. Lett. B **195**, 41 (1987) doi:10.1016/0370-2693(87)90883-5

[27] J. Distler and S. Kachru, "Duality of (0,2) string vacua," Nucl. Phys. B **442**, 64-74 (1995) doi:10.1016/S0550-3213(95)00130-1 [arXiv:hep-th/9501111 [hep-th]].

[28] V. Braun, Y. H. He and B. A. Ovrut, "Yukawa couplings in heterotic standard models," JHEP **0604**, 019 (2006) doi:10.1088/1126-6708/2006/04/019

[29] V. Bouchard, M. Cvetic and R. Donagi, "Tri-linear couplings in an heterotic minimal supersymmetric standard model," Nucl. Phys. B **745**, 62-83 (2006) doi:10.1016/j.nuclphysb.2006.03.032 [arXiv:hep-th/0602096 [hep-th]].

[30] L. B. Anderson, J. Gray, D. Grayson, Y. H. He and A. Lukas, "Yukawa Couplings in Heterotic Compactification," Commun. Math. Phys. **297**, 95 (2010) doi:10.1007/s00220-010-1033-8 [arXiv:0904.2186 [hep-th]].

[31] E. I. Buchbinder, A. Constantin and A. Lukas, "Non-generic Couplings in Supersymmetric Standard Models," Phys. Lett. B **748**, 251-254 (2015) doi:10.1016/j.physletb.2015.07.012 [arXiv:1409.2412 [hep-th]].

[32] E. I. Buchbinder, A. Constantin, J. Gray and A. Lukas, "Yukawa Unification in Heterotic String Theory," Phys. Rev. D **94**, no. 4, 046005 (2016) doi:10.1103/PhysRevD.94.046005 [arXiv:1606.04032 [hep-th]].

[33] S. Blesneag, E. I. Buchbinder, P. Candelas and A. Lukas, "Holomorphic Yukawa Couplings in Heterotic String Theory," JHEP **1601**, 152 (2016) doi:10.1007/JHEP01(2016)152 [arXiv:1512.05322 [hep-th]].

[34] S. Blesneag, E. I. Buchbinder and A. Lukas, "Holomorphic Yukawa Couplings for Complete Intersection Calabi-Yau Manifolds," JHEP **1701**, 119 (2017) doi:10.1007/JHEP01(2017)119 [arXiv:1607.03461 [hep-th]].

[35] L. B. Anderson, J. Gray and B. Ovrut, "Yukawa Textures From Heterotic Stability Walls," JHEP **1005**, 086 (2010) doi:10.1007/JHEP05(2010)086 [arXiv:1001.2317 [hep-th]].

[36] J. Distler and B. R. Greene, "Aspects of (2,0) String Compactifications," Nucl. Phys. B **304**, 1-62 (1988) doi:10.1016/0550-3213(88)90619-0

[37] P. Candelas and X. de la Ossa, "Moduli Space of Calabi-Yau Manifolds," Nucl. Phys. B **355**, 455 (1991). doi:10.1016/0550-3213(91)90122-E

[38] Ş. Blesneag, E. I. Buchbinder, A. Constantin, A. Lukas and E. Palti, "Matter field Kähler metric in heterotic string theory from localisation," JHEP **1804**, 139 (2018) doi:10.1007/JHEP04(2018)139 [arXiv:1801.09645 [hep-th]].

[39] K. Hori and C. Vafa, "Mirror symmetry," hep-th/0002222.

[40] M. Cvetic, J. Louis and B. A. Ovrut, "A String Calculation of the Kähler Potentials for Moduli of Z(N) Orbifolds," Phys. Lett. B **206**, 227-233 (1988) doi:10.1016/0370-2693(88)91497-9

[41] D. Bailin, S. K. Gandhi and A. Love, "Kähler potentials for (2,2) heterotic string theories with Wilson lines," Phys. Lett. B **269**, 293-299 (1991) doi:10.1016/0370-2693(91)90173-N

[42] D. Bailin and A. Love, "Kähler potentials for twisted sectors of Z(N) orbifolds," Phys. Lett. B **288**, 263-268 (1992) doi:10.1016/0370-2693(92)91101-E

[43] D. Bailin and A. Love, "Orbifold compactifications of string theory," Phys. Rept. **315**, 285-408 (1999) doi:10.1016/S0370-1573(98)00126-4

[44] Y. Olguín-Trejo and S. Ramos-Sánchez, "Kähler potential of heterotic orbifolds with multiple Kähler moduli," J. Phys. Conf. Ser. **912**, no.1, 012029 (2017) doi:10.1088/1742-6596/912/1/012029 [arXiv:1707.09966 [hep-th]].

[45] W. Gu and E. Sharpe, "A proposal for nonabelian mirrors," [arXiv:1806.04678 [hep-th]].

[46] Z. Chen, W. Gu, H. Parsian and E. Sharpe, "Two-dimensional supersymmetric gauge theories with exceptional gauge groups," Adv. Theor. Math. Phys. **24**, no.1, 67-123 (2020) doi:10.4310/ATMP.2020.v24.n1.a3 [arXiv:1808.04070 [hep-th]].

[47] W. Gu, H. Parsian and E. Sharpe, "More non-Abelian mirrors and some two-dimensional dualities," Int. J. Mod. Phys. A **34**, no.30, 1950181 (2019) doi:10.1142/S0217751X19501811 [arXiv:1907.06647 [hep-th]].

[48] Z. Chen, E. Sharpe and R. Wu, "Toda-like (0,2) mirrors to products of projective spaces," JHEP **1608**, 093 (2016) doi:10.1007/JHEP08(2016)093 [arXiv:1603.09634 [hep-th]].

[49] Z. Chen, J. Guo, E. Sharpe and R. Wu, "More Toda-like (0,2) mirrors," JHEP **1708**, 079 (2017) doi:10.1007/JHEP08(2017)079 [arXiv:1705.08472 [hep-th]].

[50] W. Gu and E. Sharpe, "A proposal for (0,2) mirrors of toric varieties," JHEP **1711**, 112 (2017) doi:10.1007/JHEP11(2017)112 [arXiv:1707.05274 [hep-th]].

[51] W. Gu, J. Guo and E. Sharpe, "A proposal for nonabelian (0,2) mirrors," [arXiv:1908.06036 [hep-th]].

[52] L. B. Anderson, J. Gray, A. Lukas and B. Ovrut, "Stabilizing the Complex Structure in Heterotic Calabi-Yau Vacua," JHEP **1102**, 088 (2011) doi:10.1007/JHEP02(2011)088 [arXiv:1010.0255 [hep-th]].

[53] L. B. Anderson, J. Gray, A. Lukas and B. Ovrut, "The Atiyah Class and Complex Structure Stabilization in Heterotic Calabi-Yau Compactifications," JHEP **1110**, 032 (2011) doi:10.1007/JHEP10(2011)032 [arXiv:1107.5076 [hep-th]].

[54] L. B. Anderson, J. Gray, A. Lukas and B. Ovrut, "Stabilizing All Geometric Moduli in Heterotic Calabi-Yau Vacua," Phys. Rev. D **83**, 106011 (2011) doi:10.1103/PhysRevD.83.106011 [arXiv:1102.0011 [hep-th]].

[55] L. B. Anderson, J. Gray, A. Lukas andB. Ovrut, "Vacuum Varieties, Holomorphic Bundles and Complex Structure Stabilization in Heterotic Theories," JHEP **1307**, 017 (2013) doi:10.1007/JHEP07(2013)017 [arXiv:1304.2704 [hep-th]].

[56] J. Gray and J. Wang, "Jumping Spectra and Vanishing Couplings in Heterotic Line Bundle Standard Models," JHEP **11**, 073 (2019) doi:10.1007/JHEP11(2019)073 [arXiv:1906.09373 [hep-th]].

[57] E. R. Sharpe, "Kähler cone substructure," Adv. Theor. Math. Phys. **2**, 1441 (1999) doi:10.4310/ATMP.1998.v2.n6.a7 [hep-th/9810064].

[58] L. B. Anderson, J. Gray, A. Lukas and B. Ovrut, "The Edge Of Supersymmetry: Stability Walls in Heterotic Theory," Phys. Lett. B **677**, 190 (2009) doi:10.1016/j.physletb.2009.05.025 [arXiv:0903.5088 [hep-th]].

[59] L. B. Anderson, J. Gray, A. Lukas and B. Ovrut, "Stability Walls in Heterotic Theories," JHEP **0909**, 026 (2009) doi:10.1088/1126-6708/2009/09/026 [arXiv:0905.1748 [hep-th]].

[60] L. B. Anderson, J. Gray, A. Lukas and J. Wang, "Chern-Simons Invariants and Heterotic Superpotentials," [arXiv:2006.03082 [hep-th]].

[61] E. Calabi, "The space of Kähler metrics," in *Proceedings of the International Congress of Mathematicians, Amsterdam, 1954, vol. 2*, pp. 206–207. North-Holland, Amsterdam, 1956.

[62] E. Calabi, "On Kähler manifolds with vanishing canonical class," in *Algebraic geometry and topology, a symposium in honour of S. Lefschetz*, pp. 78–89. Princeton University Press, Princeton, 1957.

[63] S.-T. Yau, "On Calabi's conjecture and some new results in algebraic geometry," *Proceedings of the National Academy of Sciences of theU.S.A.* **74** (1977) 1798–1799.

[64] S.-T. Yau, "On the Ricci curvature of a compact Kähler manifold and the complex Monge-Ampère equations. I.," *Communications on pure and applied mathematics* **31** (1978) 339–411.

[65] S. Donaldson, "Anti Self-Dual Yang-Mills Connections over Complex Algebraic Surfaces and Stable Vector Bundles," Proc. London Math. Soc., **3**, 1, (1985).

[66] K. Uhlenbeck and S.-T. Yau, "On the existence of Hermitian Yang-Mills connections in stable bundles," Comm. Pure App. Math., **39**, 257, (1986).

[67] L. B. Anderson, "Heterotic and M-theory Compactifications for String Phenomenology," [arXiv:0808.3621 [hep-th]].

[68] L. B. Anderson and M. Karkheiran, "TASI Lectures on Geometric Tools for String Compactifications," PoS **TASI2017**, 013 (2018) doi:10.22323/1.305.0013 [arXiv:1804.08792 [hep-th]].

[69] S. Gukov, C. Vafa and E. Witten, "CFT's from Calabi-Yau four folds," Nucl. Phys. B **584**, 69-108 (2000) doi:10.1016/S0550-3213(00)00373-4 [arXiv:hep-th/9906070 [hep-th]].

[70] E. Witten, "World sheet corrections via D instantons," JHEP **02**, 030 (2000) doi:10.1088/1126-6708/2000/02/030 [arXiv:hep-th/9907041 [hep-th]].

[71] E. I. Buchbinder, R. Donagi and B. A. Ovrut, "Vector bundle moduli superpotentials in heterotic superstrings and M theory," JHEP **07**, 066 (2002) doi:10.1088/1126-6708/2002/07/066 [arXiv:hep-th/0206203 [hep-th]].

[72] E. I. Buchbinder, R. Donagi and B. A. Ovrut, "Superpotentials for vector bundle moduli," Nucl. Phys. B **653**, 400-420 (2003) doi:10.1016/S0550-3213(02)01093-3 [arXiv:hep-th/0205190 [hep-th]].

[73] C. Beasley and E. Witten, "Residues and world sheet instantons," JHEP **10**, 065 (2003) doi:10.1088/1126-6708/2003/10/065 [arXiv:hep-th/0304115 [hep-th]].

[74] V. Braun, M. Kreuzer, B. A. Ovrut and E. Scheidegger, "Worldsheet instantons and torsion curves, part A: Direct computation," JHEP **10**, 022 (2007) doi:10.1088/1126-6708/2007/10/022 [arXiv:hep-th/0703182 [hep-th]].

[75] V. Braun, M. Kreuzer, B. A. Ovrut and E. Scheidegger, "Worldsheet Instantons and Torsion Curves, Part B: Mirror Symmetry," JHEP **10**, 023 (2007) doi:10.1088/1126-6708/2007/10/023 [arXiv:0704.0449 [hep-th]].

[76] V. Braun, M. Kreuzer, B. A. Ovrut and E. Scheidegger, "Worldsheet instantons, torsion curves, and non-perturbative superpotentials," Phys. Lett. B **649**, 334-341 (2007) doi:10.1016/j.physletb.2007.03.066 [arXiv:hep-th/0703134 [hep-th]].

[77] E. I. Buchbinder and B. A. Ovrut, "Non-vanishing Superpotentials in Heterotic String Theory and Discrete Torsion," JHEP **01**, 038 (2017) doi:10.1007/JHEP01(2017)038 [arXiv:1611.01922 [hep-th]].

[78] E. Buchbinder, A. Lukas, B. Ovrut and F. Ruehle, "Heterotic Instanton Superpotentials from Complete Intersection Calabi-Yau Manifolds," JHEP **10**, 032 (2017) doi:10.1007/JHEP10(2017)032 [arXiv:1707.07214 [hep-th]].

[79] E. I. Buchbinder, A. Lukas, B. A. Ovrut and F. Ruehle, "Heterotic Instantons for Monad and Extension Bundles," JHEP **02**, 081 (2020) doi:10.1007/JHEP02(2020)081 [arXiv:1912.07222 [hep-th]].

[80] E. I. Buchbinder, A. Lukas, B. A. Ovrut and F. Ruehle, "Instantons and Hilbert Functions," [arXiv:1912.08358 [hep-th]].

[81] J. O. Conrad, "On fractional instanton numbers in six-dimensional heterotic E(8) x E(8) orbifolds," JHEP **11**, 022 (2000) doi:10.1088/1126-6708/2000/11/022 [arXiv:hep-th/0009251 [hep-th]].

[82] S. Gukov, S. Kachru, X. Liu and L. McAllister, "Heterotic moduli stabilization with fractional Chern-Simons invariants," Phys. Rev. D **69**, 086008 (2004) doi:10.1103/PhysRevD.69.086008 [arXiv:hep-th/0310159 [hep-th]].

[83] M. Cicoli, S. de Alwis and A. Westphal, "Heterotic Moduli Stabilisation," JHEP **10**, 199 (2013) doi:10.1007/JHEP10(2013)199 [arXiv:1304.1809 [hep-th]].

[84] F. Apruzzi, F. F. Gautason, S. Parameswaran and M. Zagermann, "Wilson lines and Chern-Simons flux in explicit heterotic Calabi-Yau compactifications," JHEP **02**, 183 (2015) doi:10.1007/JHEP02(2015)183 [arXiv:1410.2603 [hep-th]].

[85] W. Cui and J. Gray, "Numerical Metrics, Curvature Expansions and Calabi-Yau Manifolds," JHEP **05**, 044 (2020) doi:10.1007/JHEP05(2020)044 [arXiv:1912.11068 [hep-th]].

[86] V. Bouchard, "Lectures on complex geometry, Calabi-Yau manifolds and toric geometry," hep-th/0702063 [HEP-TH].

[87] P. Griffiths and J. Harris, *Principles of algebraic geometry*, Wiley-Interscience [John Wiley & Sons], New York, 1978. Pure and Applied Mathematics.

[88] P. Candelas, "Lectures On Complex Manifolds," Published in Trieste 1987, Proceedings, Superstrings 87, 1-88.

[89] C. T. C. Wall, "Classification problems in differential topology V. ," (1966) Invent.Math.,1-355.

[90] M. Gross, "A Finiteness theorem for elliptic Calabi-Yau three-folds," [arXiv:alg-geom/9305002 [math.AG]].

[91] A. Constantin, J. Gray and A. Lukas, "Hodge Numbers for All CICY Quotients," JHEP **01**, 001 (2017) doi:10.1007/JHEP01(2017)001 [arXiv:1607.01830 [hep-th]].

[92] L. B. Anderson, X. Gao, J. Gray and S. J. Lee, "Tools for CICYs in F-theory," JHEP **11**, 004 (2016) doi:10.1007/JHEP11(2016)004 [arXiv:1608.07554 [hep-th]].

[93] L. B. Anderson, X. Gao, J. Gray and S. J. Lee, "Fibrations in CICY three-folds," JHEP **10**, 077 (2017) doi:10.1007/JHEP10(2017)077 [arXiv:1708.07907 [hep-th]].

[94] L. B. Anderson, J. Gray and B. Hammack, "Fibrations in Non-simply Connected Calabi-Yau Quotients," JHEP **08**, 128 (2018) doi:10.1007/JHEP08(2018)128 [arXiv:1805.05497 [hep-th]].

[95] Y. C. Huang and W. Taylor, "On the prevalence of elliptic and genus one fibrations among toric hypersurface Calabi-Yau three-folds," JHEP **03**, 014 (2019) doi:10.1007/JHEP03(2019)014 [arXiv:1809.05160 [hep-th]].

[96] Y. C. Huang and W. Taylor, "Mirror symmetry and elliptic Calabi-Yau manifolds," JHEP **04**, 083 (2019) doi:10.1007/JHEP04(2019)083 [arXiv:1811.04947 [hep-th]].

[97] Y. C. Huang and W. Taylor, "Fibration structure in toric hypersurface Calabi-Yau three-folds," JHEP **03**, 172 (2020) doi:10.1007/JHEP03(2020)172 [arXiv:1907.09482 [hep-th]].

[98] Hubsch, Tristan. "Calabi-Yau manifolds—motivations and constructions." Comm. Math. Phys. 108 (1987), no. 2, 291–318. https://projecteuclid.org/euclid.cmp/1104116464

[99] P. Candelas, A. M. Dale, C. A. Lutken and R. Schimmrigk, "Complete Intersection Calabi-Yau Manifolds," Nucl. Phys. B **298**, 493 (1988).

[100] P. Candelas, C. A. Lutken and R. Schimmrigk, "Complete intersection Calabi-Yau manifolds (II). : Three Generation Manifolds," Nucl. Phys. B **306**, 113 (1988).

[101] Green, Paul; Hubsch, Tristan. "Calabi-Yau manifolds as complete intersections in products of complex projective spaces." Comm. Math. Phys. 109 (1987), no. 1, 99–108. https://projecteuclid.org/euclid.cmp/1104116713

[102] P. S. Green, T. Hubsch and C. A. Lutken, "All the Hodge Numbers for All Calabi-Yau Complete Intersections," Class. Quant. Grav. **6**, 105 (1989).

[103] A. M. He and P. Candelas, "On The Number Of Complete Intersection Calabi-Yau Manifolds," Commun. Math. Phys. **135**, 193 (1990).

[104] M. Gagnon and Q. Ho-Kim, "An Exhaustive list of complete intersection Calabi-Yau manifolds," Mod. Phys. Lett. A **9** (1994) 2235.

[105] L. B. Anderson, F. Apruzzi, X. Gao, J. Gray and S. J. Lee, "A new construction of Calabi-Yau manifolds: Generalized CICYs," Nucl. Phys. B **906**, 441 (2016) doi:10.1016/j.nuclphysb.2016.03.016 [arXiv:1507.03235 [hep-th]].

[106] M. Kreuzer, H. Skarke, "On the classification of relfexive polyhedra," Commun. Math. Phys. 185, 495-508 (1997) [arXiv:hep-th/9512204].

[107] M. Kreuzer and H. Skarke, "Complete Classification of Reflexive Polyhedra in Four-dimensions," Adv.Theor.Math.Phys.**4** (2002) 1209 [arXiv:hep-th/0002240].

[108] M. Kreuzer, H. Skarke, "Reflexive polyhedra, weights and toric Calabi-Yau fibrations," Rev. Math. Phys. 14, 343-374 (2002) [arXiv:math/0001106].

[109] L. B. Anderson, V. Braun and B. A. Ovrut, "Numerical Hermitian Yang-Mills Connections and Kähler Cone Substructure," JHEP **1201**, 014 (2012) doi:10.1007/JHEP01(2012)014 [arXiv:1103.3041 [hep-th]].

[110] M. F. Atiyah, R. Bott, L. Garding, "Lacunas for hyperbolic differential operators with constant coefficients II," Acta. Math. **131**, 145-206 (1973) doi:10.1007/BF02392039

[111] F. James, "Monte Carlo Theory and Practice," Rept. Prog. Phys. **43**, 1145 (1980) doi:10.1088/0034-4885/43/9/002

[112] M. R. Douglas, R. L. Karp, S. Lukic and R. Reinbacher, "Numerical Calabi-Yau metrics," J. Math. Phys. **49**, 032302 (2008) doi:10.1063/1.2888403 [hep-th/0612075].

[113] S. K. Donaldson, "Some numerical results in complex differential geometry," Pure Appl. Math. Q. **5**, no. 2, part 1 571-618 (2009) doi:10.4310/PAMQ.2009.v5.n2.a2 [arXiv:math/0512625].

[114] J. Keller, "Ricci iterations on Kähler classes," *ArXiv e-prints: 0709.1490*(Sept., 2007).

[115] V. Braun, T. Brelidze, M. R. Douglas and B. A. Ovrut, "Calabi-Yau Metrics for Quotients and Complete Intersections," JHEP **0805**, 080 (2008) doi:10.1088/1126-6708/2008/05/080 [arXiv:0712.3563 [hep-th]].

[116] V. Braun, T. Brelidze, M. R. Douglas and B. A. Ovrut, "Eigenvalues and Eigenfunctions of the Scalar Laplace Operator on Calabi-Yau Manifolds," JHEP **0807**, 120 (2008) doi:10.1088/1126-6708/2008/07/120 [arXiv:0805.3689 [hep-th]].

[117] A. Ashmore, Y. H. He and B. A. Ovrut, "Machine learning Calabi-Yau metrics," arXiv:1910.08605 [hep-th].

[118] L. B. Anderson, J. Gray, S. Krippendorf, N. Raghuram and F. Ruehle, "Machine learning SU(3) structure," To appear.

[119] M. Headrick and T. Wiseman, "Numerical Ricci-flat metrics on K3," Class. Quant. Grav. **22**, 4931 (2005) doi:10.1088/0264-9381/22/23/002 [hep-th/0506129].

[120] M. Headrick and A. Nassar, "Energy functionals for Calabi-Yau metrics," Adv. Theor. Math. Phys. **17**, no. 5, 867 (2013) doi:10.4310/ATMP.2013.v17.n5.a1 [arXiv:0908.2635 [hep-th]].

[121] G. Tian, "On a set of polarized K̀ahler metrics on algebraic manifolds," J. Differential Geom. **32**, no. 1, 99-130 (1990) doi:10.4310/jdg/1214445039.

[122] S. K. Donaldson, "Scalar curvature and projective embeddings II," Q. J. Math. **56**, no. 3, 345-356 (2005) doi:10.1093/qmath/hah044.

[123] Notes by Matthew Headrick
http://people.brandeis.edu/ headrick/Mathematica/strategy.pdf

[124] Jorge Nocedal and Stephen J. Wright, *Numerical Optimization, 2nd Edition*, Springer, New York, NY, USA (2006)

[125] William H. Press, Saul A. Teukolsky, William T. Vetterling, and Brian P. Flannery., *Numerical Recipes 3rd Edition: The Art of Scientific Computing*, Cambridge University Press, USA (2007).

[126] P. Candelas, P. S. Green and T. Hubsch, "Rolling Among Calabi-Yau Vacua," Nucl. Phys. B **330**, 49 (1990). doi:10.1016/0550-3213(90)90302-T

[127] P. Candelas and X. C. de la Ossa, "Comments on Conifolds," Nucl. Phys. B **342**, 246 (1990). doi:10.1016/0550-3213(90)90577-Z

[128] P. Candelas, X. C. De La Ossa, P. S. Green and L. Parkes, "A Pair of Calabi-Yau manifolds as an exactly soluble superconformal theory," Nucl. Phys. B **359**, 21 (1991) [AMS/IP Stud. Adv. Math. **9**, 31 (1998)]. doi:10.1016/0550-3213(91)90292-6

[129] P. S. Aspinwall, B. R. Greene and D. R. Morrison, "Calabi-Yau moduli space, mirror manifolds and space-time topology change in string theory," Nucl. Phys. B **416**, 414 (1994) [AMS/IP Stud. Adv. Math. **1**, 213 (1996)] doi:10.1016/0550-3213(94)90321-2 [hep-th/9309097].

[130] A. Strominger, "Massless black holes and conifolds in string theory," Nucl. Phys. B **451**, 96 (1995) doi:10.1016/0550-3213(95)00287-3 [hep-th/9504090].

[131] M. R. Douglas, R. L. Karp, S. Lukic and R. Reinbacher, "Numerical solution to the hermitian Yang-Mills equation on the Fermat quintic," JHEP **0712**, 083 (2007) doi:10.1088/1126-6708/2007/12/083 [hep-th/0606261].

[132] L. B. Anderson, V. Braun, R. L. Karp and B. A. Ovrut, "Numerical Hermitian Yang-Mills Connections and Vector Bundle Stability in Heterotic Theories," JHEP **1006**, 107 (2010) doi:10.1007/JHEP06(2010)107 [arXiv:1004.4399 [hep-th]].

[133] D. J. Gross and J. H. Sloan, "The Quartic Effective Action for the Heterotic String," Nucl. Phys. B **291**, 41-89 (1987) doi:10.1016/0550-3213(87)90465-2

[134] E. Bergshoeff and M. de Roo, "The Quartic Effective Action of the Heterotic String and Supersymmetry," Nucl. Phys. B **328**, 439-468 (1989) doi:10.1016/0550-3213(89)90336-2

[135] D. J. Gross and E. Witten, "Superstring Modifications of Einstein's Equations," Nucl. Phys. B **277**, 1 (1986) doi:10.1016/0550-3213(86)90429-3

[136] Code associated to arXiv:0908.2635, which can be found at the following URL: http://people.brandeis.edu/∼headrick/Mathematica/index.html.

[137] P. Candelas, X. de la Ossa, Y. H. He and B. Szendroi, "Triadophilia: A Special Corner in the Landscape," Adv. Theor. Math. Phys. **12**, no.2, 429-473 (2008) doi:10.4310/ATMP.2008.v12.n2.a6 [arXiv:0706.3134 [hep-th]].

[138] P. Candelas, A. Constantin and C. Mishra, "Calabi-Yau three-folds with Small Hodge Numbers," Fortsch. Phys. **66**, no.6, 1800029 (2018) doi:10.1002/prop.201800029 [arXiv:1602.06303 [hep-th]].

[139] T. Hubsch, *Calabi-Yau Manifolds — A Bestiary for Physicists*, World Scientific, Singapore, 1994.

[140] D. Huybrechts, *Complex Geometry: An Introduction*, Springer, Berlin (2004).

[141] R. Friedman, J. Morgan and E. Witten, "Vector bundles and F theory," Commun. Math. Phys. **187**, 679-743 (1997) doi:10.1007/s002200050154 [arXiv:hep-th/9701162 [hep-th]].

[142] R. Friedman, J. W. Morgan, E. Witten, "Vector bundles over elliptic fibrations," [alg-geom/9709029].

[143] L. B. Anderson, X. Gao and M. Karkheiran, "Extending the Geometry of Heterotic Spectral Cover Constructions," arXiv:1912.00971 [hep-th].

[144] C. Okonek, M. Schneider, H. Spindler, *Vector Bundles on Complex Projective Spaces*, Birkhauser Verlag, 1988.

[145] G. Horrocks and D. Mumford, "A rank 2 vector bundle on $\mathbb{P}^4$ with 15000 symmetries," Topology, 12:63-81, (1973).

[146] A. Beilinson, "Coherent sheaves on $\mathbb{P}^n$ and problems in linear algebra," Funktsional. Anal. i Prilozhen. 12 (1978), no. 3, 68-69.

[147] R. Hartshorne, *Algebraic Geometry*, Springer, GTM 52, Springer-Verlag, 1977.

[148] A. Lukas, L. Anderson, J. Gray, Y. H. He, S. J. Lee, *CICY package*, based on methods described in Refs. [17, 150, 153, 161].

[149] A. Constantin and A. Lukas, "Formulae for Line Bundle Cohomology on Calabi-Yau three-folds," Fortsch. Phys. **67**, no.12, 1900084 (2019) doi:10.1002/prop.201900084 [arXiv:1808.09992 [hep-th]].

[150] L. B. Anderson, Y. H. He and A. Lukas, "Heterotic Compactification, an Algorithmic Approach," JHEP **0707** (2007) 049 [arXiv:hep-th/0702210].

[151] A. Lukas and K. S. Stelle, "Heterotic anomaly cancellation in five-dimensions," JHEP **0001**, 010 (2000) doi:10.1088/1126-6708/2000/01/010 [hep-th/9911156].

[152] H. Hoppe, "Generischer spaltungstypumun zweite Chernklassestabiler Vektorraumbündel vom rang 4 auf $\mathbb{P}^4$, " Math. Z., **187** (1984), 345-360.

[153] L. B. Anderson, Y. H. He and A. Lukas, "Monad Bundles in Heterotic String Compactifications," JHEP **0807** (2008) 104 [arXiv:0805.2875 [hep-th]].

[154] X. Wang, "Canonical metrics on stable vector bundles," *Comm. Anal.Geom.* **13** (2005), no. 2, 253–285.

[155] R. Seyyedali, "Numerical Algorithms for Finding Balanced Metrics on Vector Bundles," *ArXiv e-prints* (Apr., 2008)

[156] R. Thomas, "A Holomorphic Casson invariant for Calabi-Yau three folds, and bundles on K3 fibrations," J. Diff. Geom. **54**, no.2, 367-438 (2000).

[157] S. K. Donaldson, "Floer Homology Groups in Yang-Mills Theory," Cambridge University Press (2002), doi:10.1017/CBO9780511543098.

[158] E. Witten, "Topological Tools in Ten-dimensional Physics," Int. J. Mod. Phys. A **1**, 39 (1986) doi:10.1142/S0217751X86000034

[159] X. G. Wen and E. Witten, "Electric and Magnetic Charges in Superstring Models," Nucl. Phys. B **261**, 651-677 (1985) doi:10.1016/0550-3213(85)90592-9

[160] Kaare Brandt Petersen, Michael Syskind Pedersen, *The Matrix Cookbook*, Technical University of Denmark (2012).

[161] Y. H. He, S. J. Lee and A. Lukas, "Heterotic Models from Vector Bundles on Toric Calabi-Yau Manifolds," JHEP **1005** (2010) 071 [arXiv:0911.0865 [hep-th]].